

Report on

Seismic Microzoning of

Chimbote Area

Perú

(Misión Japonesa)

- 1971 -

*Jorge E. Alva Hurtado*

JORGE ELIAS ALVA HURTADO  
INGENIERO CIVIL  
Reg. del Colegio de Ingenieros No. 11776

**REPORT ON  
SEISMIC MICROZONING OF  
CHIMBOTE AREA  
PERU**

**MARCH 1971**

**OVERSEAS TECHNICAL  
COOPERATION AGENCY  
— GOVERNMENT OF JAPAN**

The earthquake that hit the Province of Ancash in Peru on May 31, 1970 was the most violent one unparalleled in history. In the wake of this disaster, the Government of Peru called upon the Government of Japan, known world-wide as a seismic country that have experienced many earthquakes in the past, for the assistance in the planning of an earthquake disaster rehabilitation and reconstruction program for the devastated area.

In response to this request, the Government of Japan undertook to send a technical survey mission to that country at the earliest opportunity and entrusted the Overseas Technical Cooperation Agency with the execution of the said survey.

The Overseas Technical Cooperation Agency, being cognizant of the urgency of the rehabilitation and reconstruction program for Peru, immediately organized a five-member survey mission headed by Dr. Ryohei Morimoto, Director of the Earthquake Research Institute, The University of Tokyo, and dispatched it to the stricken area on July 19, 1970.

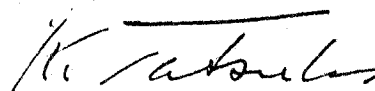
The Survey Mission, with the cooperation of various agencies of the Government of Peru, conducted extensive on-the-spot inspections of the affected area and provided necessary technical assistance to the Peruvian officials concerned over a period of 50 days until its return to Japan on September 6, 1970.

This report is the findings of various field investigations and studies made by the mission.

It is my desire that the report will prove helpful not only to the planning of a rehabilitation and reconstruction program for the severely damaged city of Chimbote to make it into an anti-seismic city but also to the planning of necessary measures against earthquakes for other cities of Peru.

Finally, I wish to take this opportunity to express my heart-felt thanks to officials of government agencies and staffs of the university and research institutes in Peru for their generous cooperation and support extended to the Mission during its stay in that country.

March 1971



KEIICHI TATSUKE

Director General

Overseas Technical Cooperation Agency

## Letter of Transmittal

31st March 1971

Mr. Keiichi Tatsuke, Director General  
Overseas Technical Cooperation Agency,  
Ichigaya, Shinjuku-ku, Tokyo 160

Dear Sir;

The undersigned, Dr. Ryohei Morimoto, Chief of the Japanese Survey Mission for Restoration of Earthquake Disaster in Peru 1970, has the honour of presenting herewith a report of the Mission on Seismic Microzoning of Chimbote, one of the most important industrial cities in Peru.

Peru and Japan are of active seismicity belonging to the same **Circum-Pacific Seismic Zone**. People of both countries are destined to suffer severe earthquakes at times. Therefore, when the tragedy brought about by the Earthquake of 31st May 1970 which shook the Departamento de Ancash of Peru was reported, it was felt as if it were an event in this country. The people in both countries always have to think about the way to protect themselves from earthquakes or to minimize the earthquake disasters. Prevention of earthquake disaster is a common subject given to both governments. In general, ground movement and the destruction of constructions due to earthquakes are essentially governed by the magnitude and epicentral distance of the earthquake concerned, but local heterogeneity in damage distribution in a certain limited area is mainly ascribed to local difference in subsoil condition roughly identified by local microtopography. "Proper constructions on proper land" is a simple and important principle for preventing earthquake disaster. It was quite reasonable and appropriate for the Peruvian Government, therefore, to request the Japanese Government to send a Survey Mission for the preparation of the seismic microzoning map of the hard hit city of Chimbote in order to rehabilitate this seismic city for national economy.

The Mission arrived at Lima on 20th July 1970 and immediately contacted the Ministro de Vivienda and Presidente de Comision de Reconstruccion y Rehabilitacion de la Zona Afectada por El Teremoto del 31 de Mayo de 1970 of the accepting Government. The first ten days of the stay in Peru were spent with the officials of the abovementioned organizations for discussions on the survey schedule and for preliminary surveys of the whole affected area along the coast (25-28th July) and the Callejón de Huaylas (30-31st July) kindly arranged by the Peruvian Government. The working group for the preparation of the seismic microzoning map of Chimbote consisted of all members of the Japanese Mission and Peruvian officials. Peruvian scientists and engineers who had once been in Japan at the Earthquake Research Institute and the International Institute of Seismology and Earthquake Engineering played an important role in the working group. The survey in Chimbote was a typical example of international technical cooperation of Peruvian and Japanese personnels and this cooperation may be said to go back to ten years ago when the first trainee was sent from Lima to Tokyo in 1961. Among many foreign missions visiting Peru after the great earthquake, the long lasting cooperation between the two seismic countries across the Pacific ocean through seismology and engineering seismology must be highly esteemed.

In order to elucidate the behaviour of the ground in Chimbote at time of earthquakes and its effects on the response of structures, all available methods and means such as field surveys of surface geology, geological interpretation of aerophotographs, collection of pre-existing boring data, 18 borings with standard penetration tests, observation of microtremors and after-shocks, and investigation of earth changes were used for the working project. The subsoil of the Chimbote area consists mainly of thick sandy deposit on the hard compact bedrocks composed of Crétaceous volcanics, shale, sandstone, and granitic rocks intruding the formers. The foundation is rather stable against the earthquake. The subsoil condition in Chimbote as a whole is anti-seismically better than that in large cities of Japan where soft Alluvial deposits develops extensively. Locally, however, the natures of these deposits are different in different places and the damage to constructions by earthquake is also different accordingly. Local difference in water level is important factor controlling subsoil conditions. Through various procedures mentioned above, Chimbote area was divided into four zones. In Zone I the subsoil consists of dense gravels or rocks and the water table is at least 10m deep below the ground surface. A large portion of the area belonging to this Zone is higher than 10m in altitude, where no subsidence of buildings and the ground is expected, but seismic force acting on buildings may be a little stronger than in other Zones. Therefore, problem of soil-structure interaction must be considered for any structures in this Zone. In Zone II area is covered with loose to medium dense sand of several metres in thickness underlain by either dense sand or cemented compact sand formation with water table being about 5m below the surface. No appreciable settlement is expected for ordinary residential buildings less than two stories, except those on the outer edge of sand dune. It is preferable for buildings higher than two stories to be supported by piles reaching the dense sand. As to the constructions on sand dune, foundations should be improved by means of vibrofloatation. In Zone III the subsoil consists mainly of sandy soil covered with thin agricultural soil. Gravel beds lie deeper than 10m with ground water level being a few meters in depth. Loose fine sand seating in some depths may liquefy during the earthquake. There is a possibility of damage to constructions due to local liquefaction of sands lying in some depths below the ground surface. No appreciable settlement of building will occur with a few exceptions. However, careful consideration should be given to the design of substructures of buildings higher than two stories. Zone IV is characterized by high water table which is almost the same in height as the ground surface. Most of the land is covered with water. Average elevation of the land belonging to Zone IV is lower than 5 m above sea level. The soil consists mainly of sand covered with a very thin layer of organic silt. Damage to buildings in this Zone is ascribed mainly to the settlement and partly to seismic force. Liquefaction of the sand up to the surface will occur at time of severe earthquakes. Piling for building and improvement of the foundation to certain depth are essential in Zone IV. The area lower than 5m in elevation facing directly the wide mouth (the southern mouth) of the Bay of Chimbote may subject to tsunami (marimoto) The study on the possibility of tsunamis had to be excluded from this survey owing to time limit.

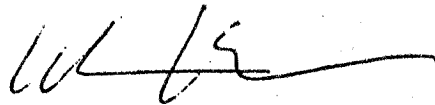
It is believed that the seismic microzoning map mentioned above is useful for the reconstruction of Chimbote as an anti-seismic city, and the methods used by this Survey Mission are also applicable to other cities. It is very encouraging to hear that a similar investigation had been started by Peruvian personnels themselves in Huaraz. There are many approaches to prevent, or at least to minimize, the earthquake disasters. For this purpose, seismology and engineering seismology in association with other related sciences, including researches for the predication of earthquakes and of mud flow due

to fall of ice-cap should be promoted. The adobe construction which collapsed by seismic force actually aggravated the casualties in the recent earthquake, as well as damage by mud-flow due to ice fall. Improvement of quality and some aseismic design for adobe construction are urgent and most essential questions. Since it takes long time and requires huge amount of money to implement these recommendations, the initiative must be taken by the central government to start these projects as soon as possible. The establishment of a kind of Composite Research Institute for Earthquake Disaster Prevention covering the above-mentioned research fields and exchange of scholars and students between the two countries will facilitate the implementation of these projects.

Strictly to say, modes of occurrence of any disaster depend upon not only natural but also social environment of the affected area. Therefore, most appropriate way of prevention should be established by the people who know their own land in detail. In this means, it is strongly hoped that the time will come soon when all anti-seismic designs are implemented by the Peruvian people themselves against the earthquakes attacking their own territory.

Finally, the undersigned wishes to take this opportunity to express his heart-felt thanks to Sr. Contralmirante Luis Vargas Caballero, Ministro de Vivienda and Sr. Genral de Brigada E P, Carlos Villa Pazos, Presidente de la Comisión de Reconstrucción y Rehabilitación de la Zona Afectada of Peruvian Government for their kind cooperation and assistance extended to the undersigned as well as to all members of the Mission in spite of their busy schedule in the time of emergency. It is hoped that the recent survey serves as a milestone not only of the farther scientific and technical cooperation between Peruvian and Japanese people but also of future friendship between the two seismic countries.

Yours sincerely,



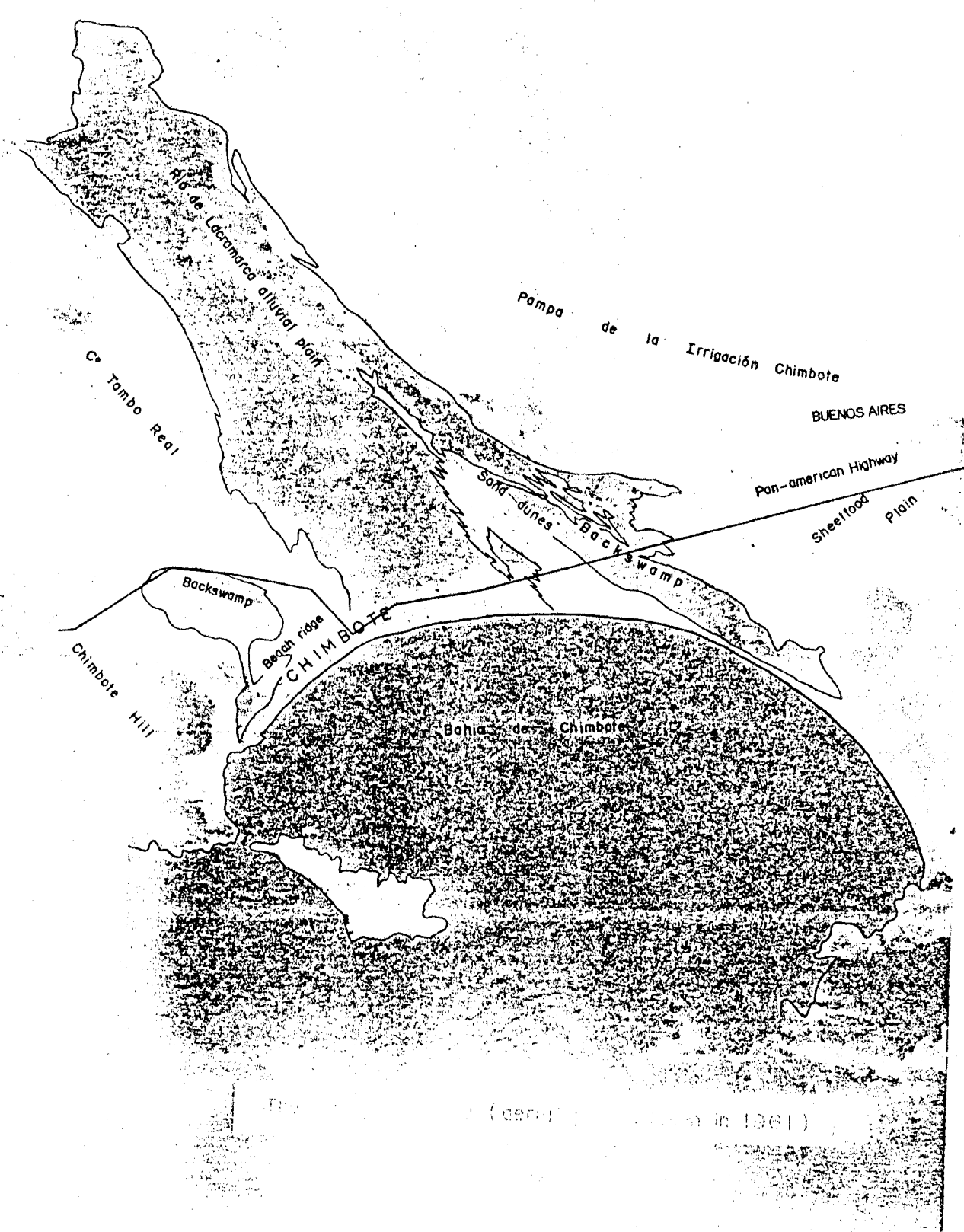
Dr. Ryohei MORIMOTO  
Chief of the Japanese Survey Mission  
for Restoration of Earthquake  
Disaster in Peru 1970.

JORGE ELIAS ALVA HURTADO  
INGENIERO CIVIL  
Reg. del Colegio de Ingenieros N° 11776

# REPORT ON SEISMIC MICROZONING OF CHIMBOTE AREA

## C O N T E N T S

Preface		
Letter of Transmittal		
Chapter 1	Introduction	1
Chapter 2	Geology of the Chimbote Area	7
Chapter 3	Soil Conditions	22
Chapter 4	Observations of Micro-Tremors	28
Chapter 5	Observations of Aftershocks	33
Chapter 6	Analysis of the Ground Motion	41
Chapter 7	Survey on Damage to Buildings	53
Chapter 8	Geological Aspect of Damage	56
Chapter 9	Microzoning of the Chimbote Area	77
Chapter 10	General Recommendations	80
Appendix		
1	Comparison of the two penetration tests	A- 1
2	Field records of borings and penetration tests	A- 3
3	Results of Grain size analysis	A-16
4	Pre-existing of water-wells and borings	A-25
5	Micro-tremor records in Chimbote area	A-32
6	Frequency-periods curve of micro-tremor records in Chimbote area	A-35



Map of the coastal region of Chile (centered on Valparaíso in 1961)

Scale 1:50,000





The Chimote area (aerial photos taken in 1961)

## Chapter 1 Introduction

A severe earthquake attacked the Ancash Area of Peru on the 31st of May, 1970. It was one of the most destructive earthquakes in the world history. Many human lives were lost and thousands of buildings and other structures collapsed.

This earthquake is reported to be 7.8 in Magnitude by U.S.C.G.S. and the hypocenter of it is located in  $9.2^{\circ}$  S,  $78.8^{\circ}$  W, 43 km in depth.

The city of Chimbote located 380 km north of Lima, has the largest harbour in the country and is one of the most important industrial cities with groups of fish mills and a steel factory. The city had grown rapidly and its population had reached about 180,000. (Figs. 1-1, 2) The city was severely damaged by this earthquake and its reconstruction was an urgent matter. Prior to the start of the new city planning, the seismic microzoning of the city was required, and a mission comprising the following members was sent by the Japanese Government to Peru. The micro-zoning map of the city of Chimbote was prepared after many tests and surveys;

Chief	Ryohei Morimoto
Member	Yasunori Koizumi
Member	Tokihiko Matsuda
Member	Motohiko Hakuno
Member	Isao Yamaguchi

Now, why is the micro-zoning map of the said city necessary for the protection of the city from the anticipated earthquake damage in the future?

For the purpose of protecting the city from damage, all structures and earthstructures in seismic active regions should be constructed to withstand earthquake.

The basic design coefficient of seismic force is mainly determined by two factors: (1) seismic activity, (2) ground condition. The design coefficient for buildings may be modified according as their uses and their structural characteristics. The factor concerning seismic activity could be determined statistically based on past seismic activities. At the present time the Peruvian territory has been divided into three regions, in each of which the different value of regional seismic factors has been proposed.

It has been found during past destructive earthquakes that damage to structures in a limited area has much local irregularities. This indicates that the seismic force acting on a structure is affected in a large extent by the topography and subsoil condition at the site.

Therefore, if the effect of ground condition is to be taken into consideration more detailed zoning map in a proposed area should be made.

In order to establish the most reasonable utilization of land in a city planning, micro-zoning in the area is recommended to be done from the view point of earthquake engineering.

The microzoning map will be made on basis of geological survey, precise ground explorations, observations of microtremors and of actual earthquakes. If the area has experience earthquake damage, the investigation on feature of damage relating to the subsoil conditions is very important.

The following investigations were made in the Chimbote areas.

A) Geological Survey

This is to determine the structure of subsoil through field surveys and interpretation of aerophotograph of the area from a geological view point and provide the mission with macroscopic information about the subsoil condition. This survey greatly contributed to the preparation of the micro-zoning map of the Chimbote areas along with the boring results.

B) Borings and Standard Penetration Tests

This is to get the subsoil condition directly and to know the level of water table, the grain size distribution and the hardness of the subsoil. From the above two surveys, it is possible to obtain information whether the subsoil would be spoiled by 'Liquifaction' or not during earthquake,

In the Chimbote areas, borings and penetration tests were made at eighteen points indicated in Fig. 3-1. These results were very useful to the preparation of the micro-zoning map along with the results of geological surveys.

C) Survey on Damage to Buildings, Roads, and Ground Failure

Many factors including the intensity of earthquake and dynamic properties of the ground have a great influence on the extent of damage to structures. For this reason, a survey on the damage to structures is very important. Since the adobe construction in the Chimbote area were destroyed almost completely, an extensive survey was made on the brick construction with frame covering the whole city and in down town area of the city a study was made on the relation between the damage of structures and the failure of ground surface.

D) Observations of After Shocks

This observation is carried out to obtain dynamic properties of the ground surface utilizing the After-Shocks following a big Earthquake.

In the Chimbote areas two seismometers of the same type were provided for after-shock observation. One meter was fixed on the rock base as the standard (reference) seismometer, and the other was moved from point to point after some good results were obtained.

Observations were made at six boring points No. 1, 2, 3, 4, 5, 7.

From the results of analysis of after-shocks, it was confirmed that the intensity of the earthquake on the alluvial layer is less than that on the rock ground surface.

E) Observation of Micro-Tremor on the Ground Surface

The ground surface is always vibrating in very small amplitude. This vibration of the ground is mostly natural vibration of the ground surface layers.

Dynamic properties of the surface layers, such as the predominant period may be obtained through analysis of this micro-tremor.

In the Chimbote area observations were made at more than twenty points shown in Fig. 4-5 and the surface ground was considered to be very hard and dense from the standpoint of dynamic property. *Chimbote*

F) Geophysical Survey of the S-wave Velocity in Each Layer

The S-wave velocity may be obtained from the relation between the distance propagated and time spent.

Sometimes on artificial shock source like a dynamite blast under the ground is used for generating the S-waves. However, this survey was not conducted in the area of Chimbote.

G) Analysis of Ground Surface Motion by Computer

By utilizing the data on subsoil condition, the motion of the ground surface can be calculated with the 'Shear Wave Reflection Theory'. According to the computed results, the predominant periods, and dynamic complication behavior of the surface layers may be assumed.

In the Chimbote areas, the surface ground motion was calculated by means of the so called 'Multi Reflection theory', which utilizes the assumed S wave velocity derived from N value.

Many surveys of different type were carried out in Chimbote as stated previously. The buildings which will be constructed in this city in the near future may be low structures such as adobe or brick type whose natural period is very short, (Recently, a measurement was made on the natural period of one story house made of adobe with a micro-tremor meter and the period shown was less than 0.04 second) and the structure is considered to be quite rigid against the earthquake motion.

These findings on the properties of the structure led to the conclusion that from the view-point of damages to structures, specially to brick and adobe construction, the main cause of damages to the structures on the hard ground is the intense earthquake force applied to the super structures and the damage to the structures on the soft ground is caused mainly by the settlement of buildings due to the compaction or liquifaction of loose sand, and is not the dynamical resonance of structures and the ground. Therefore, the results of the dynamical tests such as the ones stated at articles D), E), F), G), are useful for the more deflectable structure, but could not be used directly to make a micro-zoning map. However, the tendency of the results obtained from all the previously mentioned methods were qualitatively coincident with each other.

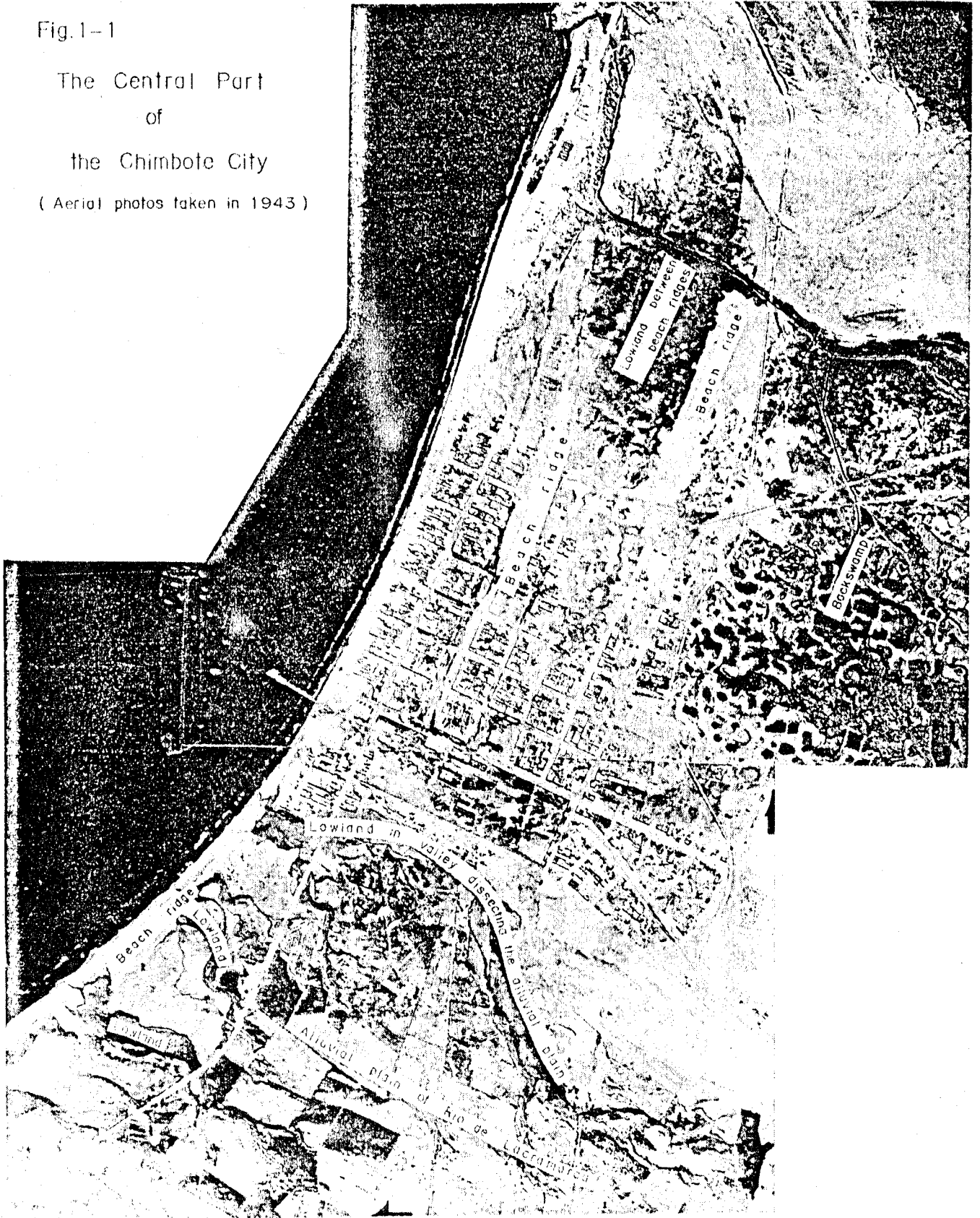
The micro-zoning map was made mainly on the basis of the results obtained from the geological survey, and the borings and damage distribution of structures.

The mission wishes to express its sincere appreciation and gratitude to the officials of the Peruvian Government and institutions for kind cooperation and support extended to the mission during the survey.

Fig.1-1

The Central Part  
of  
the Chimbote City

( Aerial photos taken in 1943 )



## Chapter 2. Geology of the Chimbote Area

The most of the city of Chimbote is located on the alluvial plain of the Rio de Lacramarca along the coast of the Bahia de Chimbote. To the north and southeast of the city there are rocky mountains and hills which are covered partly with eolian sands. The surface geology of the Chimbote area may be classified as follows: (See Fig. 2-1).

- A: Bedrocks
  - A': Bedrocks covered with the older eolian sands
- B: Alluvial deposits
  - B1: Alluvial deposits of Rio de Lacramarca
  - B2: Remnant of the older alluvial deposits of Rio de Lacramarca
  - B3: Sheetflood deposits
- C: Beach ridges
  - C1: Present beach ridges
  - C2, C3, C4: older beach ridges
- D: Eolian Sands
  - D1: Present eolian sand
  - D2: Older eolian sand
- E: Backswamps
- F: Lowlands in valleys dissecting the alluvial plain

Brief explanations will be given below.

### 2-1 Bedrocks

The main constituents of bedrocks are Cretaceous andesitic volcanics with shale and sandstones and granitic rocks intruding it. The volcanic rocks, called the Casma formation, are more or less metamorphosed by the intrusion of the granites. They are exposed largely on the hills north of the city (Chimbote Hill and C<sup>o</sup> Tambo. Real) (Fig. 2-3), while the granites, probably a part of the Andean batholith, constitute hills southeast of the city (Pampa de la Irrigación Chimbote east of Rio de Lacramarca alluvial plain).

### 2-2 Alluvial plain

There are a few alluvial fans extending towards the lowland on which Chimbote City lies. The most important one is an alluvial plain of Rio de Lacramarca (B<sub>1</sub>). The other two are sheetflood alluvial fans (B<sub>3</sub>) developed on the foot of the Chimbote Hill and the Pampa de la Irrigación Chimbote (Figs. 2-4, 2-7a).

- (1) Rio de Lacramarca alluvial plain (B<sub>1</sub>): The alluvial plain is developed filling the valley of Rio de Lacramarca ca. 10 km long and ca. 5 km wide at the coast. The water of Rio de Lacramarca disappears near the head of the alluvial fan beneath the ground surface. No definite river floor is recognized on the alluvial surface. The seaward margin of the alluvial plain

is truncated obliquely by the coast line in the northern part, where the alluvial plain has 3 m - 5 m height above the sea level at the coast and it is fringed there by a beach ridge. In the southern part of the alluvial fan, on the other hand, the plain is gradually lowered and continues to backswamps or lagoons.

The alluvial plain has a soil layer suitable for cultivation on the surface. Figs. 2-2 and 2-11 show a near-surface profile of geology in the near-shore part of the plain between the coastal line and Pan American Highway. Subsurface geology of this alluvial plain is shown in Fig. 3-2, based on data of borings and the pre-existing data (Appendix 2 and 4). Generally speaking, the alluvial deposits consist mainly of various kinds of sands, interbedded with thin clay and gravel. The shallowest gravel beds lie between ca. 10 m - 20 m in depth in the inland part of the studied area, becoming thinner and deeper seaward. At the near-shore localities no remarkable gravel beds are found down to ca. 20 m from the surface. Instead, marine sands with fragments of shell in thickness of 5-7 m are interbedded in a horizon between 7-15 m down from the ground surface. Clay and silt are not significant in the geologic profile down to 25 m, although there are several layers less than 3 m in thickness. The following two facts are probably favourable for subground liquefaction: the first is that sands in the upper part of the deposits are well-sorted fine sand probably of the reworked eolian sand, and the second is that the level of the ground-water table is quite shallow (1-2 m in depth) and sometimes even pressured.

The data of boring performed at Fabrica Pescamar near the coastal line indicate that the base of this alluvial deposits lies shallower than 90 meters in depth from the ground surface. In the core sample, probably fluvial granitic coarse sand to granule deeper than 52 m change into the undoubted granitic basement at ca. 90 m. The exact boundary between the alluvial deposits and the basement was obscure because of the possible occurrence of weathering products of the granitic basement.

(2) Remnant of older alluvial deposits of Rio de Lacramarca (B<sub>2</sub>):

A terrace-like narrow bench is attached on the lower part of the hill-slope along the northern margin of the alluvial plain of Rio de Lacramarca. The terrace is 10-50 m in width and about 20 m high above the present alluvial plain. The inner angle of the terrace is covered with eolian sand. The outer edge is marked by a sharp cliff, where weakly consolidated gray, sandy mud and dirty very fine sands of about 2 m in thickness are exposed on the uppermost part of the terrace cliff.

The deposits contain numerous plant remains and have no indication of marine environment of deposition. They are considered to be a remnant of old alluvial plain escaped from the subsequent fluvial erosion.

(3) Sheetflood plain around Chimbote Hills and Pampa de la Irrigación Chimbote (B<sub>3</sub>):

Rocky mountains in this region have gentle-sloping, broad skirts of plain around themselves. These plains consist of fairly thick deposits of coarse sands and gravels with subangular boulders.



A typical and largest plain extends westwards to the coast from the Pampa de la Irrigación Chimbote, on which Buenos Aires is present (Fig. 2-7). This alluvial plain is considered to have been formed by sheetflood because of absence of definite valleys on this flat plain. An alluvial plain similar to the above is one south of Chibote Hill, on which the steel plant of Chimbote stands. As shown in pre-existing boring data and as seen in the cutting in the steel plant (Fig. 2-8), the plain consists of alternation of angular debris derived from the mountains behind and sorted sand probably of reworked eolian origin. The alluvial fan north of the harbour of the steel plant consists largely of reworked eolian sand interbedded with rock debris (Fig. 2-9). Water table is fairly deep in the sheetflood plain. In Buenos Aires the water table lies 16 m below the ground surface at boring No. 5.

### 2-3 Beach-ridges

In and around the city of Chimbote, there are present and older beach ridges along the present coast (Fig. 2-5).

- (1) Present beach ridge  $C_1$ : The present beach ridge is developed along the coast of the Bahía de Chimbote. The beach ridge is generally 20-100 m in width and 3-5 m high above sea level and it consists of coarse grained laminated beach sand layers with fragments of shells. As shown in Fig. 2-2, the beach sand interfingers partially with clay on its backside slope in the central part of Chimbote.
- (2) Older beach ridges ( $C_2, C_3, C_4$ ): The northern part of the city of Chimbote consists of three beach ridges, of which two inland are beach ridges of the older time when the coastal line was there. The innermost one is the most distinct and 7 m in high above the present sea level. Avenida Jose Olaya is just on the crest of this beach ridge. Another old beach ridge ( $C_4$ ) is recognizable in the middle of lagoonal area of the southern part of Chimbote, limiting the eastern extremity of Barrio Vialla Maria. This old beach ridge is only 1 m higher in elevation than the surrounding lagoonal area.

### 2-4 Eolian Sands

A prevailing wind from the ocean is transporting inlandward fine sands toward NNE to form sand dunes in the southern part of the Chimbote area. The main source area of sands is the southern coast of Bahía de Chimbote and the northern coast of Bahía de Samanco. Besides this presently-moving sand dunes, old eolian sand are distributed on the north side of the Chimbote area.

- (1) Present eolian sands ( $D_1$ ): The most thick eolian sands cover the southern part of the Rio de Lacramarca alluvial plain. The sand dunes are 10 – 20 m high above the surface of the alluvial plain, and elongated and arranged parallel to the direction of the prevailing wind. The sand dune consists of well-sorted fine sand rich in quartz grains. The deposits have commonly cross laminations.
- (2) Older eolian sands ( $D_2$ ): The southern slope of hills ( $C^0$  Tambo Real) north of Chimbote is covered by sands. Borrio San Pedro, Cementario and Reservorio are located on this sandy

slope (Fig. 2-12). The sand consists of fine to coarse sands containing small fragments of shells. The thickness is not known, but it is estimated at less than a few meters in thickness. Beneath the loose sands, semi-consolidated sand layers are exposed on steep slopes or cliffs, which are cross-bedded and more than a few meters thick. The sand layers consist of fine to coarse sands with shell fragments. The calcareous matter is served as cement. The superficial loose sands and the underlying semi-consolidated sands mentioned above are very similar to each other. The both sands are considered as old eolian sands (or beach sands reworked by wind) which were formed when the coastal line was situated more closely to the foot of these hills than the present situation. This seems reasonable from the fact that well-preserved beach ridges lie in the area between this sandy hill and the present coastal line and that the coarse sand and larger fragments of shell are commonly included in the deposits.

## 2-5 Backswamp

Backswamps are developed in enclosed lowlands on alluvial plain (Figs. 2-3, 2-5 and 2-6). They are formed in areas where the ground water is coming up to the surface and the surrounding highs such as beach ridges prevent to drain the ground water.

The largest backswamp in the Chimbote area lies in the southeastern Chimbote, which developed on the southern margin (the lowest portion) of the Rio de Lacramarca alluvial fan. The backswamp is divisible into the outer and inner portions which are separated incompletely by an old beach ridge (C<sub>4</sub>) near the Pan-American Highway. The water in the backswamp is supplied from numerous gushing springs in the inner portion of the backswamp and flows out into the sea through the high of sand dune and a beach ridge. The source of the ground water is Rio de Lacramarca, of which stream water submerges under the ground surface at the head of the alluvial fan. Geological profile of this backswamp consists largely of medium to coarse sands down to 25 meters, although gravel and silty clay beds are interbedded in some horizons. (see boring data, No. 4). It is noteworthy that no muddy sediments are found beneath the swamp bottom.

Another backswamp is developed in the lowland in the northern Chimbote. It is surrounded by hills on the north (Chimbote hill) and east (C<sup>o</sup> Tambo Real) and Rio de Lacramarca alluvial cone on the south and beach ridges on the west (Fig. 2-3). A drain channel goes to the coast through the beach ridges to the west. The backswamp is less than 5 meters above sea level and incloses many irregular or linearly-elongated sand dunes in it. Some gushing springs supplies the water to the backswamp. This backswamp was originally a lagoon which was formed by growth of beach ridges. The oldest beach ridge is C<sub>3</sub> in Fig. 2-1. The narrow lowland between these ridges turned to a part of the backswamp as the present beach ridge develops. In the lower portion of the backswamp, a black organic soil layer is developed near the surface as seen in the trench wall along the drain-channel. However, deposits of the backswamp down to 25 meters are mainly sandy deposits of fluvial, eolian and beach origin (see boring data of No.1). Generally speaking, the northern section of this backswamp contain coarse detritus of alluvial fan extending from the northern hill, while the southern section

consists mainly of fluvial sand and gravel of the Rio de Lacramarca alluvial fan. A marine sand layer containing abundant shell fragments lie in 4 meters from the ground surface, which is nearly the same elevation as that in the backswamp in the southern Chimbote (cf. Boring No. 1 and 4 in Fig. 3-2). It is to be noticed that unlike the present surface appearance, there are no remarkable clay or muddy soft deposits even near the top of the sedimentary sequence beneath the backswamps in the Chimbote area.

#### 2-6 Lowlands in valleys dissecting the alluvial plain

As shown in geologic map (Fig. 2-1), the Rio de Lacramarca alluvial fan is dissected by young small valleys in its northern marginal portion. These valleys are developing to inland by head erosion from the sea cliff of 2 or 3 meters high above the sea level. The heads of the valleys reach generally 1 km or less far from the coastal line. The largest valley just south of the center of Chimbote, has about 2 km in length.

The valley-floor is a flat lowland about 100 m wide and 3 meters lower than the Rio de Lacramarca alluvial plain at the estuary, becoming narrower and shallower to the inland. The lowland has a stream channel carrying running water. The water tend to be dammed by the beach ridge at the estuary, resulting in formation of small backswamps behind the beach ridge. The surface soil in the lowland consists of soft, wet, silty fine sand or sandy mud with or without plant remains. The thickness of the deposits filling the valley is not known exactly, but it seems to be less than a few meters as judged from boring data.

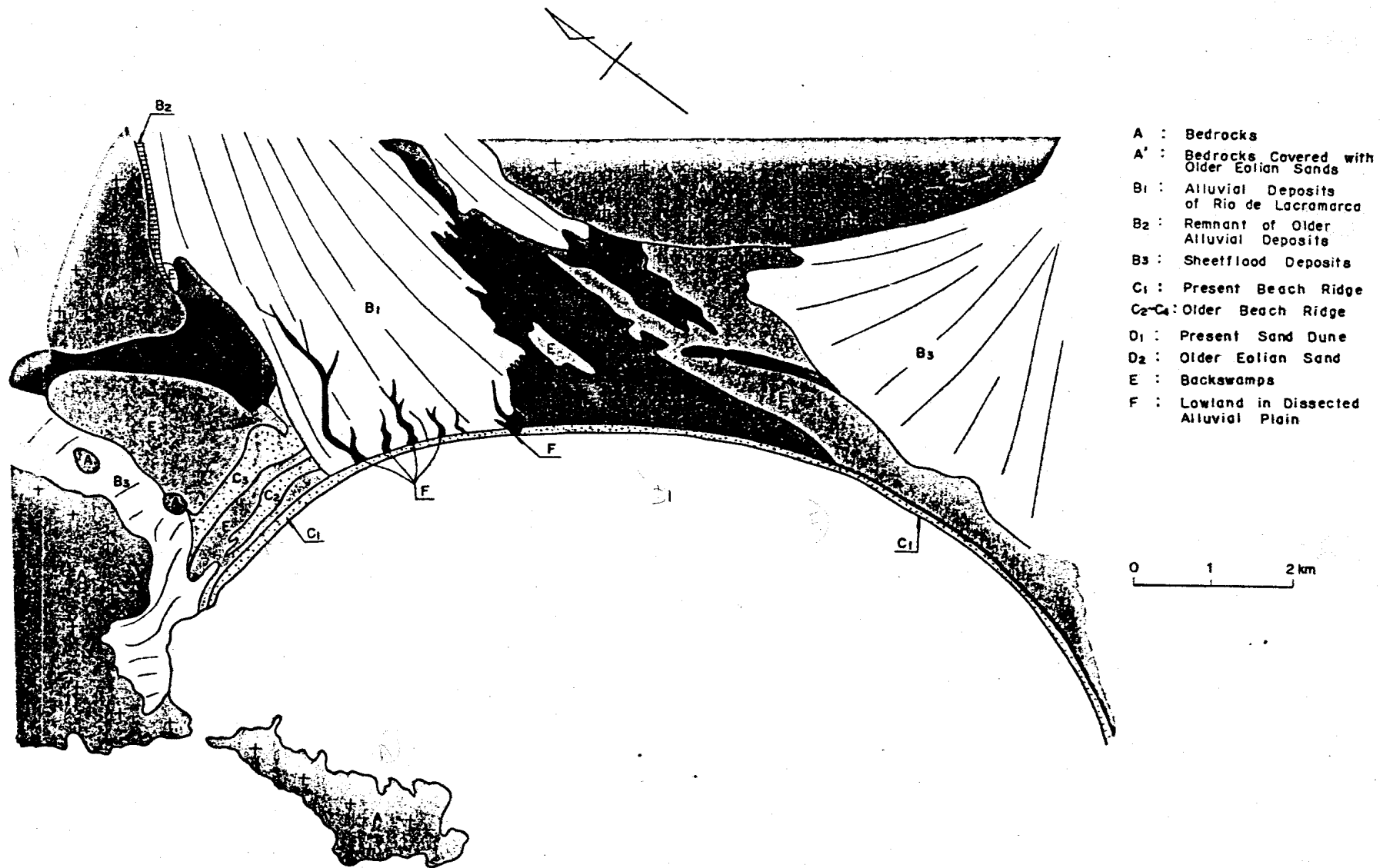


Fig. 2-1 GEOLOGIC MAP OF THE CHIMBOTE AREA

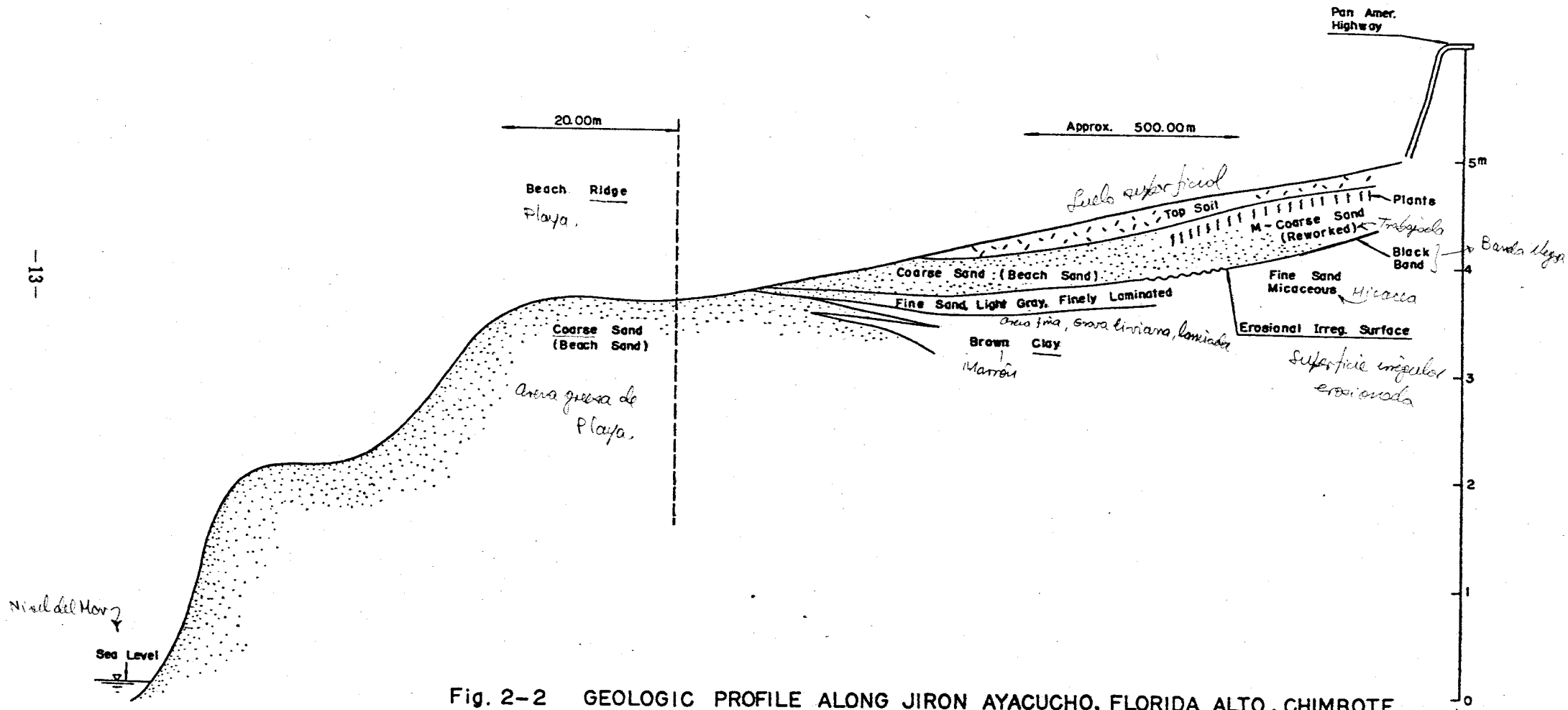


Fig. 2-2 GEOLOGIC PROFILE ALONG JIRON AYACUCHO, FLORIDA ALTO, CHIMBOTE

*a lo largo* ↗

Fig. 2-3  
Chimbote Hill and  
backswamp  
(looking from  
San Pedro)

*Chimbo Chimbote  
(Vista desde San Pedro)*



Fig. 2-4  
Sand dunes and the  
Rio de Lacramarca  
alluvial plain  
(southern Chimbote)

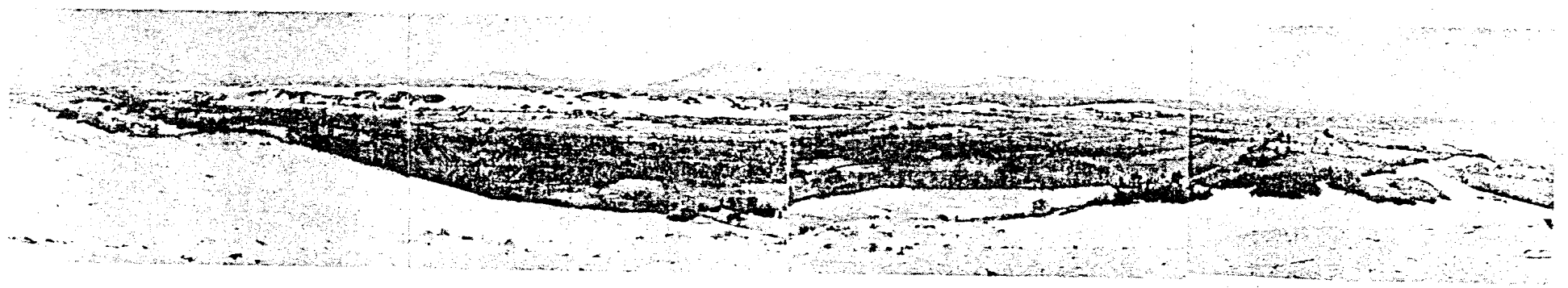


Fig. 2-5  
Beach ridge and  
lagoonal swamp  
at the estuary  
(Miramar Baja)

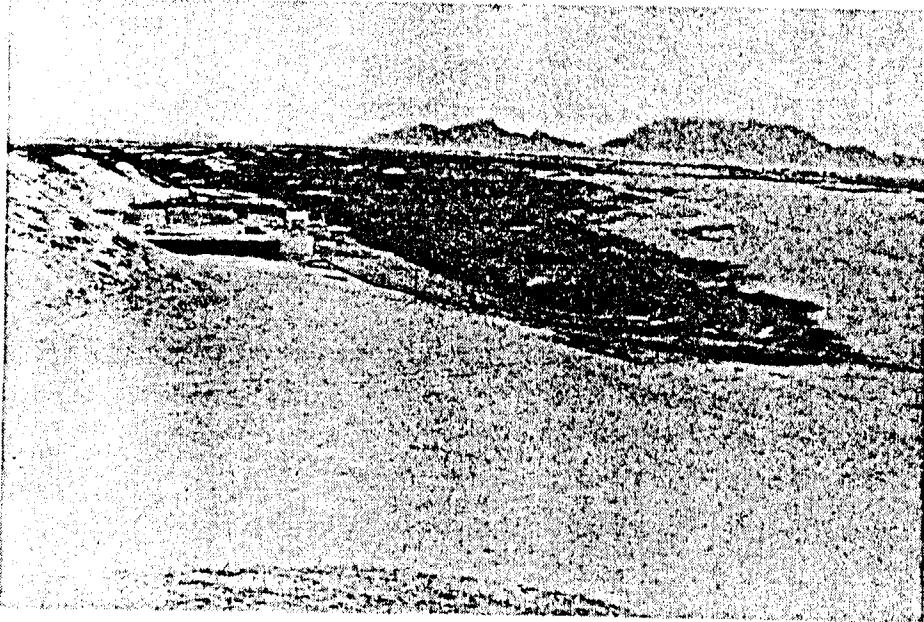
(a)



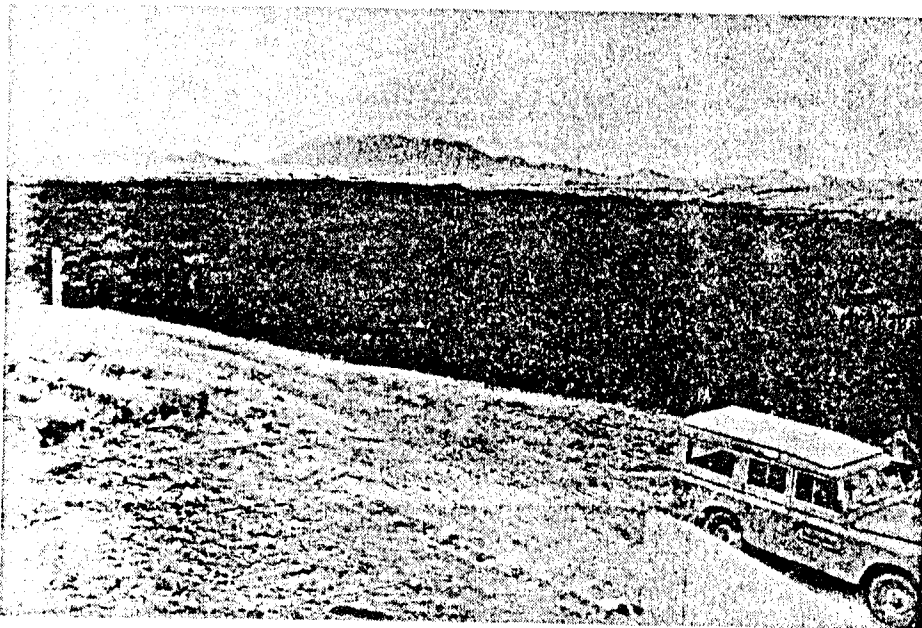
(b)



Fig. 2-6  
Backswamp and sand  
dunes  
(southern Chimbote)



(a)



(b)

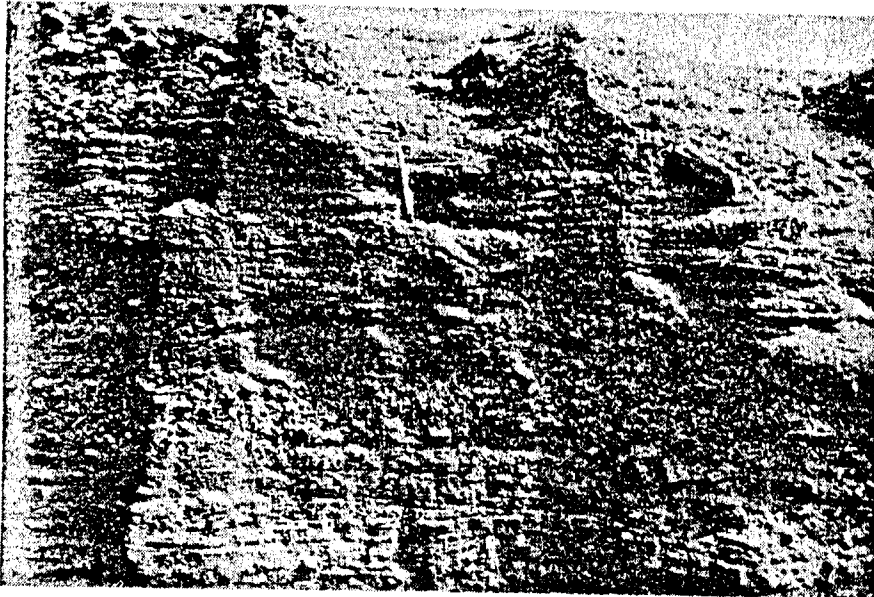


Fig. 2-7  
Sheetflood deposits,  
west of Buenos Aires.

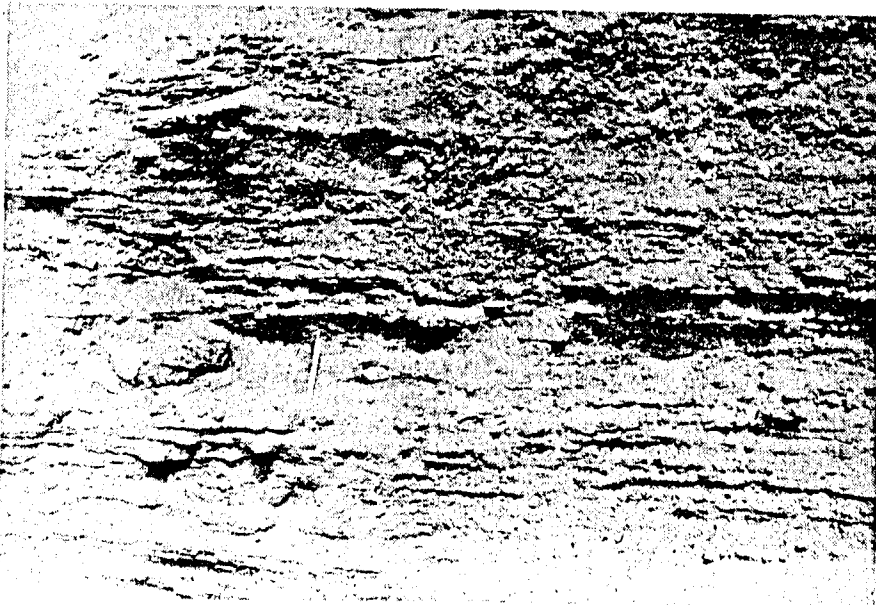
*este* ↗



(a)

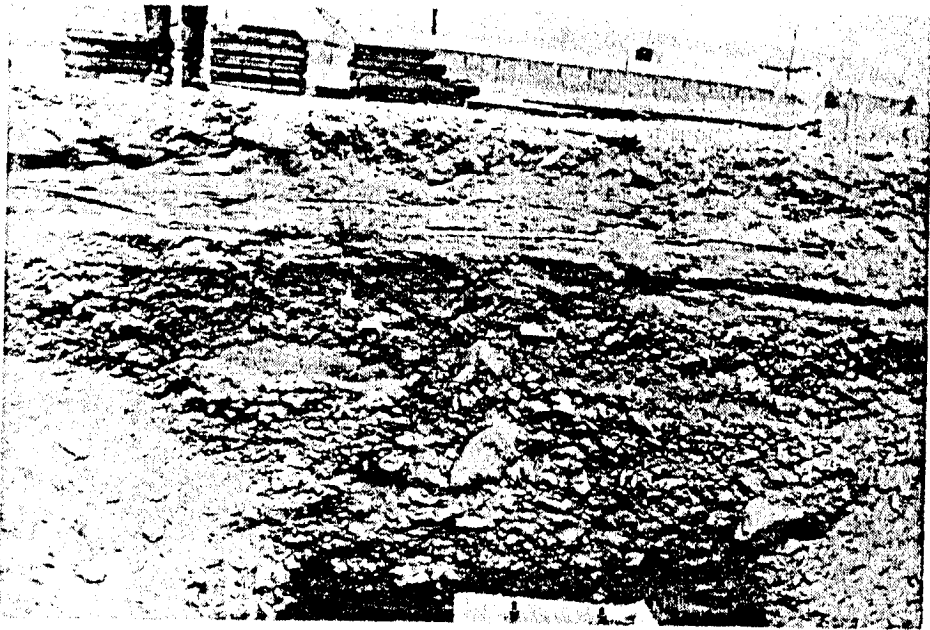


(b)

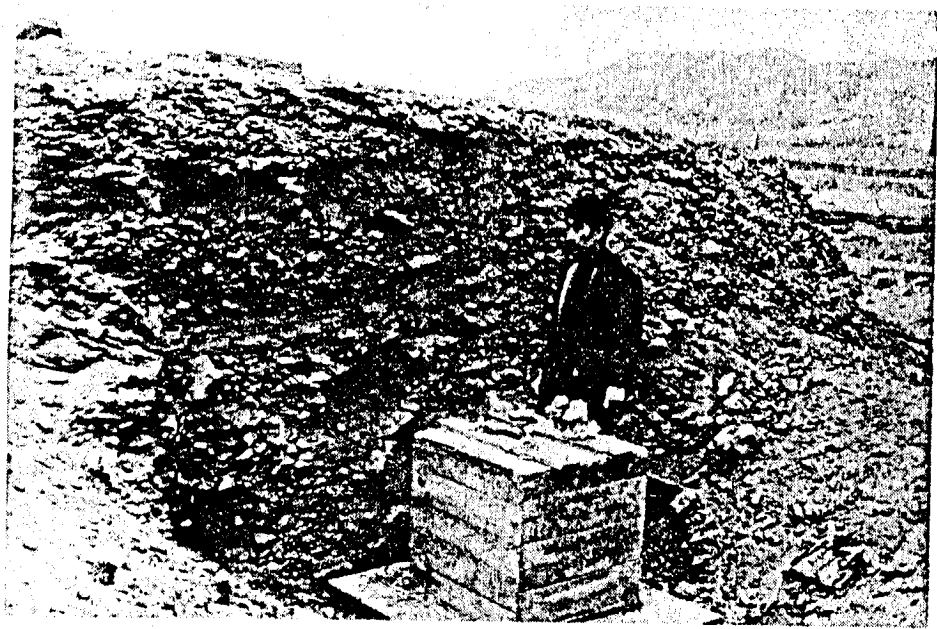


(c)

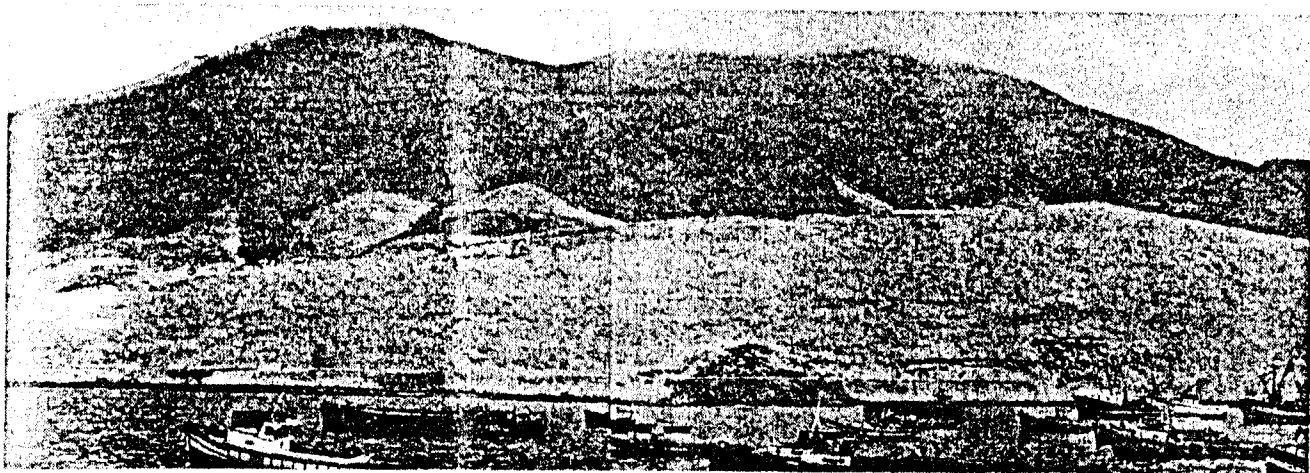
*Abancos* *Tarapaca*  
Fig. 2-8  
Sheetflood deposits  
and reworked eolian  
sands of the alluvial  
fan (B 3), south of  
Chimbote Hill.  
(Steel plant of  
Chimbote)



(a)



(b)



(a)



(b)



(c)

Fig. 2-9  
Alluvial fan, north  
of the Chimbote  
harbour, consisting  
of reworked eolian  
sands and debris  
derived from steep  
mountain-slopes  
behind.

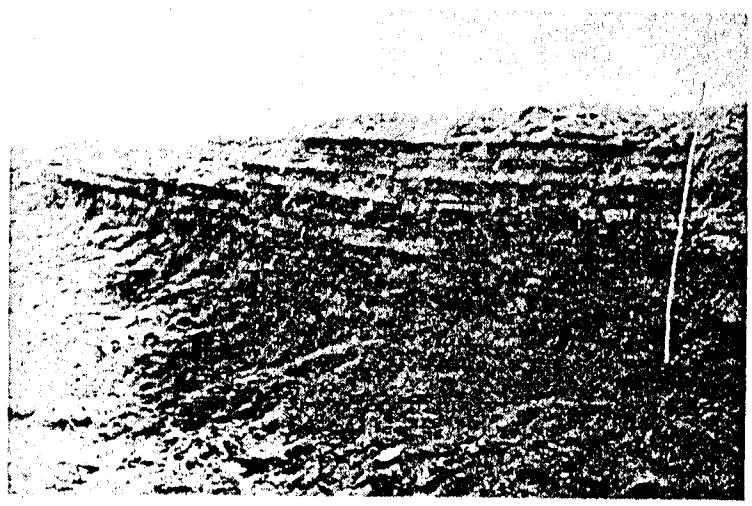
*harbour*

*debris*

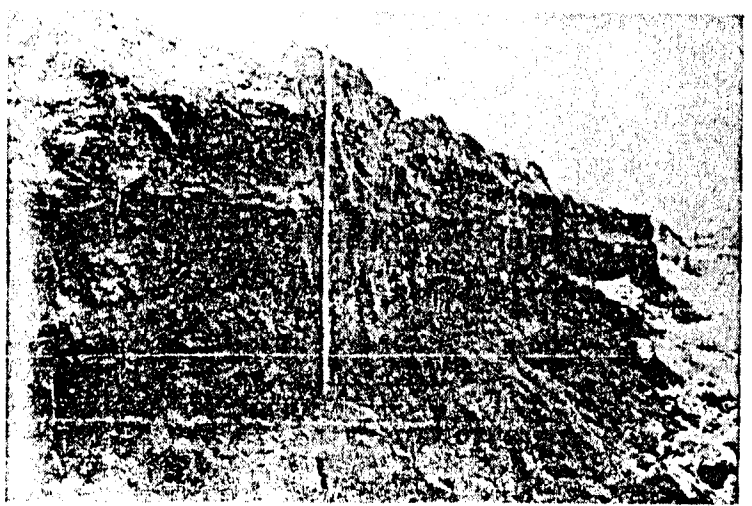


(a)

*Tamro*  
Fig. 2-10  
Soil profile along a  
trench in Jiron  
Ayacucho, Florida  
Alto. Darker layers  
are brown clay, light  
coloured layers are  
sand.  
*Alfaro*



(b)



(c)

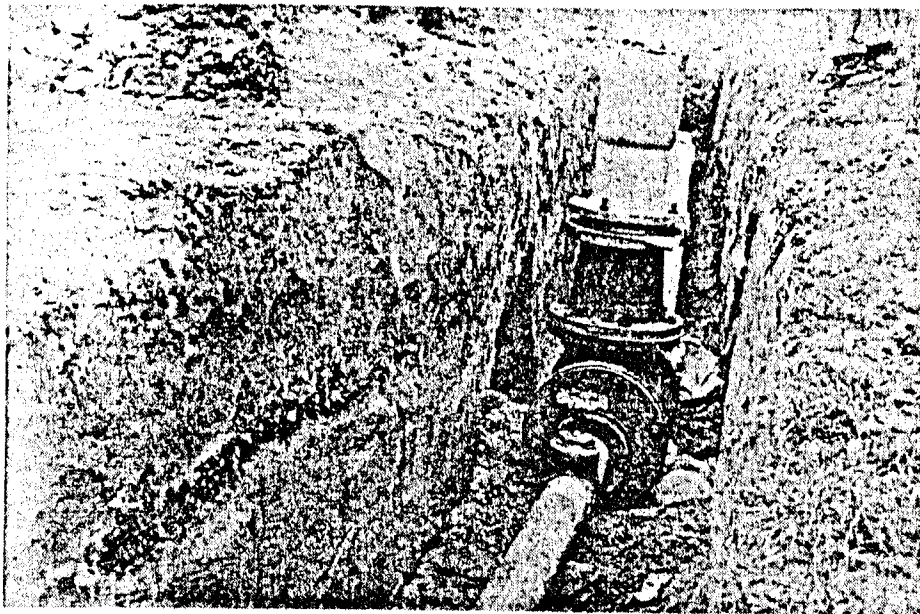


Fig. 2-11  
Soil profile at  
Servopesca on the  
Rio de Lacramarca  
alluvial plain.



Fig. 2-12  
Southern slope of  
Co Tambo Real,  
covered largely  
by old eolian sand. *Barrio*  
Houses on the slope  
are Barrio San Pedro.

### Chapter 3 Soil Conditions

To investigate the subsoil conditions, records of pre-existing borings and water-well as much as available were examined, and a total of 16 borings were made at locations as shown in Fig. 3-1. Depths of most of them were about 25 m below the ground surface. The penetration test was accompanied every one meter in each of the boreholes, counting the number of blows  $N'$  necessary for the split spoon sampler with an outer diameter of 2.5 in. to produce the penetration of a foot under the repeating impact of 210 lb x 20 in. Later,  $N'$ -values obtained by this method were compared with  $N$ -values for the standard penetration test (2 in. split spoon sampler), and it has been found that the good correlation of  $N=0.88 N'$  exists between them (Appendix 1). Additionally, hand borings were made with an auger down to depths of about 3 m to investigate the surface soil conditions and the water table. Grain size analysis was also conducted for some of samples taken by the spoon sampler (Appendix 3).

Somewhat simplified geological cross section with  $N$ -values have been constructed by Ing. C. La Puente basing on the boring records (Appendix 2), and are shown in Fig. 3.1 (a) (b).

As described in the previous Chapter, the subsoil of the Chimbote area consists mainly of a thick sandy deposit. In most parts of the area, medium dense sand deposit with  $N$ -values ranging 10 to 30 overlies the very dense sands ( $N > 50$ ) and/or gravel extending to the bedrock. The overlying sand increases in its thickness towards the sea, with thickness of 0 - 5 m in the inland and of 10 - 20 m in the coastal area. Underlying very dense sand is intervened, in some area, by layers of loose fine sand and stiff clay (No. 3 and No. 11). Bedrock is found at a depth of about 60 m at a site near No. 11 in the coastal area.

In a part of the North Port reclamation has been made by loose sand. The areas between the old sand dunes ( $C_1, C_2, C_3$  in Fig. 2-1) and other very limited areas in the city are also supposed to have been filled by sand.

The contour lines of the ground water table are shown in Fig. 3-3. The depth of the ground water has a general tendency to become shallower towards the sea, and is close to the ground surface in the coastal area and low lands, being located at depths of 1 or 2 m.

In general, sands tends to contract under a vibrating force. The ground subsidence occurred during the earthquake due to compaction of sands in a large area. Details will be discussed in Chapter 8. It is clear that the looser the sand and the greater the thickness of the sand, the greater the subsidence.

Compaction of sands which seats below the water table will be accompanied by squeezing out the pore water. It will result in a rise of the ground water and in upward water flow. From this reason, the lowlands were submerged and the ground water was observed to spout in someplaces during the earthquake.

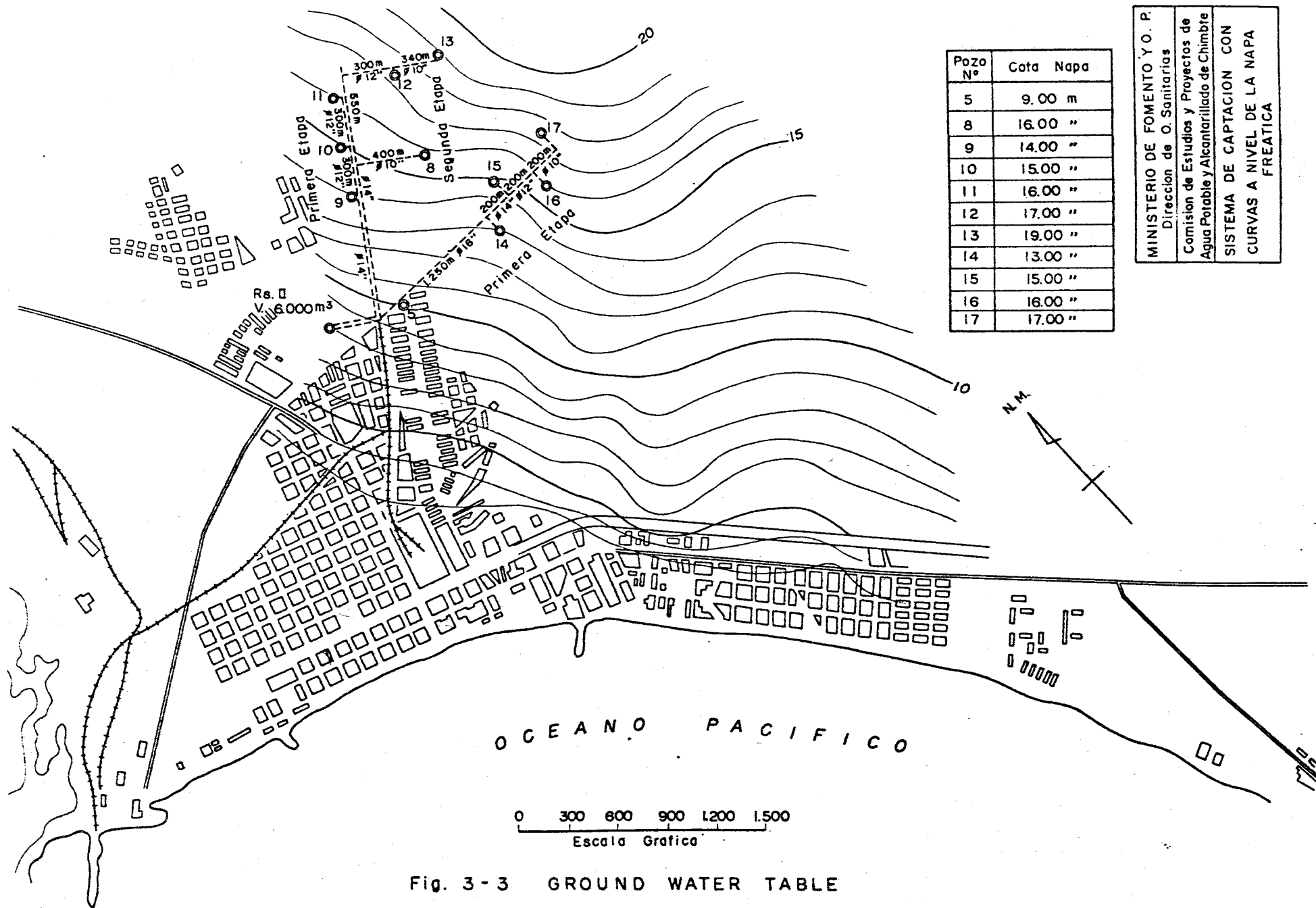
Since for a loose saturated sand a considerable amount of compaction takes place in almost undrained condition during an earthquake, the pressure of pore water increases and results in the

decrease in the shearing resistance of the sand, sometimes into a liquid state. This is known as liquefaction of sand. It is believed that a layer of loose fine sand of about 2 m thick in boring Nos 3 and 11 liquefied during the earthquake. The liquefied sand was jetted out with ground water during this earthquake. However since this type of liquefaction was limited in a layer several meters below the ground surface, no appreciable settlement of buildings was found. On the other hand, in the above-mentioned areas where the reclamation was made by loose sand, liquefaction reached near the ground surface and many buildings settled severely. It is deemed that the upward seepage flow from deeper stratum was also responsible to this type of liquefaction. Even the densest sand and gravel seating in great depths contract due to crushing of grains and possibly originate the upward water flow. Therefore, the latter type of liquefaction is likely to occur in areas where thick sand deposit exists without intervention of impervious layers.



Fig. 3-1 LOCATION OF BORINGS *Penetecr Stador*





## Chapter 4. Observations of Micro-Tremor

### 4-1 Objective of the Measurement

In general, ground surface consists of soft layers in upper parts, harder layers in deeper and under those layers, there is a hard base rock.

At the time of an earthquake, wave comes through the medium of earth from the hypocenter and when the wave appears on a ground surface, its incidental angle is almost  $90^\circ$  to the ground surface because of the difference of wave velocity mainly depending on the hardness of the layers. (Referring to Fig. 4-1). In that case, a model of the ground surface will be something like Fig. 4-2.

In Fig. 4-2, the model is considered to be two layers as the simplest case. Now assuming that the lower layer is rigid as an extreme case, the upper strata will generate the so called a natural vibration.

In reality, it is recognized that different points on the ground surface have each predominant period in its earthquake ground motion from many observed earthquake records in Japan and the theory to explain this phenomenon is called 'Multiple Reflection Theory'. Then, how the predominant period of some point on the ground can be determined.

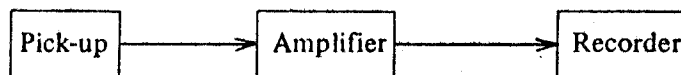
At present, many methods are used for the purpose of obtaining the predominant period, and the micro-tremor method is one of them. Micro-tremor is a vibratory phenomenon of the ground surface a few micron in amplitude even without the special exciting sources, and its frequency domain is almost 1 to 10 Hz. The cause of this vibratory phenomenon is considered to be traffic load and so on, however, details are not so clear.

This micro-tremor is generated by many sources, therefore, it would include a large amount of the natural vibration of a surface layer of the ground. Therefore, it is possible to obtain a predominant period from this micro-tremor through adequate analysis.

### 4-2 Equipment

'Micro-tremor' is very small vibration in amplitude, so a highly sensitive equipment is required.

The equipment consists of a system shown in the chart below:



Pick-up	Electro Magnetic Type
Amplifier	Transisterized Max. Sensitivity 60 DB
Recorder	Pen Oscillograph of Data Recorder

#### 4-4 The results and consideration

Measurement was made mainly midnight to avoid noise tremor due to traffic or the operation of factories. Some examples of records are represented in Appendix. Fig. A-5. The curves of predominant periods analyzed from those records are shown in Fig. A-6 in Appendix, and it is known from these curves that Chimbote area is divided into three parts from the view point of dynamic properties of ground surface. Those results were put together and the following Table 4-1 was obtained.

Table 4-1

Points measured	Predominant Periods	Maximum Periods
No. 1	0.24 (sec.)	0.66 (sec.)
No. 3	0.09	0.41
No. 4	0.09	0.84
No. 5	0.15	1.06
No. 6	0.15	0.96
No. 13	0.09	1.20
No. 7	0.28/0.90	1.71
No. 15	0.33	1.23
No. 16	0.27	1.53
No. 20	0.28	1.20
No. 21	0.28/0.33	2.0/1.16
No. 10	0.18/0.60 0.93/1.35	3.56
No. 19	0.27	1.26
No. 24	0.22	2.10

Predominant Periods from the micro-tremor measurement

Measuring points are shown in Fig. 4-3.

Divided three parts of Chimbote area are as follows:

(1) Northern parts

This area includes such villages as San Pedro, SOGESA and coastal parts connecting the hill. The predominant periods in this area are approximately 0.1 second. This shows that the base ground in this area seems to be hard and dense.

(2) Central parts

The shape of the curves in this region are slightly more flat than those in northern part and predominant periods are in the range of 0.2 - 0.3 second.

This fact seems to show that the ground surface of this area is a little soft in dynamical view point. This area is a flooded place of Rio de Lacramarea, so it seems that the thickness of an alluvial layer is more thick than in other area.

(3) Southern part

This area includes the region of Buenos Aires and connecting sandy flat place separated by the Panamerican highway, continuing to the coast.

The period - frequency curves in this area show several predominant periods and this means that surface layers in this area consists of not only one, but multiple strata in dynamical properties.

4-5 Concluding remarks

From the previous mentioned results, the following conclusion will be derived, if the surface layer would not be broken, that is, they remain in a linear range. Dynamical properties of the ground surface in the city of Chimbote will divide the city area into the previously stated three parts from the view point of their dynamical properties, and generally speaking, this area is much harder compared to Tokyo area in Japan which has 0.3 - 0.6 sec. as the predominant periods.

Main work related to the micro-tremor measurement was performed under the guidance of Eng. Victor Konno, Ministerio de Vivienda, with an assistance of several students of Peruvian National University of Engineering.

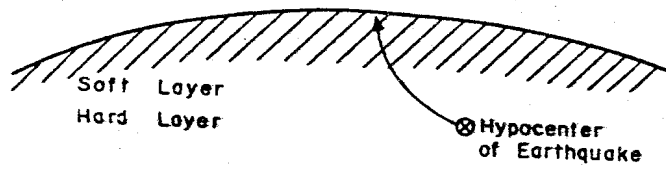


Fig. 4-1 RUNNING PATH OF EARTHQUAKE WAVE

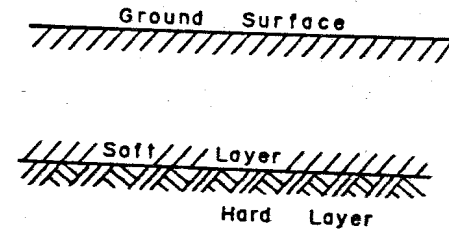


Fig. 4-2 MODEL OF GROUND SURFACE

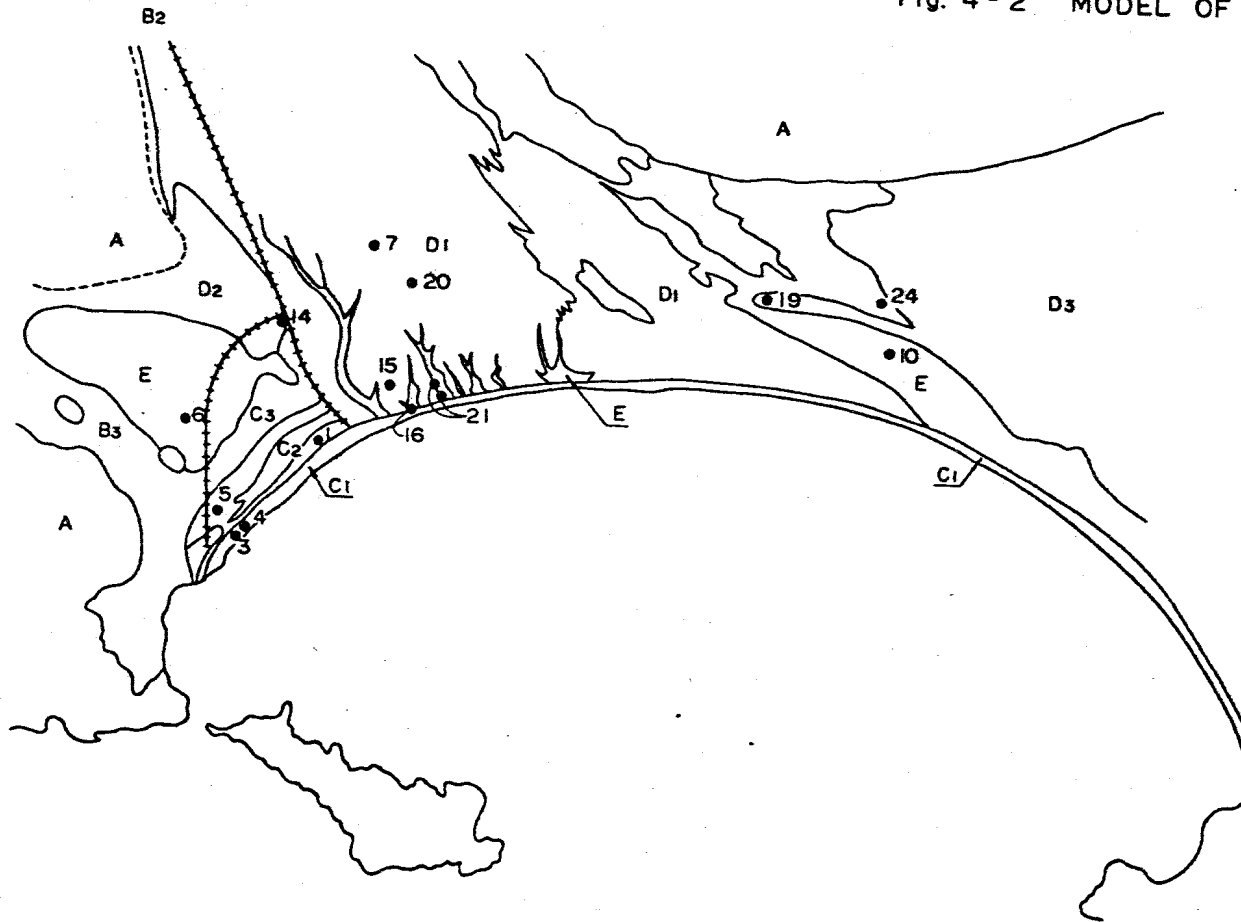
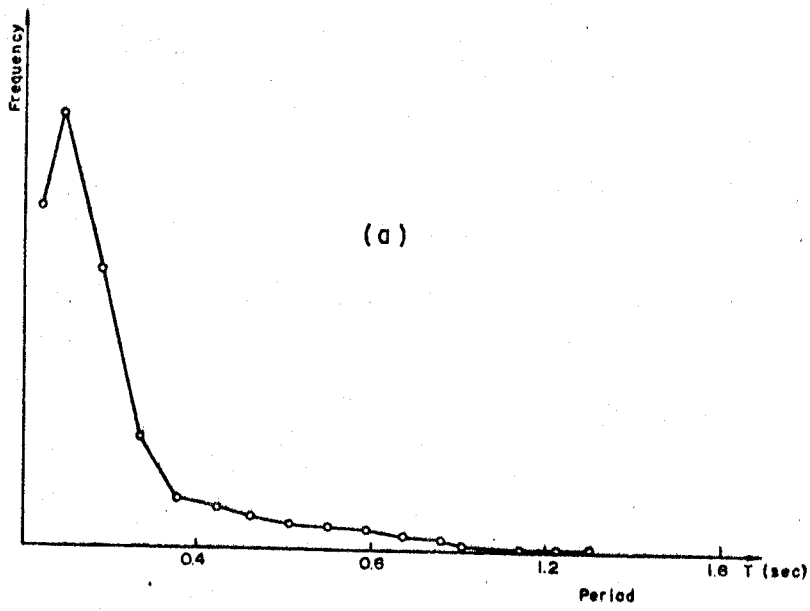
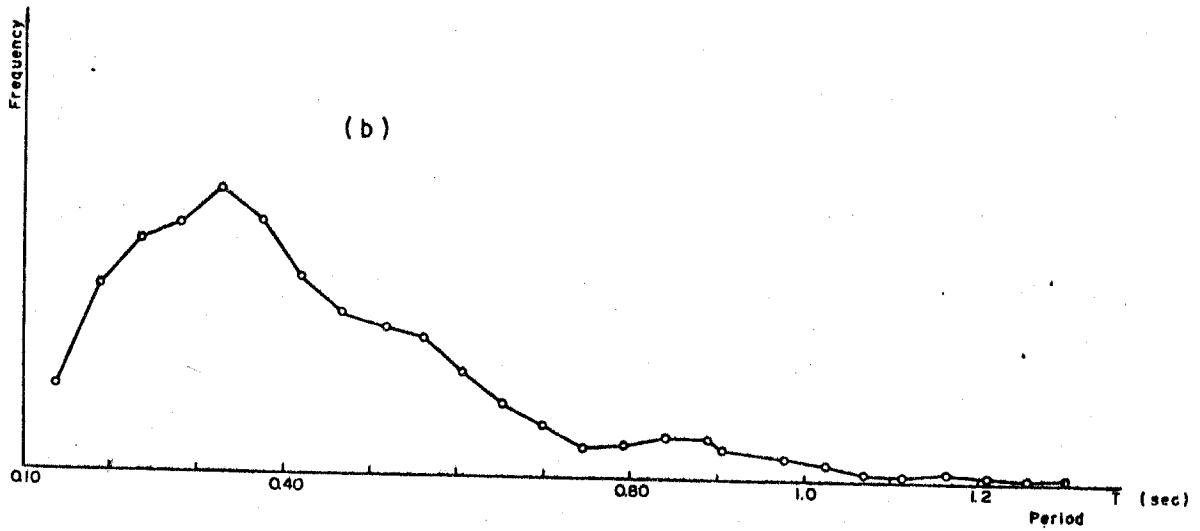


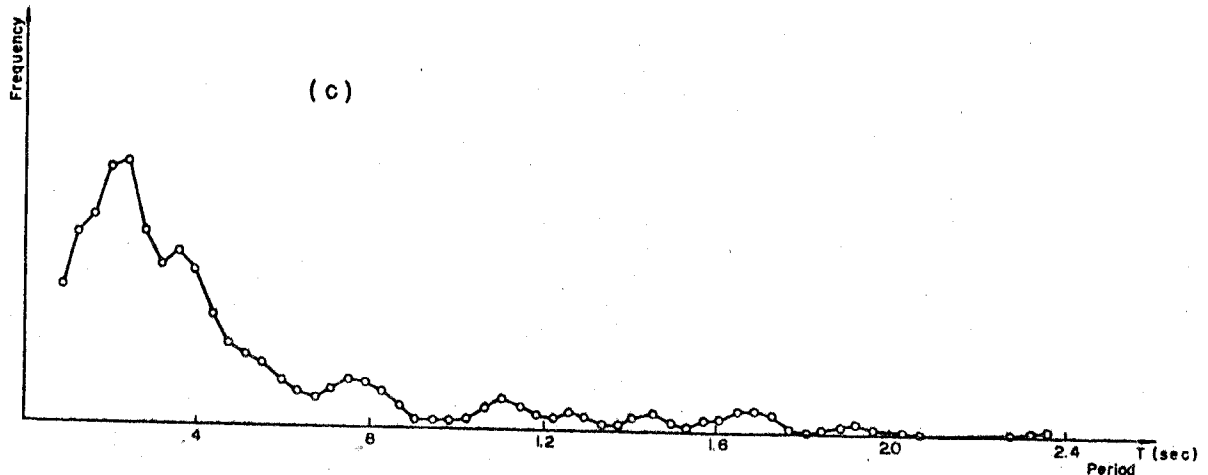
Fig. 3 OBSERVATION POINTS OF MIC TREMOR



POINT No. 13 San Pedro  
Pick No. 2



POINT No. 15  
Jr. Union - Cuadra 6  
Pick No. 1



POINT No. 24 (Barrio Villa Maria)  
Pick No. 2

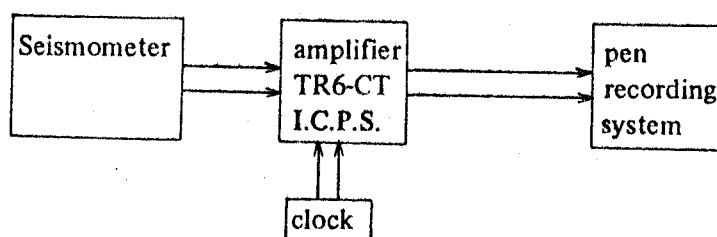
Fig. 4-4 PERIOD-FREQUENCY CURVES FOR MICRO-TREMORS

## Chapter 5. Observation of Aftershocks

The aftershocks were observed on each boring point to determine the behavior of the soil conditions in Chimbote City and also for comparison with the micro tremor results of the older destructive earthquakes experienced by the Peruvian area. For this purpose one seismic station was installed on the foundation rock basement as a reference station in Koisko, 10 km to the north of Chimbote City, and the other one was moved, from one boring point to another after recording one or two aftershocks. A total of 8 aftershocks were recorded at point 1 through point 7 installation on point 6 was not possible due to lack of facilities for ensuring the equipment). The results of the frequency period analysis show a predominant period on the short range. The amplitude ratio between the maximum amplitude of the aftershocks recorded in Koisko (foundation rock basement) and the same aftershocks recorded on the boring points (soft soil), shows that on the soft soil the amplitude decreases compared with the amplitude recorded on the base rock. This observation was made by a group of Peruvian Geophysical Institute whose leader is Ing. E. Deza.

### 5-1 Instrumentation

The two velocity type vertical seismographs used in this observation were identical. The seismometer has a natural frequency of one second (geophone type Hall & Sears). The amplifier developed by Carnegie Institution of Washington TR6-CT, has selective filters and works with a pen recording system developed also by Carnegie. The diagram below shows schematically the seismograph arrangement.



The TR6-CT amplifier has band pass filters ranging from 0.5, 1.5, 3, 6 and 20 c.p.s.; during this observation only 1.5 c.p.s. filter was used. The magnification is also selective, ranging from 0.1, 0.25, 0.5, 1.0, 2.5, 5.0, 10, 25, 50 to 100; the gain during these observations was set up from 0.1, 0.25, 0.5, 1.0, 2.5 to 5, taking always into account the fact that the amplitude of the noise must not be more than 2 mm. On each gain position, electrical pulses from 100  $\mu$ V, 200  $\mu$ V, 500  $\mu$ V and 1000  $\mu$ V, was fed into the recording system through the amplifier for measuring the recorded amplitude of the aftershock.

The system has slight damping, then, when a shock was recorded, the seismograph records besides the vibration of the soil, the natural frequency of the system.

Time was controlled by a crystal clock Toyo type.

Each time after changing the record the calibration test was done, feeding one pulse of 1.5 volts to the seismometer through the amplifier. The recording speed should be the same for both stations but it was different due to the lack of gears; anyhow the recording speed of the movil station was about

600 mm/sec, and the recording speed of the base station was almost the half (250 mm/sec).

## 5-2 The field procedure method of Analysis

After recording one or two felt aftershocks in one of the boring points the station was moved to the next point and so on. This procedure took place during 20 days, while the Koisko station placed on volcanic rock directly remained more-less the last 15 days on the same place because it was the reference station. The locations of the seismic stations can be seen on Fig. 5-1.

Two different kinds of analysis of the records were carried out, the first one was the frequency period analysis for each recorded aftershock. It was performed taking into consideration only the first 20 seconds of the shock. The zero line drawn on the aftershock record was divided in seconds; every time that the zero line crossed the recorded aftershock curve, it was counted, then the average period for each division (1 second) was easily calculated and plotted against the number of times it appears for 'p' and 'SV' waves. Analysis was made on 8 aftershocks which are shown on Table No. 1, sometimes only one peak of Predominant period was seen and other times two peaks were seen as is shown on the attached figures and also on the Table No. 2, with the exception of point 1, near Sogesa factory, where the predominant periods of 'P' and 'SV' waves are 0.22 sec. and 0.28 sec., and point 2, in the Calle Garcilazo de la Vega, where the periods are very short (for P waves 2 peaks were observed, 0.072 sec. and 0.088 sec. and for S waves, only one peak of 0.084 sec. was observed,) the other values that were from the stations 3 to 7 vary from 0.10 to 0.20, which are almost the predominant periods of the seismic waves in Koisko, the base station.

The second analysis carried out was to find the amplitude ratio between the maximum amplitude of the SV. wave recorded on soft soil and the corresponding wave in the Kosko Station. Here only 4 aftershocks were analyzed. The amplitudes were measured in uV, after getting the average value of the 1000 uV signal. The ratio changes from 1.80 to 2.80 as may be seen in Table No. 3. This would mean that, for these predominant earthquake periods in soft soil, there is absorption of the energy, or, that the parameters of the seismic waves propagation in soft soil are favorable for decreasing the amplitude of the vibration.

## 5-3 Brief Discussion

In general, it can be said as a first approximation, that the structures having short period have suffered less damage due to local earthquakes vibration when they are located on soft soil with longer predominant periods than the same kind of structures placed on comparatively hard ground, where the predominant periods are shorter.

Anyhow, it seems that the soil layers of Chimbote city are not so thick that the predominant period of the aftershocks recorded in Koisko station are almost the same for those recorded in the city of the same time. Besides, the soil layers seem to behave as a filter for the short period seismic waves, that is why brick houses built up on soft soil did not suffer so much damage.



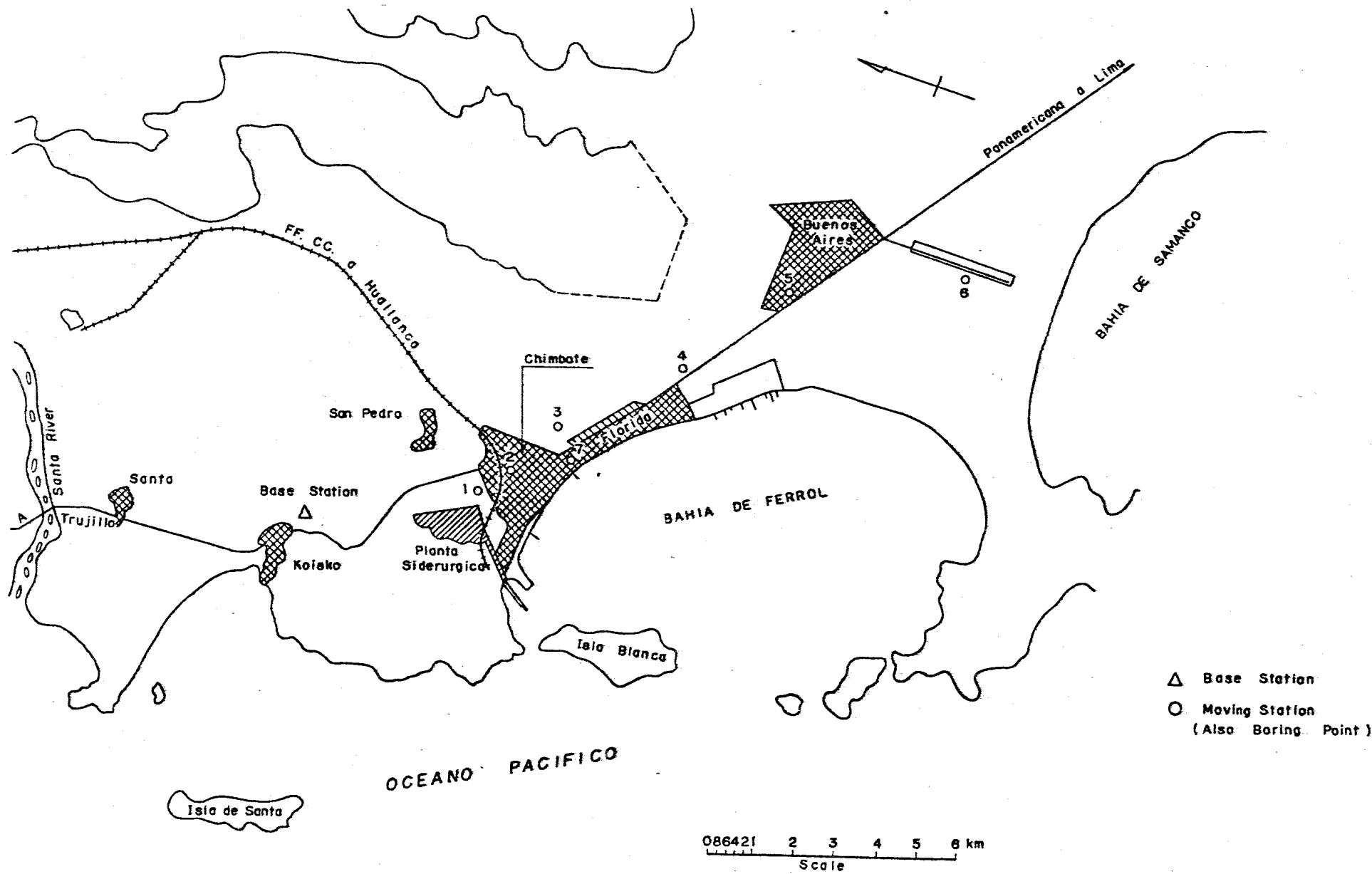
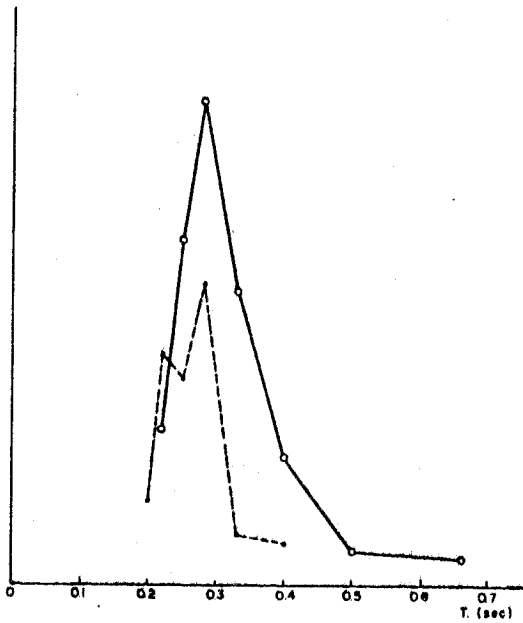


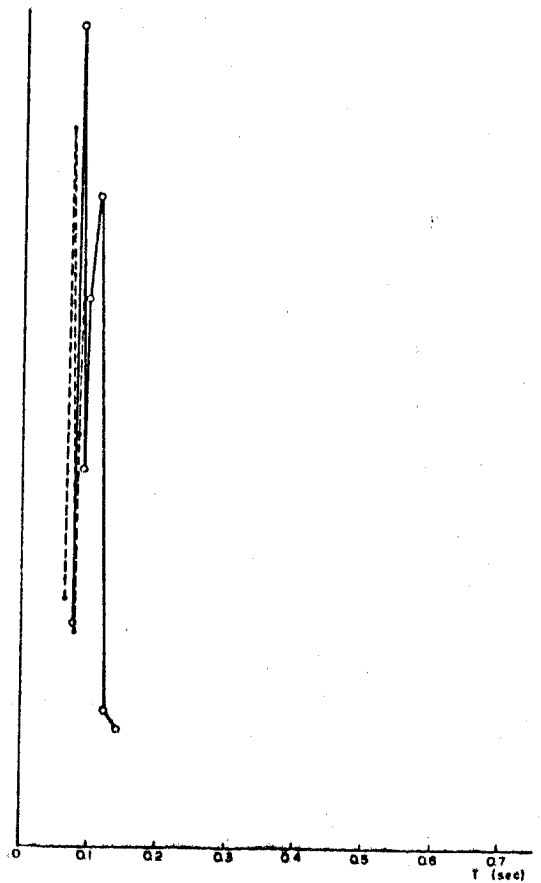
Fig. 5-1 OBSERVATION OF AFTERSHOCKS  
 LOCATION OF THE SEISMIC  
 STATIONS IN CHIMBOTE AREA



--- P Waves  
 — SW Waves

**POINT No. 1**  
 Aftershock No. 1  
 Date GMT.  
 August 07-1970 IP= 042654.3  
 Chimbote IS= 2907.3  
 Near to Steel Factory

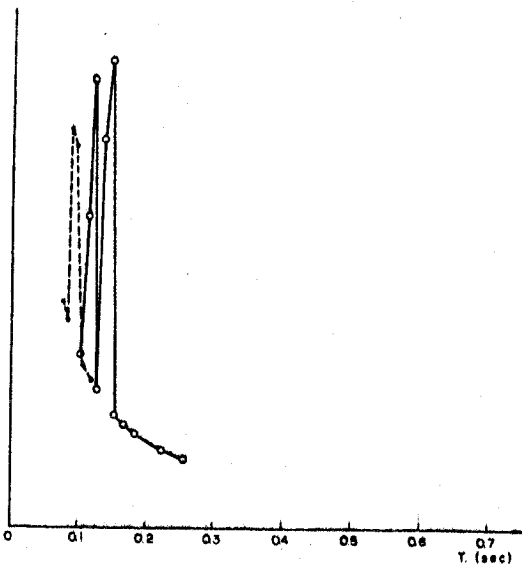
Fig 5-2 (a) PERIOD - FREQUENCY CURVE



--- P Waves  
 — SW Waves

**POINT No. 2**  
 Aftershock No. 2  
 Date GMT.  
 August 08-1970 IP= 022140.9  
 Chimbote IS= 2151.7  
 Calle: Garcilaso de la Vega

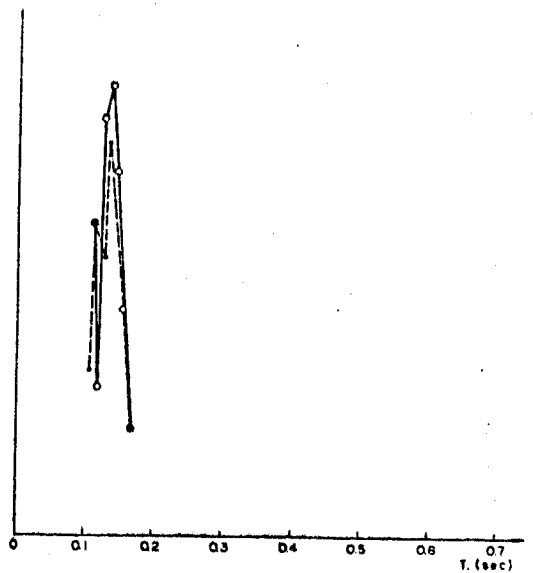
Fig 5-2-(b)



--- P Waves  
 — SW Waves

**POINT No. 3**  
 Alto Peru - Chimbote  
 Aftershock No. 3  
 Date GMT.  
 IP = 084118.7  
 IS = 4128.7

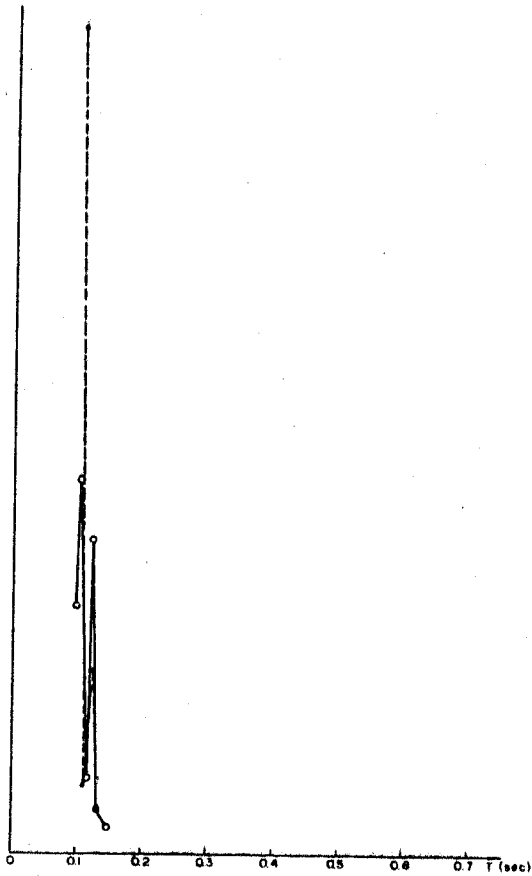
Fig 5-2-(c)



--- P Waves  
 — SW Waves

**POINT No. 3A'**  
 Alto Peru - Chimbote  
 Aftershock No. 3A'  
 Date GMT.  
 IP = 221131.4  
 IS = 1204.2

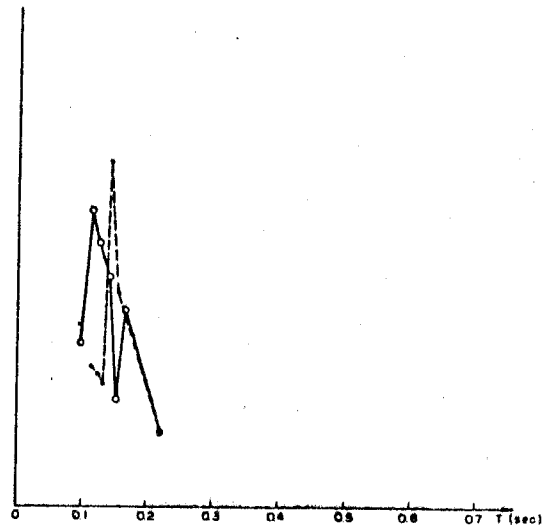
Fig. 5-2 (d)



POINT No. 3A  
 Kaitoko - Chimbote  
 Aftershock No. 3A  
 GMT.  
 IP - 221153.4  
 IS - 1206.9

--- P Waves  
 — SW Waves

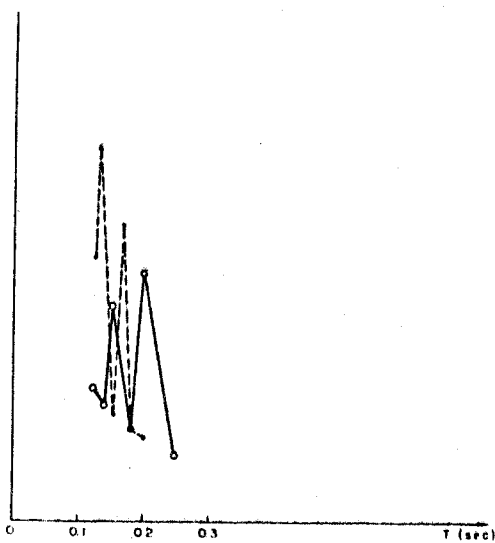
Fig. 5-2-(e)



POINT No. 4  
 Panamericana - Chimbote  
 Aftershock  
 GMT.  
 IP - 025927.8  
 IS - 5937.3

--- P Waves  
 — SW Waves

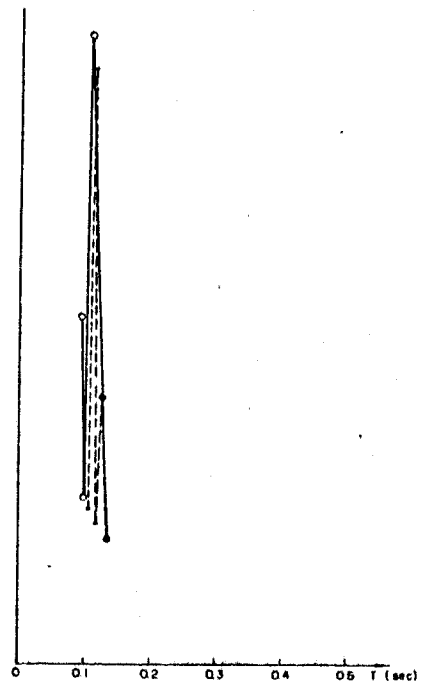
Fig. 5-2-(f)



POINT No. 4  
 Kaitoko - Chimbote  
 Aftershock No. 4  
 GMT.  
 IP - 025927.5  
 IS - 5937.0

--- P Waves  
 — SW Waves

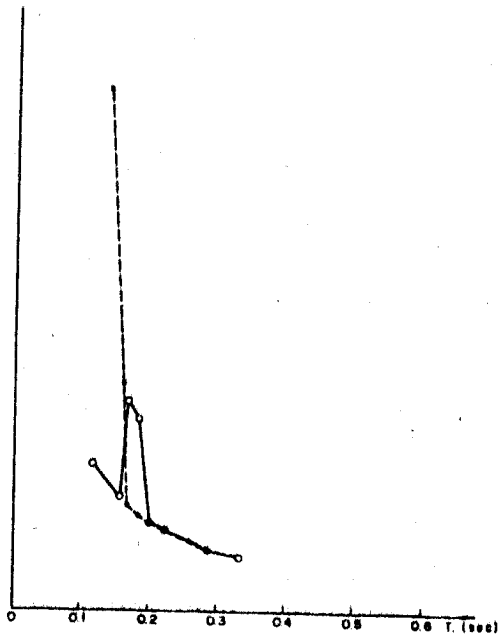
Fig. 5-2-(g)



POINT No. 5  
 Buenos Aires - Chimbote  
 Aftershock No. 5  
 GMT.  
 IP - 000832.35  
 IS - 0841.4

--- P Waves  
 — SW Waves

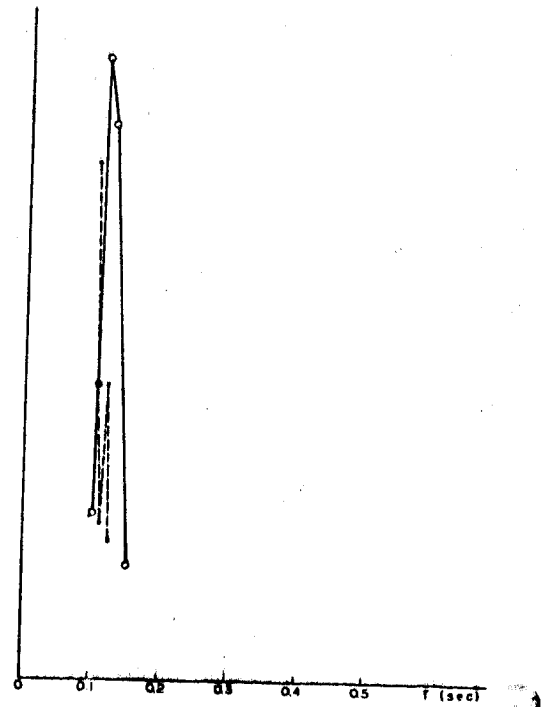
Fig. 5-2-(h)



POINT No. 5  
 Koisho - Chimbote  
 Aftershock No. 5  
 GMT.  
 IP - 000831.1  
 IS - 0839.4

--- P Waves  
 --- SW Waves

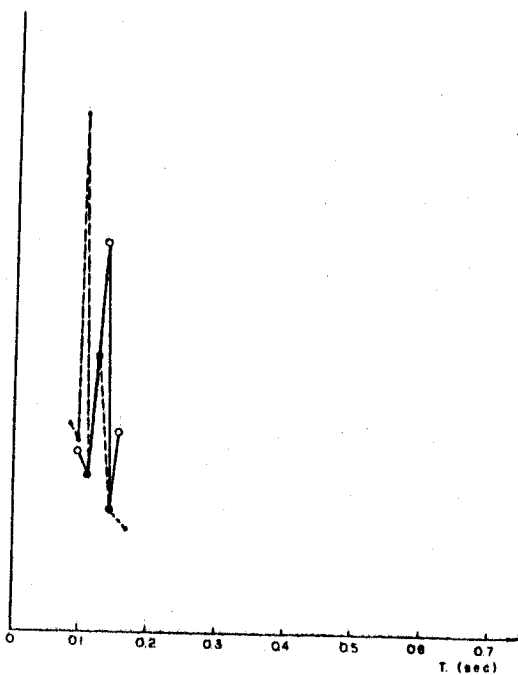
Fig. 5-2 (I)



POINT No. 5A  
 Buenos Aires - Chimbote  
 Aftershock No. 5A  
 GMT.  
 IP - 003708.8  
 IS - 2717.9

--- P Waves  
 --- SW Waves

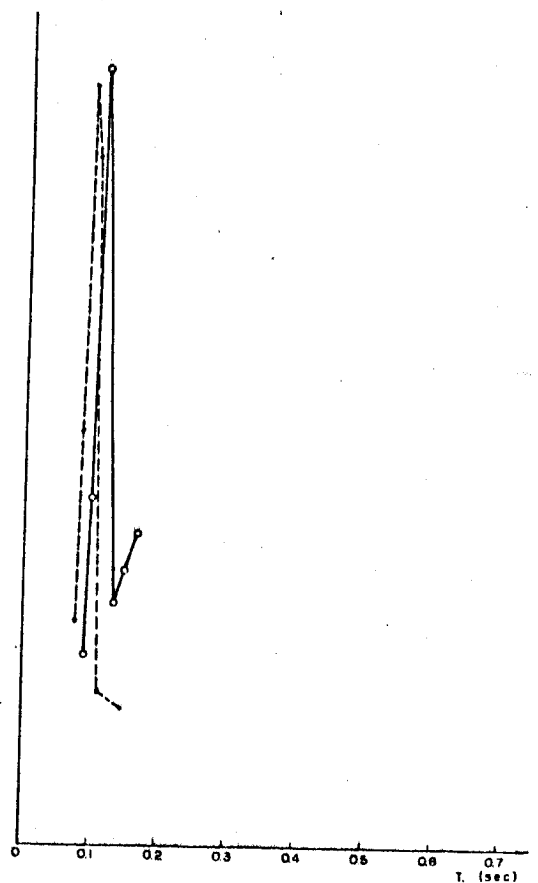
Fig. 5-2-(J)



POINT No. 7  
 Miramar - Chimbote  
 Aftershock No. 7  
 GMT.  
 IP - 212321.0  
 IS - 2332.3

--- P Waves  
 --- SW Waves

Fig. 5-2-(K)



POINT No. 7A  
 Koisho - Chimbote  
 Aftershock No. 7A  
 GMT.  
 IP - 212323.5  
 IS - 2338.2

--- P Waves  
 --- SW Waves

Fig. 5-2-(L)

Table No. 5-1 Aftershocks Recorded in Chimbote Area

Boring points No.	Movil Station Place	Date	Phase and time time GM	S-P SEC	KM.	Base Station Koisko Phase and Tj- ME GMT	S-P	KM.
1	Cerca Sogesa	06-08-70	iP 042854.3 iS 2907.3	13.0	111			
2	Calle Garcila so de la Vega	08-08-70	iP 922140.9 iS 2151.7	10.8	88			
3	Alto Peru	10-08-70	iP 964116.7 iS 4126.7	10.7	87			
4	Panamericana	15-08-70	iP 020123.5 iS 0131.3	07.8	64			
3-A	Alto Peru	11-08-70	iP 221151.4 iS 1204.2	12.8	108	iP 221153.4 iS 1206.9	13.5	116
4	Panamericana	15-08-70	iP 025927.6 iS 5937.3	09.7	84	iP 025927.5 iS 5937.0	09.5	83
5	Buenos Aires	17-08-70	iP 000832.3 iS 0841.4	09.1	79	iP 000831.1 iS 0839.4	08.3	70
7	Miramar	20-08-70	iP 212321.0 iS 2332.3	11.3	93	iP 212323.5 iS 2336.2	12.7	107
5-A	Buenos Aires	17-08-70	iP 003708.8 iS 3719.9	09.1	79	iP 003708.8 iS 3720.0	09.2	80

Table No. 5-2 Predominant Period of Aftershocks in Chimbote Area

Boring point and After-shock No.	Place	Predominant Periods in seconds				Predominant Periods Nase Rock - Koisko			
		P-waves		SV-waves		P-waves		SV-waves	
		T1	T2	T1	T2	T1	T2	T1	T2
1	near Sogesa	0.22	0.28	0.28	-	-	-	-	-
2	Garcia de la Vega	0.072	0.088	0.084	0.111	-	-	-	-
3-A	Alto Peru	0.111	0.133	0.111	0.133	0.105	0.125	0.125	0.125
4	Panamericana	0.144	-	0.118	0.168	0.132	0.168	0.154	0.20
5	Buenos Aires	0.111	0.125	0.105	-	-	-	-	-
5-A	" "	0.100	0.118	0.111	-	0.134	-	0.168	-
7	Miramar	0.100	0.125	0.132	-	0.142	-	0.162	-

Table No. 5-3 Ratio of Amplitudes of SV waves

Boring point No.	Mobile Station place	Mobile Station maximum amplitude in uV : A	Base Station Koisko amplitude in uV : Ao	Ratio $\frac{Ao}{A}$	Mangification	
					A	Ao
3-A	Alto Peru	1042	1875	1.80	2.5	2.5
4	Panamericana	2185	4650	2.12	1.0	1.0
5-A	Buenos Aires	2105	5680	2.80	0.5	1.0
7	Miramar	1724	4645	2.70	0.5	1.0

## Chapter 6. Analysis of the ground motion

### 6-1 Objective of computation

As previously stated, when an earthquake attack the city it comes upwards almost perpendicular to the ground surface. And the intensity of the earthquake at each observation point is said to be different from one another even in a small city. This phenomenon may be explained to as a kind of resonance of the ground surface layers, and in this way the theoretical background by 'Multiple Reflection Theory' may be obtained. It is from this idea that the calculation of the motion of the surface layers can be made with this theory.

Two methods are now used to apply this theory for the computation of ground motion. The difference between the two methods is the difference in the kind of Incidental wave to be considered.

The one deals with a stationary random white noise and the other an actually recorded earthquake.

The former 'white noise' procedure was developed by Prof. Etsuzo Shima, Earthquake Research Institute, University of Tokyo, and the latter 'Actual Earthquake' Method was established by Prof. Hiroyoshi Kobayashi, Tokyo Institute of Technology.

### 6-2 Response to White Noise

Prof. Estuzo Shima developed the method by considering the damping effect inside of each ground layer in the following manner. (Fig. 6-1).

A shear rigidity of a layer is represented by the following complex form.

$$G^* = G + iG' = G \left(1 + \frac{i}{Q}\right)$$

where,  $G' / G = Q^{-1}$

In case of the constant value of  $Q$ , the frequency response spectrum  $A$  of the ground surface to the white noise is calculated by the following equation.

$$A = \frac{2}{\left| \cos \frac{\omega H}{V_1} + i \frac{\rho_1 V_1^*}{\rho_2 V_2} \cdot \sin \frac{\omega H}{V_2^*} \right|} \quad (6-1)$$

where  $V_i^*$  satisfies the following relation between  $V_i$  and  $Q_i$ .

$$V_i^* = V_i \left(1 - i \frac{1}{2Q_i}\right)$$

This equation is a function of  $\omega$ ,  $H$  etc. and usually the relation between  $A$  and  $\omega$  gives the predominant period of the ground surface layer. Equation (6-1) is a formula for computing the frequency response spectrum for the case of only one surface layer upon the base rock, but the similar formula can be obtained for computing the response function of  $n$  layers on the base.

### Calculated Results

Borings were made at many points in Chimbote area and the N value distribution at each point was obtained.

As the wave propagation test was not made, the velocity in each layer must be obtained by some means or other. In Japan some experimental formulas are used to obtain the sheer wave velocity from the N value. One of them is given as follows.

$$V = 76 N^{0.36} \quad (\text{m/sec})$$

Utilizing the above formula and equation (2-1), the frequency response function of the ground surface layers may be obtained.

Several results are shown in Fig. 6-2.

### Consideration of the Computed Results

Fig. 6-2 shows the computed results. A horizontal axis represents a frequency of the incidental sinusoidal wave unity in amplitude and the vertical axis is the amplification factor of the ground surface layer, that is, a ratio of an amplitude on the ground surface to the one on the base rock. In the case of on surface layers, that is, a half infinite elastic body, this ratio is two.

Therefore, this curve is a transfer function of the surface layers.

If the incidental wave is a white noise which has a constant component in all frequency domain, above mentioned transfer function is identical to the spectral components on the ground surface.

Next, let us consider the characteristic of the transfer function curves. The beginning value of this curve on the left hand side is always 2.0 and has the predominant frequency 3-7  $H_z$  corresponding to the results of micro-tremor measurement.

If the height of the curve at the predominant frequency is bigger, the natural vibration tends to appear in the ground motion.

### 6-3 Response to Past Observed Earthquake

This method is a numerical response analysis of multi-layered ground due to actual earthquakes under the condition of shear wave propagation and each layer is parallel and horizontal.

The equation of shear wave propagation is indicated as equation (6-2)

$$\frac{\partial^2 u}{\partial t^2} = \left(\frac{\mu}{\rho}\right) \frac{\partial^2 u}{\partial x^2} \quad \dots (6-2)$$

and its solution is given by equation (6-3), which shows a propagation of shear waves.



$$u = F_1 \left( t - \frac{x}{V} \right) + F_2 \left( t + \frac{x}{V} \right) \quad \dots (6-3)$$

$$V = \sqrt{\frac{\mu}{\rho}}$$

In multi-layered soil shear waves transmit and reflect at each boundary where elastic properties are different.

The relation of waves at boundary are shown equation (6-4).

$$F_2 = \frac{2}{1 + \alpha} F_1 + \frac{\alpha - 1}{1 + \alpha} G_2$$

$$G_1 = \frac{1 - \alpha}{1 + \alpha} F_1 + \frac{2\alpha}{1 + \alpha} G_2 \quad \dots (6-4)$$

$$\alpha = \frac{\rho_2 V_2}{\rho_1 V_1}$$

After transforming the first two equations,

$$F_2 = \gamma F_1 + \beta' G_2$$

$$G_1 = \beta F_1 + \gamma' G_2 \quad \dots (6-5)$$

where,

$F_k$  is upward waves and  $G_k$  is down ward waves. Suffix 1 and 2 indicate upper and lower layer.

$\gamma$  is transmission coefficient and  $\beta$  is reflection coefficient.

In multi-layered ground shown in Fig. 6-3, equation (6-6) is obtained from equation (6-5).

In this equation suffix k indicates layer K and  $F_0$  is incidental wave..

$$G_1(t) = F_1 \left( t - \frac{H_1}{V_1} \right)$$

$$F_1(t) = \gamma_1 F_2 \left( t - \frac{H_2}{V_2} \right) + \beta_1' G_1 \left( t - \frac{H_1}{V_1} \right)$$

$$G_2(t) = \beta_1 F_2 \left( t - \frac{H_2}{V_2} \right) + \gamma_1' G_1 \left( t - \frac{H_1}{V_1} \right)$$

$$F_2(t) = \gamma_2 F_3 \left( t - \frac{H_3}{V_3} \right) + \beta_2' G_2 \left( t - \frac{H_2}{V_2} \right)$$

$$G_k(t) = \beta_{k-1} F_k \left( t - \frac{H_k}{V_k} \right) + \gamma_{k-1}' G_{k-1} \left( t - \frac{H_{k-1}}{V_{k-1}} \right)$$

$$F_k(t) = \gamma_k F_{k+1} \left( t - \frac{H_{k+1}}{V_{k+1}} \right) + \beta_k' G_k \left( t - \frac{H_k}{V_k} \right)$$

$$G_n(t) = \beta_{n-1} F_n \left( t - \frac{H_n}{V_n} \right) + \gamma_{n-1}' G_{n-1} \left( t - \frac{H_{n-1}}{V_{n-1}} \right)$$

$$F_n(t) = \gamma_n F_0(t) + \beta_n' G_n \left( t - \frac{H_n}{V_n} \right) \quad \dots (6-6)$$

From equation (6-6), all  $F_k$  and  $G_k$  at any time are determined with previous  $F_k$  and  $G_k$ .

So  $F_k$  and  $G_k$  are calculated step by step.

In equation (6-6), any kinds of dimension of  $F_k$ ,  $G_k$  are available. From equation (6-6), the ground motion at each boundary layer due to an incidental wave  $F_0(t)$  may be obtained.

#### Incidental Wave

At the time of analysis, the incidental wave must be determined. There are two kinds of waves, the one is the incidental wave for El Centro earthquake, another is the one for Taft earthquake.

Both of these incidental waves are calculated by Prof. Yutaka Osawa and Prof. Teiji Tanaka, Earthquake Research Institute, University of Tokyo, by means of previously explained 'Multi Reflection Theory' utilizing the boring data at El Centro and Taft.

#### Calculation of wave Velocity from N-Value

The best way to use the dynamite method for the purpose of obtaining the shear wave velocity of surface layers.

As there was no opportunity to use it, the following experimental formula was used.

$$V_s = 76 \times N^{0.36}$$

For computation, the average value of several similar layers is used as the velocity, and for that purpose, four or five layers are considered.

#### Computation and Results

An example of the computed motion of each layer and incidental wave are shown in Fig. 6-4.

From Fig. 6-4, it is easily recognized that the incidental wave is transformed a little after passing through each layer.

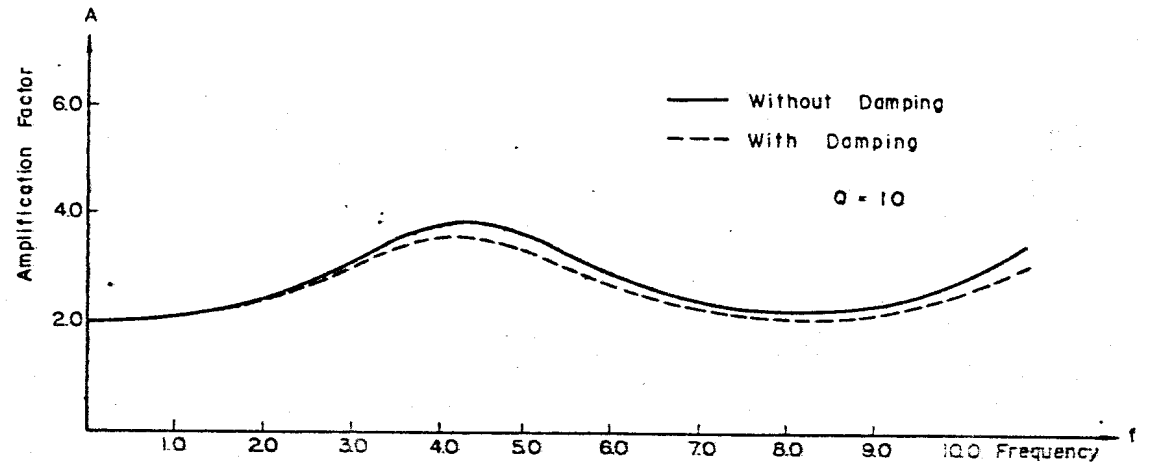
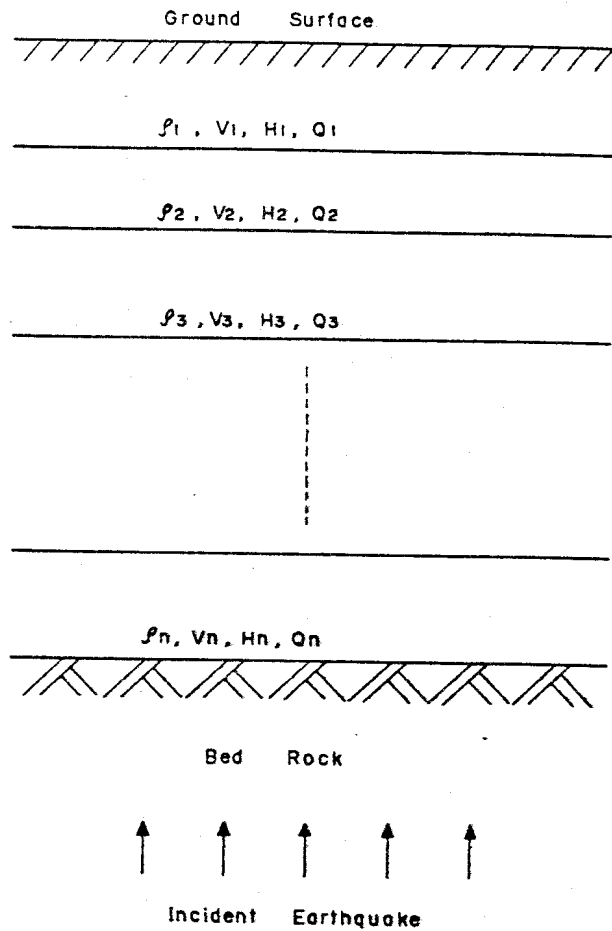
By comparing the same kinds of computed ground motion, tables 6-1, 2, have been developed. These tables show the boring number averaged N value and the ratio of the maximum acceleration of the ground surface at the boring point to the max. acceleration of the incidental wave.

#### 6-4 Consideration

Although we find a slight difference among the ratio of maximum acceleration on the ground surface to the incidental wave, all results indicate almost same value ranging from 2.0 to 3.0 shown Table 6-2. The difference depending on the incidental waves is negligible small.

The maximum acceleration of Boring No. 1 and 17 is comparatively large, this seems to be caused from that the uppermost layer of both site are soft, judging from the N-Value.

Generally speaking, the subsoil condition of the Chimbote area is very hard as a whole compared to the one in Japan, even if we can find the small difference of N-Value, for example, 23, 35 or something like that, and such a difference of N-Value under the condition of being more than 20 of absolute value would not affect on the ground surface motion.



Boring No. 2  
Fig. 6-2 (a)  
SPECTRAL RESPONSE WITH DAMPING

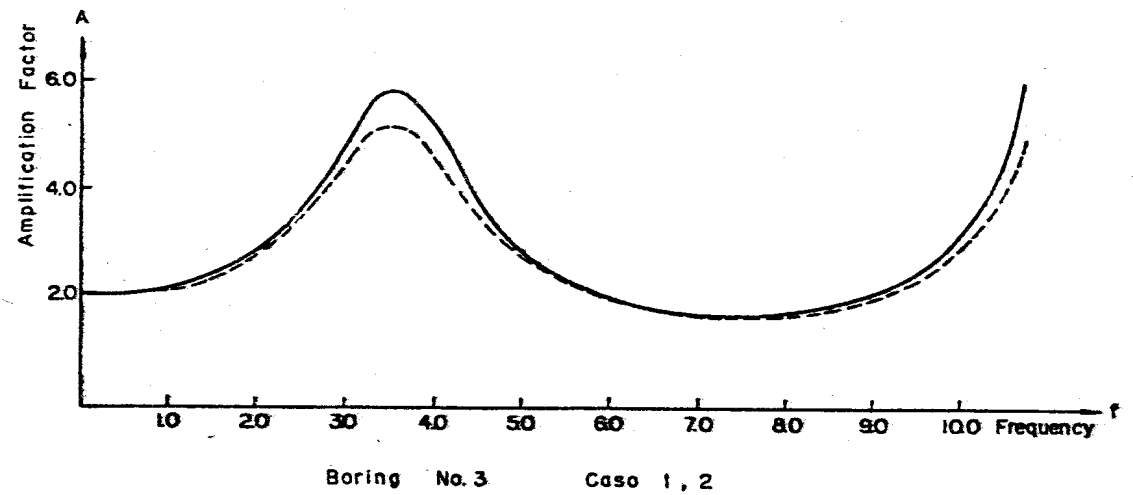
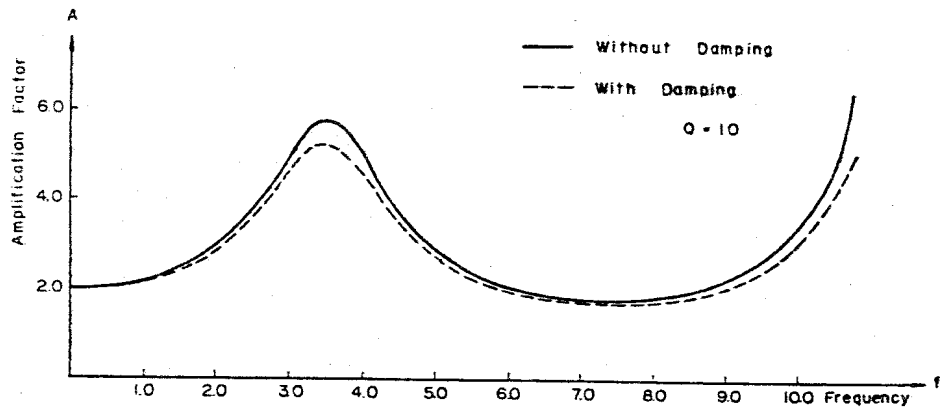


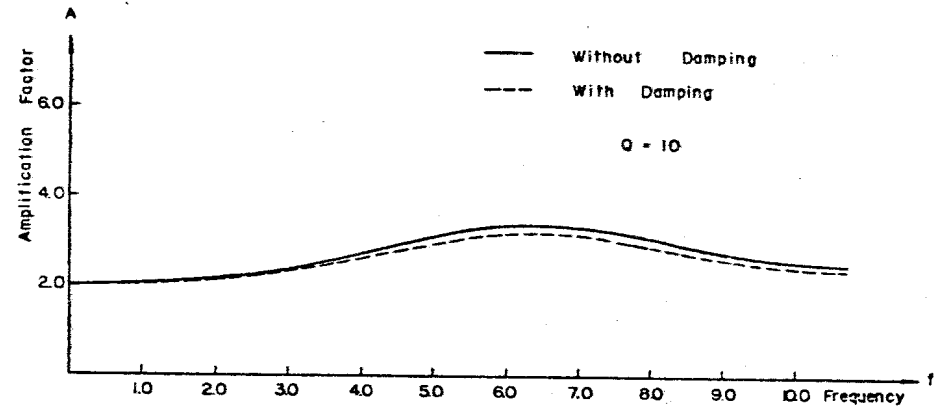
Fig. 6-2 (b)

Fig. 6-1 MULTI-LAYERED GROUND SURFACE



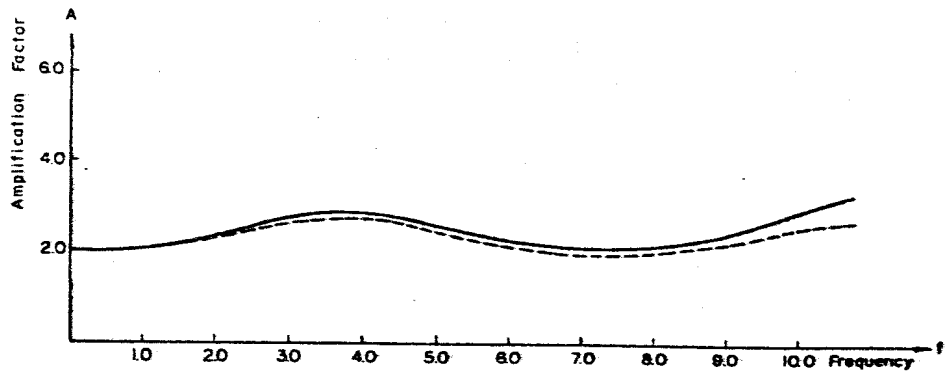
Boring No. 3 Case 3, 4

Fig. 6-2 (c)



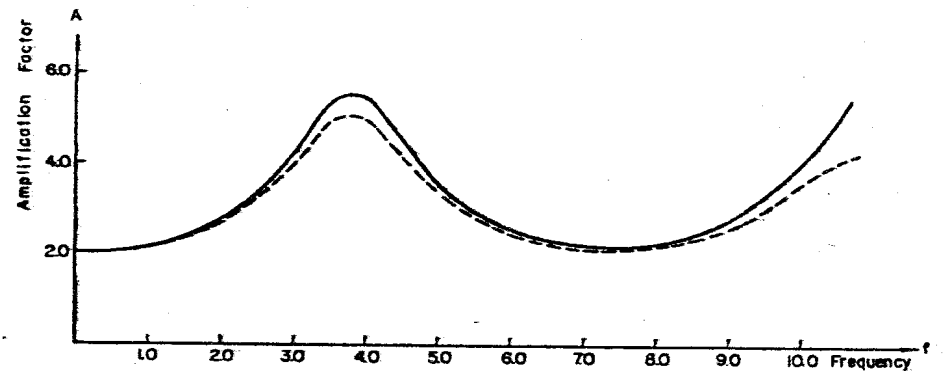
Boring No. 5

Fig. 6-2 (e)



Boring No. 4

Fig. 6-2 (d)



Boring No. 7

Fig. 6-2 (f)

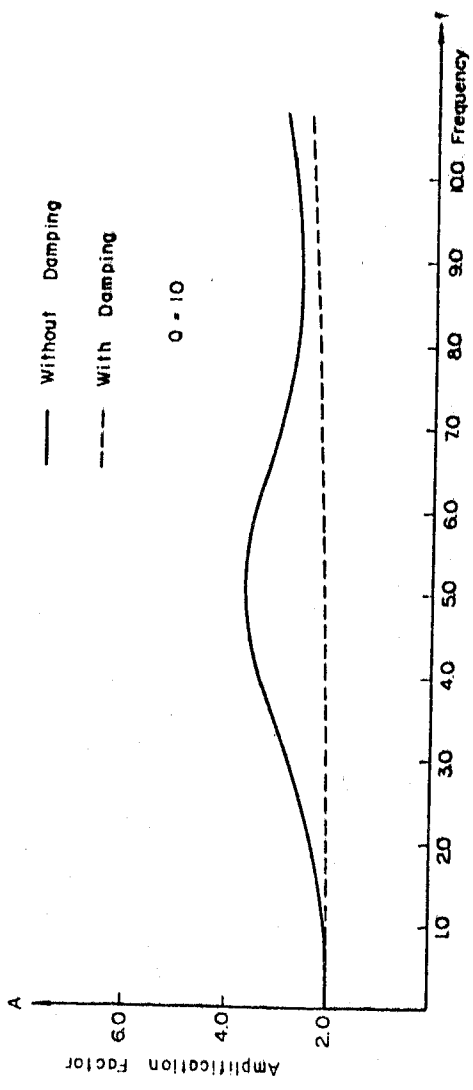


Fig. 6-2 (g)

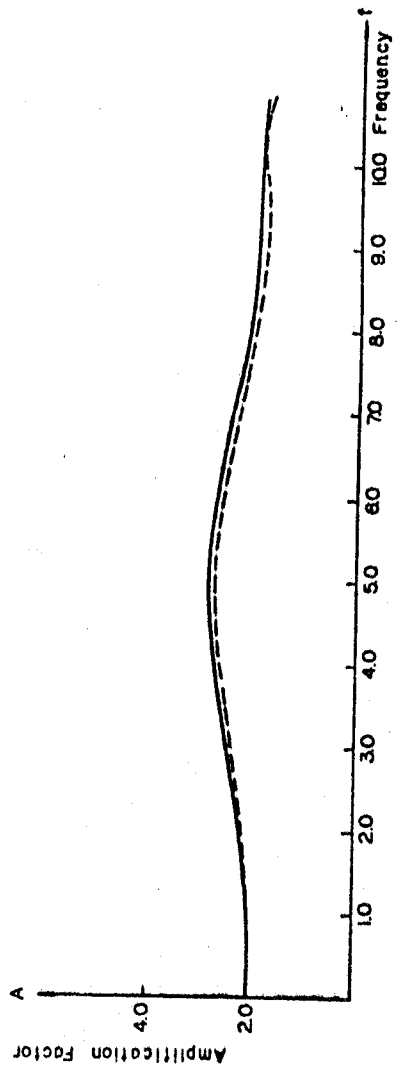


Fig. 6-2 (h)

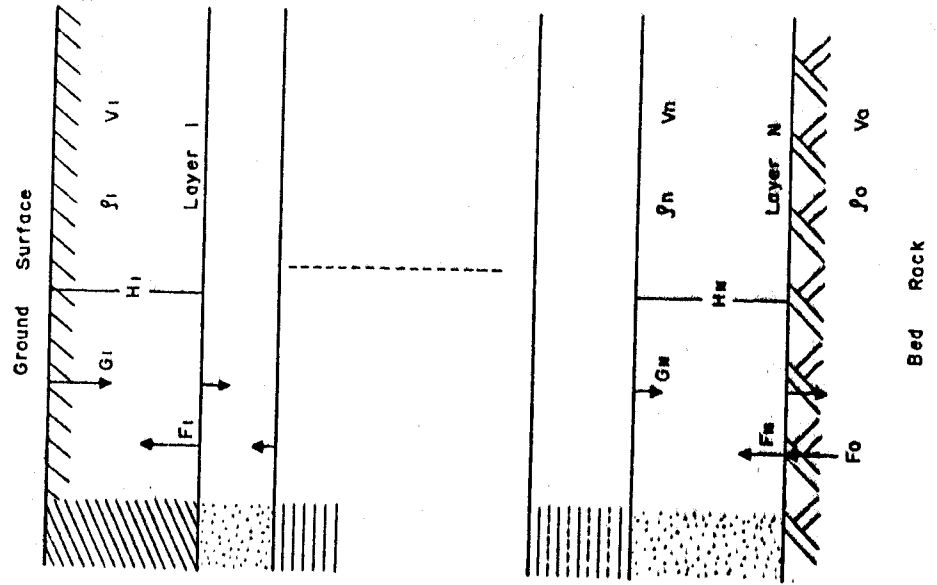


FIG. 6-3 REFLECTION IN MULTI-LAYERED SURFACE

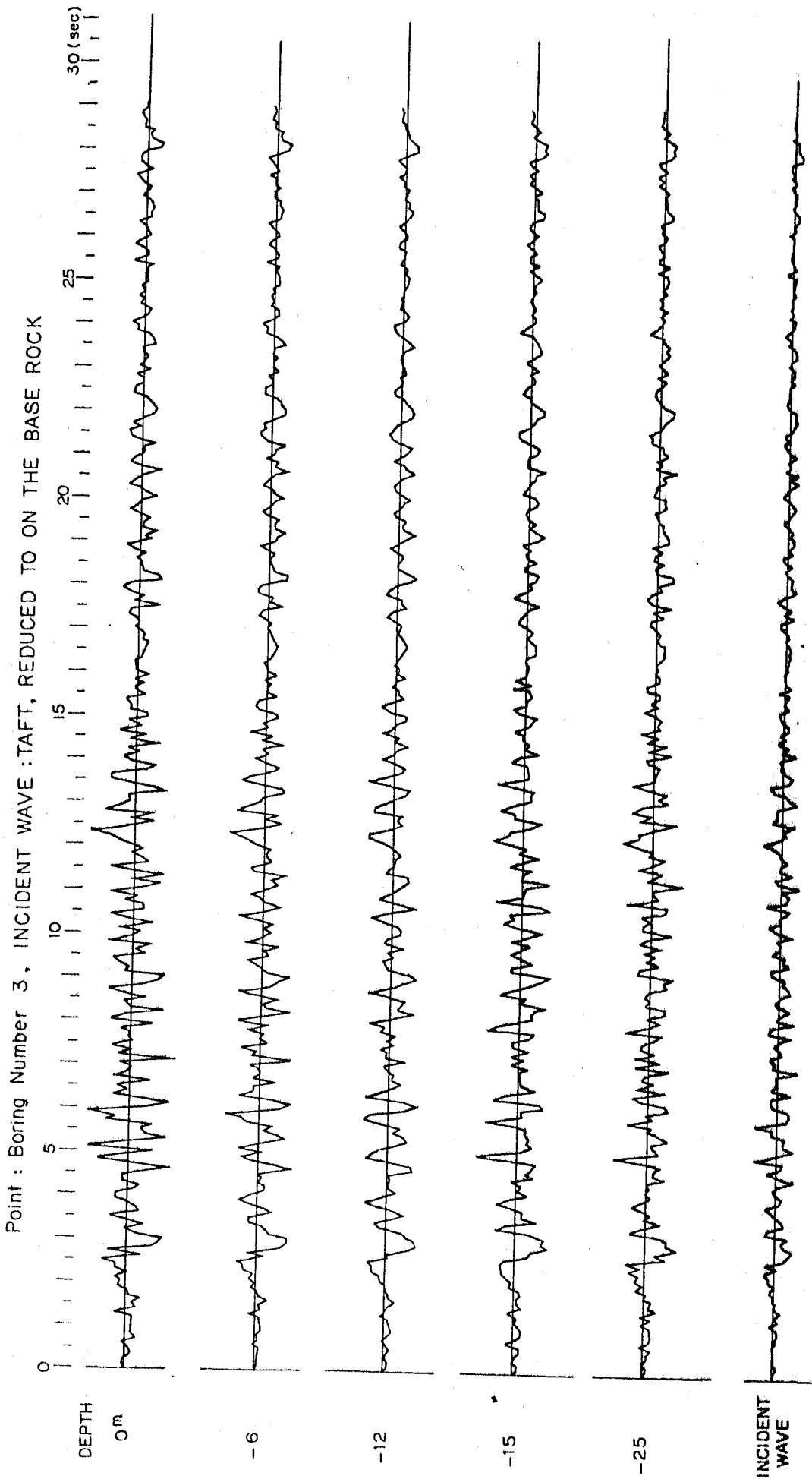


Fig. 6-4 (a) Response of Ground Surface Layers to Earthquake Input

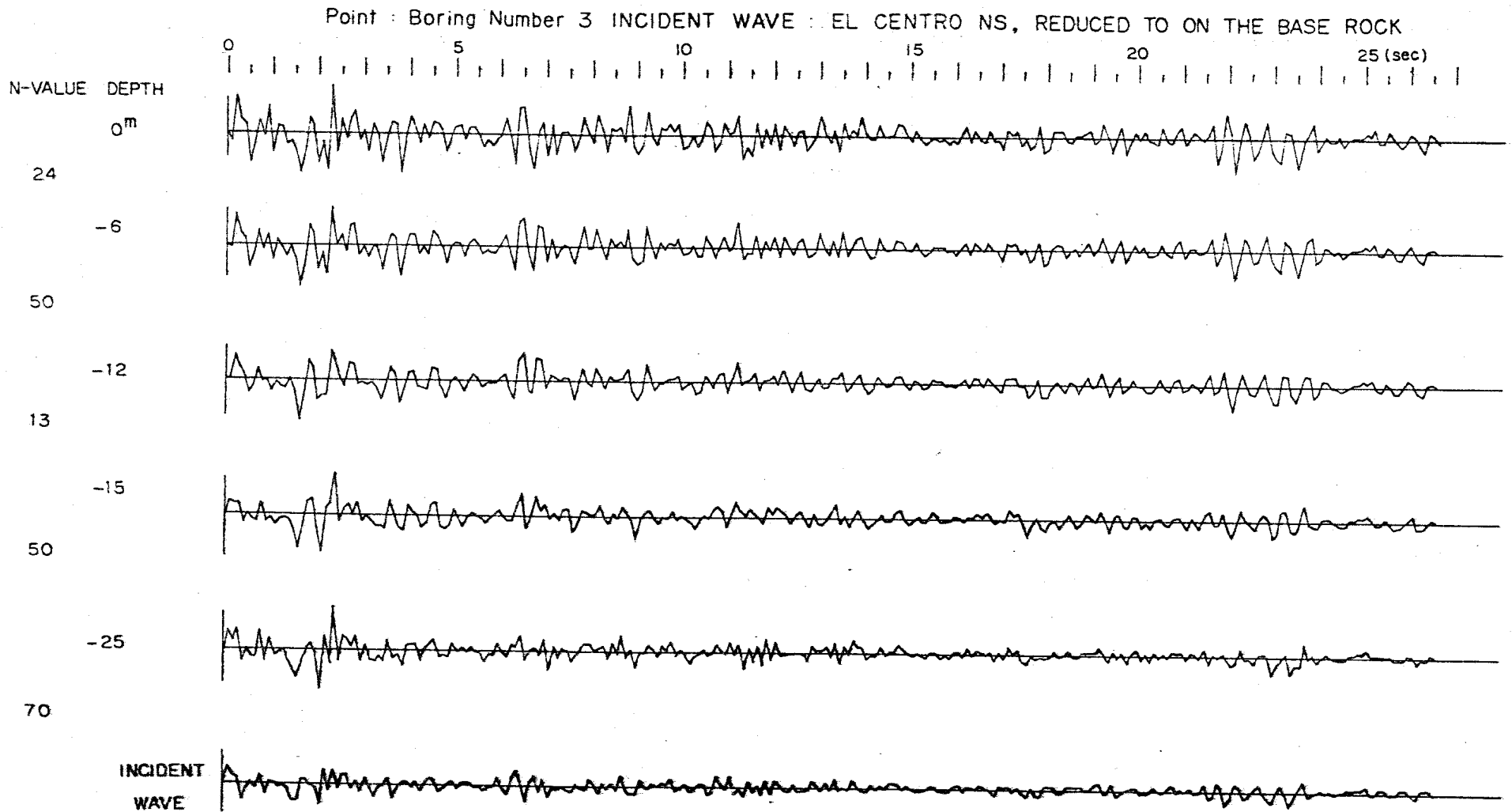


Fig. 6-4 (b) Response of Ground Surface Layers to Earthquake Input



Table 6-1 Adopted Parameters for Computation

Boring number	Density of soil ton/m <sup>3</sup>	Thickness of layer m	Averaged N-value
1	{ 2.0 2.0 2.2	3.5	6
1		21.5	50
		Base Rock	70
2	{ 2.0 2.0 2.2	3.5	30
		21.5	50
		Base Rock	70
3	{ 2.0 2.2 2.0 2.2 2.2	6.0	24
		6.5	50
		2.5	13
		10.0	50
		Base Rock	70
4	{ 2.2 2.2	25.0	50
		Base Rock	70
5	{ 2.2 2.2 2.2	5.0	50
		20.0	50
		Base Rock	70
7	{ 2.0 2.0 2.0 2.2 2.2	9.5	37
		4.0	38
		5.0	38
		6.5	50
		Base Rock	70
8	{ 2.0 2.0 2.2 2.2 2.2	6.0	32
		4.23	37
		6.22	55
		8.55	70
		Base Rock	70
11	{ 2.0 2.2 2.0 2.2 2.2	5.5	36
		4.5	47
		2.3	31
		12.7	46
		Base Rock	70
17	{ 2.0 2.2 2.2 2.2	2.0	5
		3.0	44
		20.0	70
		Base Rock	70

Table 6-2 Ratio of Max. Acceleration of Ground Surface to Max. Acceleration of Incidental Wave

	Max Acc.	Ratio of Max. Acc. of Ground Surface to Max. Acc. of Incidental Wave
<b>El Centro Incident Wave</b>	<b>-55.77</b>	
Boring No. 1	-187.15	3.35
2	-128.58	2.31
3	-138.73	2.49
4	-118.91	2.13
5	-119.14	2.14
7	-135.76	2.43
8	-142.76	2.58
11	120.13	2.15
17	-156.91	2.80
<b>Taft Incident Wave</b>	<b>-33.46</b>	
Boring No. 1	-85.81	2.57
2	-70.88	2.12
3	-69.17	2.07
4	-68.89	2.08
5	-68.86	2.06
7	-73.69	2.21
8	-79.54	2.38
11	-70.51	2.11
17	-71.95	2.15

## Chapter 7. Survey on Damage to Buildings

The buildings damage survey at Chimbote were made in August 1970 (5th to 23rd) under a leadership of Prof. Julio Kuroiwa. The results are as follows according to him:

The buildings located at the Casco Urbano (Downtown Chimbote that include 42 blocks) were checked in detail, using special filling forms for each construction. The data were classified using a computer.

Because of the time limitation, it was not possible to study in such a detail the rest of whole city, so the attention were concentrated in the settlements and the damage of three types of buildings: adobe houses, brick constructions with frames and brick constructions without frames. The result is included in Table 7-1 and Figs. 7-1, 7-2, 7-3, basing on the statistical estimation from taking average of randomly chosen blocks in each area. In Fig. 7-2 is shown the distribution of settlement of buildings in the center of the city.

From Table 7-1 it is evident that the destruction of adobe houses have been severe, ranking from 100 % at San Pedro to about 80 % in Pensacola. It is interesting to point out that in Pensacola the land is flat and the adobe houses have 'good' concrete foundation.

The brick construction with frame have suffered moderate damages, from 10 % at Antonio de Mayolo and other places to about 30 % at Los Pinos and at Buenos Aires (Fig. 7-1).

It was found that two stories constructions of the same type were damaged more severely at Los Pinos (30 %) than at La Caleta (10 %). At Antonio de Mayolo there were found seven blocks of one story brick constructions with practically no damages but there were moderate amount of settlement.

The brick constructions without frames have suffered severe damage. More than 70 % of this type of buildings were damaged so that they became impractical to repair. At Buenos Aires there is a group of houses of this type that have been completely destroyed.

At Laderas del Norte there are two types of one story brick construction (about 50 of each type). In the first model, the columns confine the facade wall very well but in the second one, since the facade is not in the same plane, the column do not confine one side of the wall. The second type of facade was almost completely destroyed, but the damages to the first type were moderate.

It is interesting to point out that cantiliver walls at Laderas del Norte, Los Pinos and at Buenos Aires have suffered more severe damages than in the other places. From the damage observation at Chimbote area it became evident that buildings designed correctly and constructed carefully have suffered negligible damages. If in the future buildings are designed and constructed carefully with consideration on Earthquake Engineering principles, the lost of lives and property will be substantially reduced.

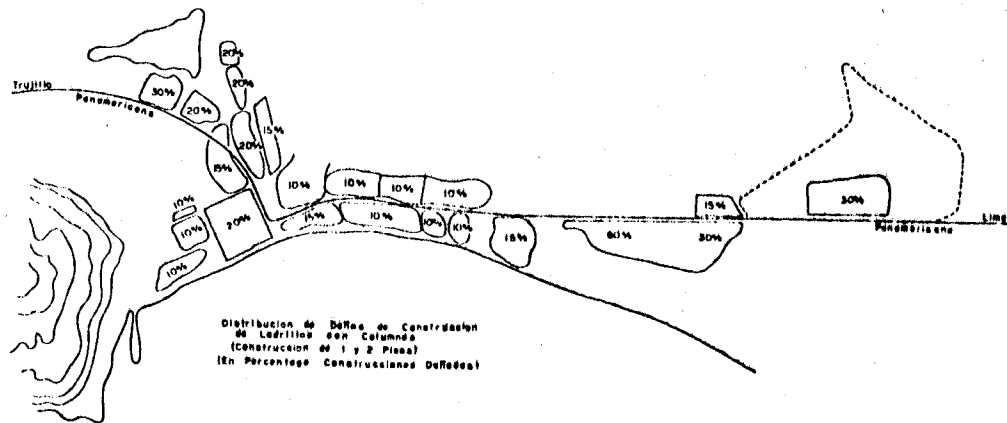


Fig. 7-1 DAMAGE DISTRIBUTION OF BRICK CONSTRUCTION WITH FRAME (1 & 2 STORIES HOUSES, IN PERCENTAGE OF DAMAGED BUILDINGS)

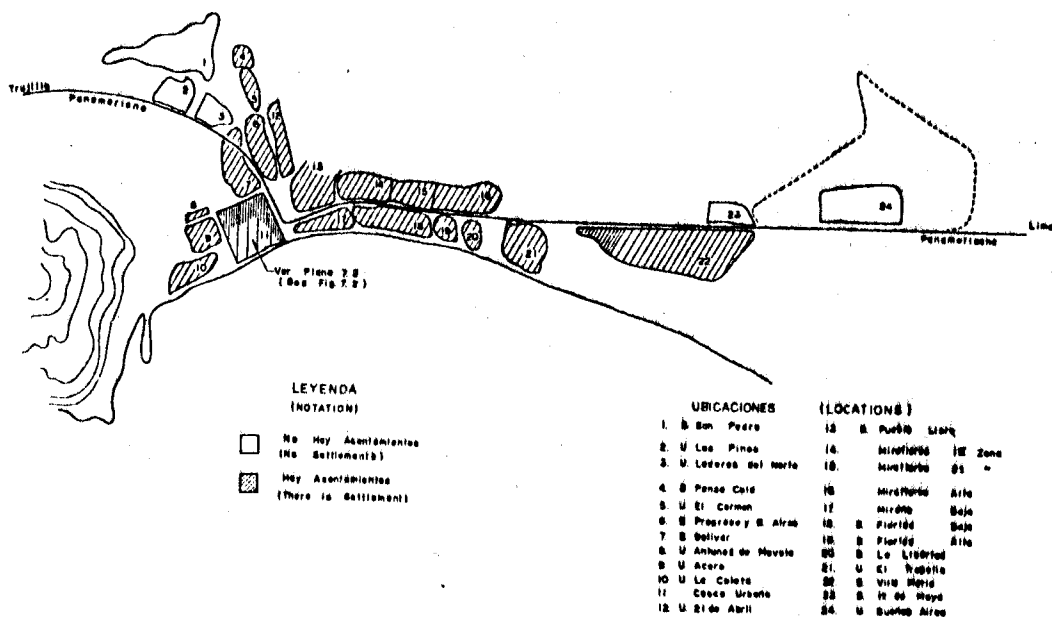


Fig. 7-2 DISTRIBUTION OF PERCENTAGES OF SETTLED BUILDINGS

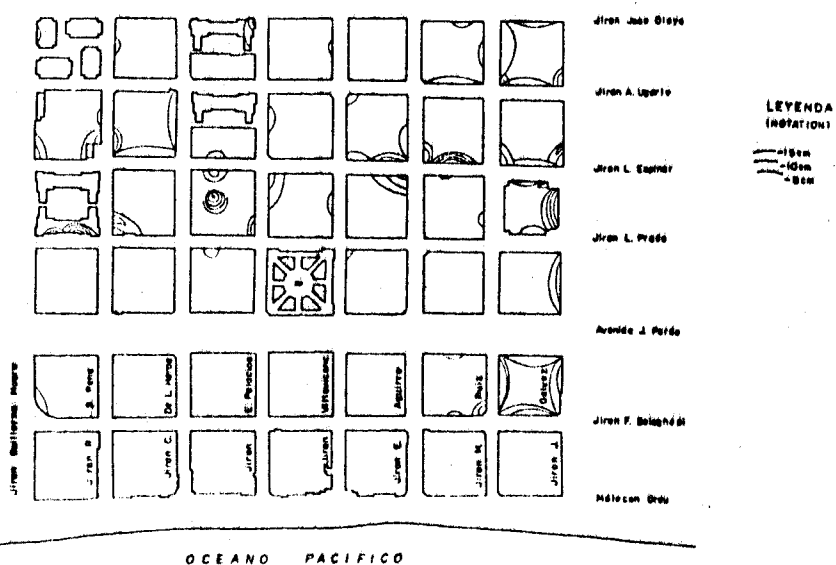


Fig. 7-3 DISTRIBUTION AND AMOUNT OF SETTLEMENT AT THE CENTER (DOWNTOWN) OF THE CHIMBOTÉ CITY

Table 7-1 Damage to Constructions

Ubicación (Location)	Asent. (Settl)	Tipo de Construcción (Construction type)			Comentarios (Comments)
		Adobe	LCC	LSC	
1	No	100%	-	-	
2	No	-	30%	-	
3	No	-	20%	70%	L.S.C. -Pano confinado en un solo lado (Ver foto)
4	Si(Yes)	80%	20%	-	(span confined only at one side)
5	Si(Yes)	-	20%	-	
6	Si(Yes)	80%	20%	-	
7	Si(Yes)	90%	15%	-	
8	Si(Yes)	-	10%	-	Casas de 1 piso construidas masivamente (one story houses of the same type)
9	Si(Yes)	100%	10%	-	
10	Si(Yes)	-	10%	-	Casas del mismo tipo que el area 2
11	Si(Yes)	90%	20%	-	Casco Urbano (Down town)
12	Si(Yes)	-	15%	-	
13	Si(Yes)	90%	20%	70%	
14	Si(Yes)	90%	10%	70%	
15	Si(Yes)	90%	10%	70%	
16	Si(Yes)	90%	10%	70%	
17	Si(Yes)	95%	10%	60%	
18	Si(Yes)	100%	10%	60%	
19	Si(Yes)	-	10%	70%	
20	Si(Yes)	-	10%	60%	
21	Si(Yes)	-	15%	-	
22	Si(Yes)	-	30%-90%	-	30% en el extremo sur y 90% en el extremo norte (30% at the south end and 90% at the north end)
23	No	-	15%	60%	
24	No	-	30%	85%	

L.C.C. = Ladrillo con columna (Brick with frame)

L.S.C. = Ladrillo sin columna (Brick without frame)

8-1 Damage in the Rio de Lacramarca alluvial plain

The most significant effect of the May 31, 1970 earthquake in this area was ground cracking which was associated with extrusions of water and sand (Figs. 8-2, 3, 4 and 5). The extrusions resulted in numerous 'sand volcanoes' which straddled the cracks in the ground. Distribution of the sand volcanoes and cracks are shown in Fig. 8-1. basing on the investigation made by J. La Cruz and V Taype. They appeared most commonly in the middle of this alluvial plain, particularly in the cultivated fields between San Jose and Clementia and around the Cucalda along the Camino Peru. In these areas, several water-wells were destroyed either by subsidence or tilting of concrete pipe (Figs. 8-6b and 6c) or by bending of steel pipe in the well. The railway was destroyed by wavy deformation of the ground (Fig. 8-6a).

The cracks were open fissures, both side were of the same height. However, the cracks which were formed on gentle slopes at the margin of the alluvial plain showed displacements by stepping downslope. Even in this case, no bulging such as seen commonly at the terminal part of landslides were observed. With the cracking, a vast amount of water temporary covered the ground. These features indicate that the cracks are of tensional nature and are caused by compaction of alluvial deposit. The large amount of water resulted from shaking and readjusted of particles which in turn resulted in smaller pore spacing and resulted in the compaction of the underground deposits.

Neither settlement nor tilting of houses (mostly of adobe) was observed in this area.

8-2 Damage to beach and dune areas

Collapse of sand dune by seismic vibration and crackings associated with the subsidence of the nearby ground occurred (Figs. 8-7b, c and 8-8b), e.g. cracks observed in the sand dune area at Tres Cabezas in the southern Chimbote, where cracks appeared along the margin of a backswamp which is surrounded by sand dunes. The down-thrown side of the cracks was always on the downslope side. Houses built over these cracks were destroyed by differential settling and lateral spreading of the foundation (Fig. 8-10). At Urbanizacion la Caleta on the coast of Chimbote, a series of cracks had developed along the narrow zones on the inland side of a beach ridge. Subsidence occurred on the downslope side of the crack (Figs. 8-12c and 13a, b).

Near Hotel Chimu, located on a beach ridge, cracks occurred almost parallel to the beach line. The cracks were probably formed by an incipient seaward slumping of the beach ridge or gravitational spreading.

On hill slopes at San Pedro area in the northern Chimbote, slabs of semi-consolidated old eolian sand (see Chapter 2) slipped down along the slope to form many cracks (Fig. 8-9). The heavy destruction of adobe houses in San Pedro (Chapter 7) can be explained by strong seismic intensity induced on the hard ground of this area (semi-consolidated sand layers and bedrocks beneath it).

### 8-3 Damage in the Backswamp and Lowland Areas

In these areas, the damage is characterized by regional and local ground subsidences due to compaction of underground deposits, the settlement of constructions and the submergence of the ground. For example, the lowlands along shallow valleys dissecting the Rio de Lacramarca alluvial plain such as in Miramar Bajo and Miraflores Baja, were submerged ca. 0.5 meters immediately after the earthquake, the water level decreased subsequently. The submergence was caused both by an abrupt rise of ground-water level and by a subsidence of the ground itself which is probably due to compaction of unconsolidated deposits filling the valley bottoms. The adobe houses in the lowland sank by ca. 0.5 m at maximum relatively to the ground surface around them (Fig. 8-14).

Subsidence of the ground and houses (e.g. in Barrio villa Maria) and a rise (ca. 1 m) of water table occurred also in the backswamp area in the southern Chimbote (Fig. 8-15). An enlargement of the water basin of the backswamp occurred not only by an increase of amount of water extruded from the backswamp, but also by ground subsidence of the backswamp area. These two phenomena are probably caused by compaction of water-saturated deposits of this area during the earthquake. Fig. 8-15c shows a drain channel which was made after the earthquake. A similar rise (ca. 1m in amount) of water level occurred also in the backswamp at the northern Chimbote. Further, a low-lying area surrounded by sand dunes at Miraflores Alto was covered by water to form a new lake (Fig. 8-16). In all cases the water level rose immediately after the earthquake, subsiding subsequently. In late August 1970, the water level was still higher than at pre-earthquake level.

Some buildings settled in some limited areas in the center of the Chimbote city (Fig. 8-17), where buildings and highways were damaged by the differential settlement. (Fig. 7-2 and Figs. 8-18, and 8-12ab). These areas more damaged in the center of the city are located in low-lying area between beach ridges or in former backswamps. These areas can be easily recognized in aerial photographs taken in 1943 by their darker tones (Fig. 1-1). Damage to Pan-American Highways in the Chimbote area was limited to such low-lying, wet areas where the the ground (both natural and man-made) subsided differentially.

### 8-4 Damage in the Sheetflood Area

Cracking, subsidence of the ground or water extrusion did not occur in the area of sheetflood deposits. In these areas (e.g. Buenos Aires), damage to houses was caused only by the direct effect of seismic vibration of the ground.

### 8-5 Damage to Man-made Ground at Chimbote Harbour

In Chimbote harbour, a rock-fill pier settled ca. 0.3 m. The fill extended from a wharf; water with sands and shell fragments gushed out from the numerous fissures that appeared during the earthquake. As a result, the fill had subsided by about 2 meters, in part submerging below sea level (Fig. 8-20b). Liquefaction is inferred to have occurred.

In summary: based on the nature of damage the Chimbote area can be divided into the following four areas (see also Table 8-1);

Zone I: areas of no damage to the ground itself.

Damage to constructions is only due to seismic vibration. — Sheetflood plain and Bedrock areas.

Zone II: areas of damage characterized by differential subsidence of the ground accompanied with small scale slumpings and crackings of the ground. — Beach ridge and Sand dune areas.

Zone III: areas characterized by appearance of open cracks with 'sand volcanoes' and by destruction of water-wells, which probably indicate an occurrence of subsurface liquefaction. — Rio de Lacramarca Alluvial Plain.

Zone IV: areas of ground subsidence and rise of water table which would be caused by compaction of loose, water-saturated deposits or by general liquefaction. — Backswamps and Lowland in the alluvial Plain.

These categories are significant for the seismic microzoning of the Chimbote area, because the nature of damage to a certain area caused by this earthquake can be expected to reappear in the same area during future earthquake and in other areas of similar geological conditions.

Table 8-1 Nature of the Damage in Relation to the geologic Province, and Classification of the Area

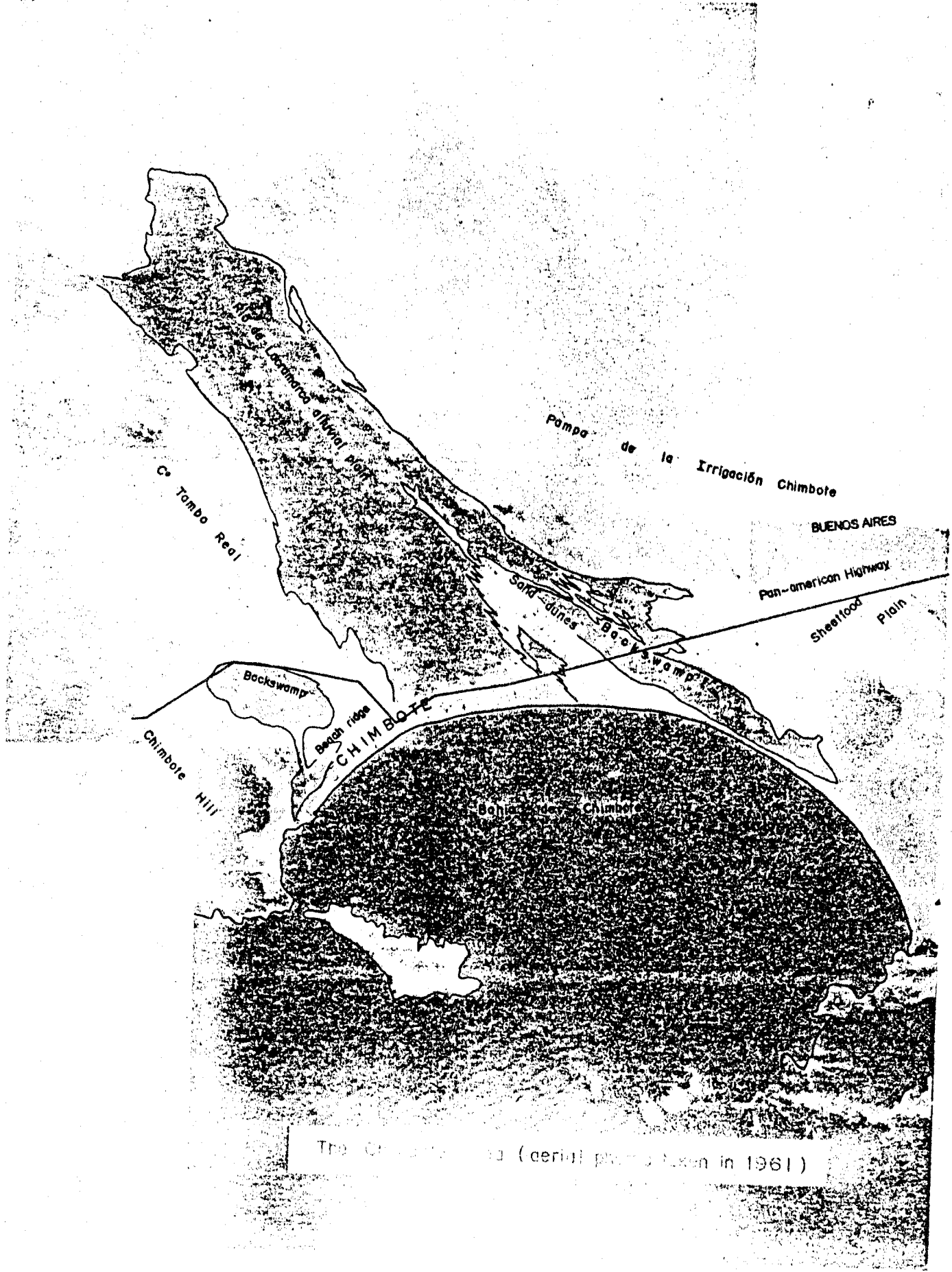
Geologic Province	Subsidence of foundation of constructions	Ground subsidence		Rise of ground water table and submergence	Sand volcanoes, Damage to wells	Nature of ground cracks	Zoning of the area	Major cause for damage to the ground	Characteristic damage to constructions
		Slumpint	Compaction						
A (Bedrock area)	○	○	○	○	○	no crack	Zone I		Damage due to seismic vibration
B <sub>3</sub> (Sheetflood plain)	○	○	○	○	○				
C (Beach ridge)	△	●	○	○	○	slumping gravitational	Zone II	Collapse of sand dune	Differential settlement and lateral spreading of the foundation
D (Sand dune)	△	○	○	○	○				
B <sub>1</sub> (Alluvial plain of Rio de Lacramarca)	△	○	○	○	●	cracks with sand volcanoes	Zone III	Subsurface liquefaction	Damage to underground constructions such as
E (Backswamp)	●	○	●	●	( )	cracks due to differential compaction of deposits	Zone IV	General liquefaction	Subsidence of the foundation and rise of water table
F (Lowland in alluvial plain)	●	○	●	●	( )				

● Remarkable

△ Negligible

○ Absent





The City of Valparaíso (aerial photo taken in 1961)

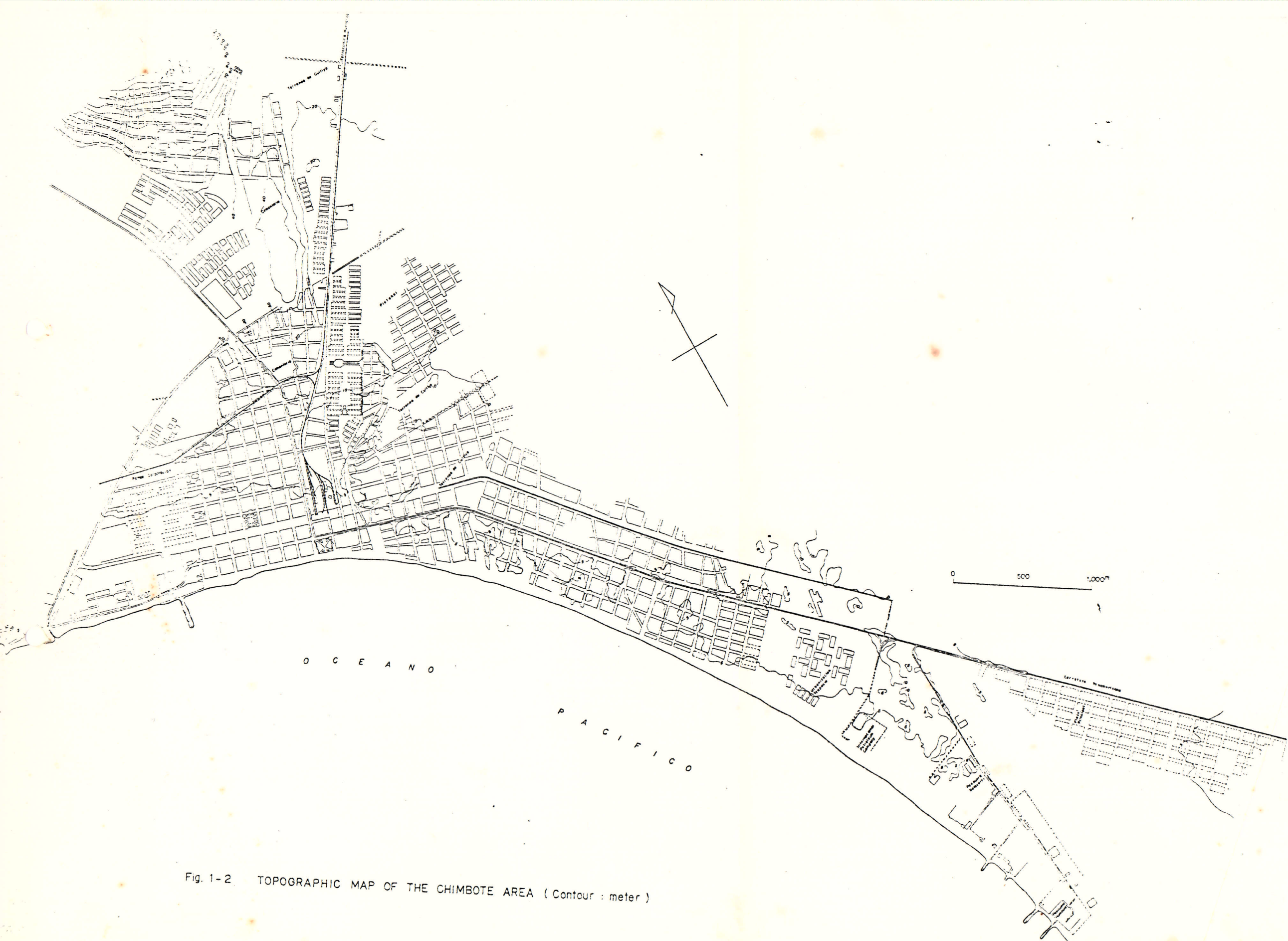


Fig. 1-2 TOPOGRAPHIC MAP OF THE CHIMBOTE AREA ( Contour : meter )





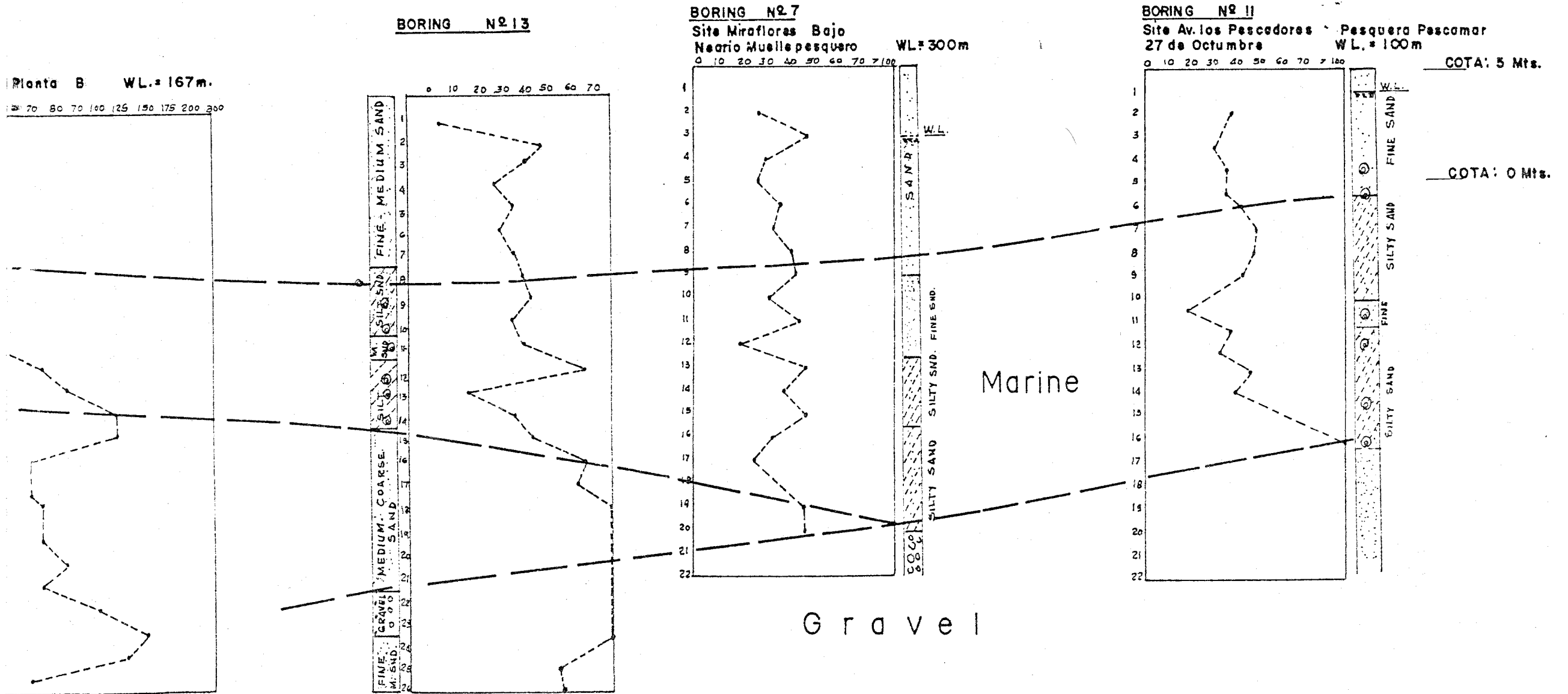
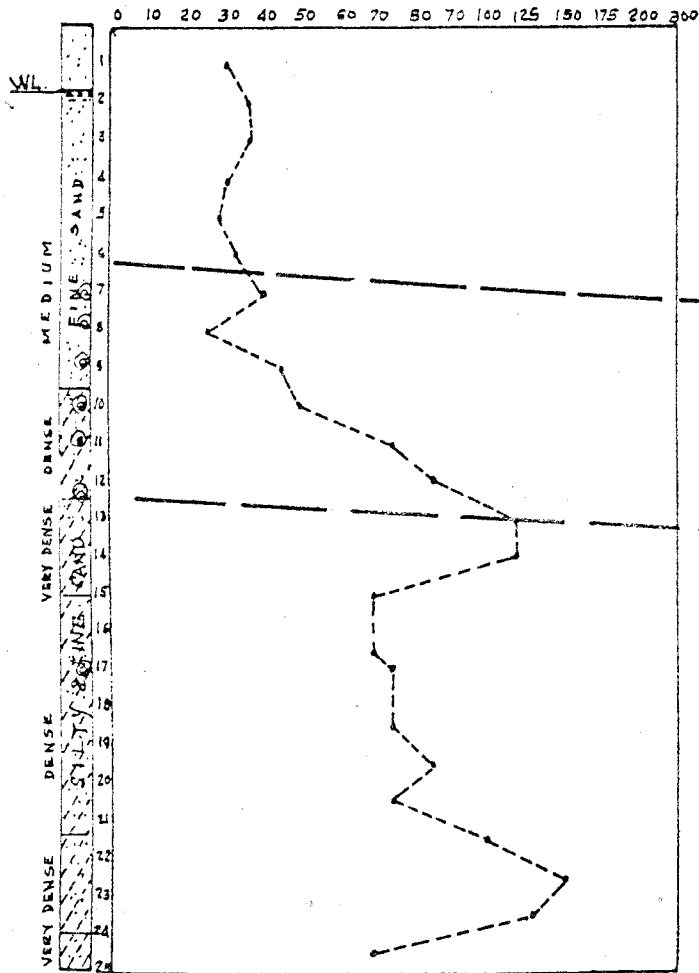


Fig. 3 - 2 (b) Boring logs and N-values

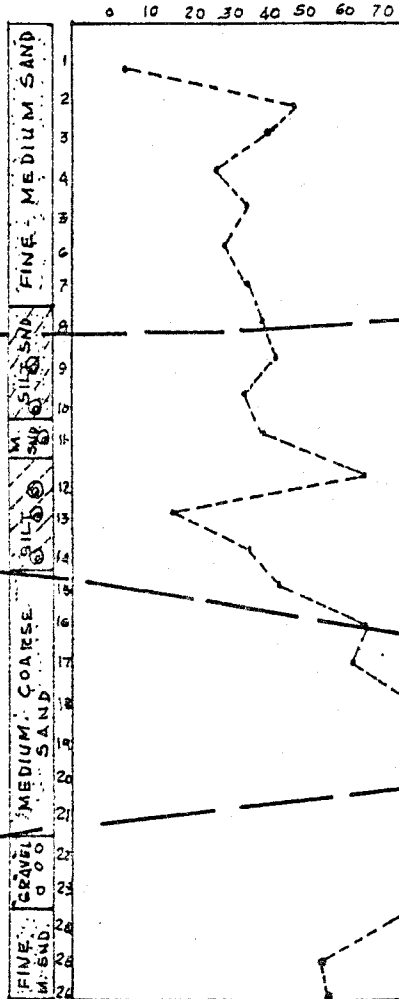
**BORING Nº 8**

Site la Caleta

Maritima Pesquera Planta B WL: 167m.



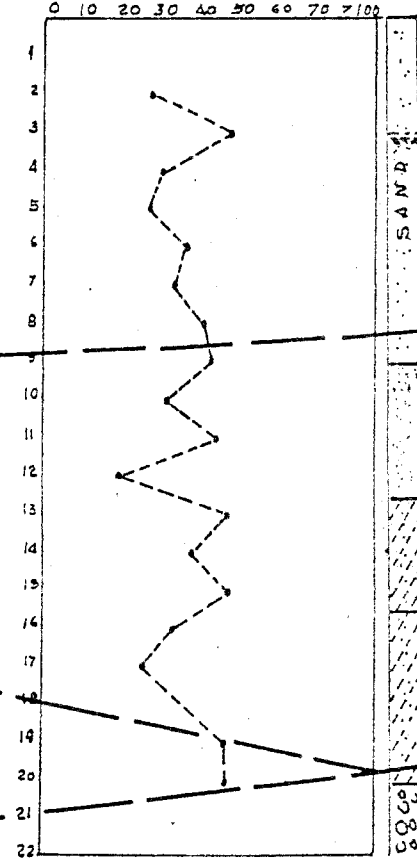
**BORING Nº 13**



**BORING Nº 7**

Site Miraflores Bajo  
Neario Muelle pesquero

WL: 300m



**BORING Nº 9**

Site Av. los Pa  
27 de Octum



Marine

Gravel

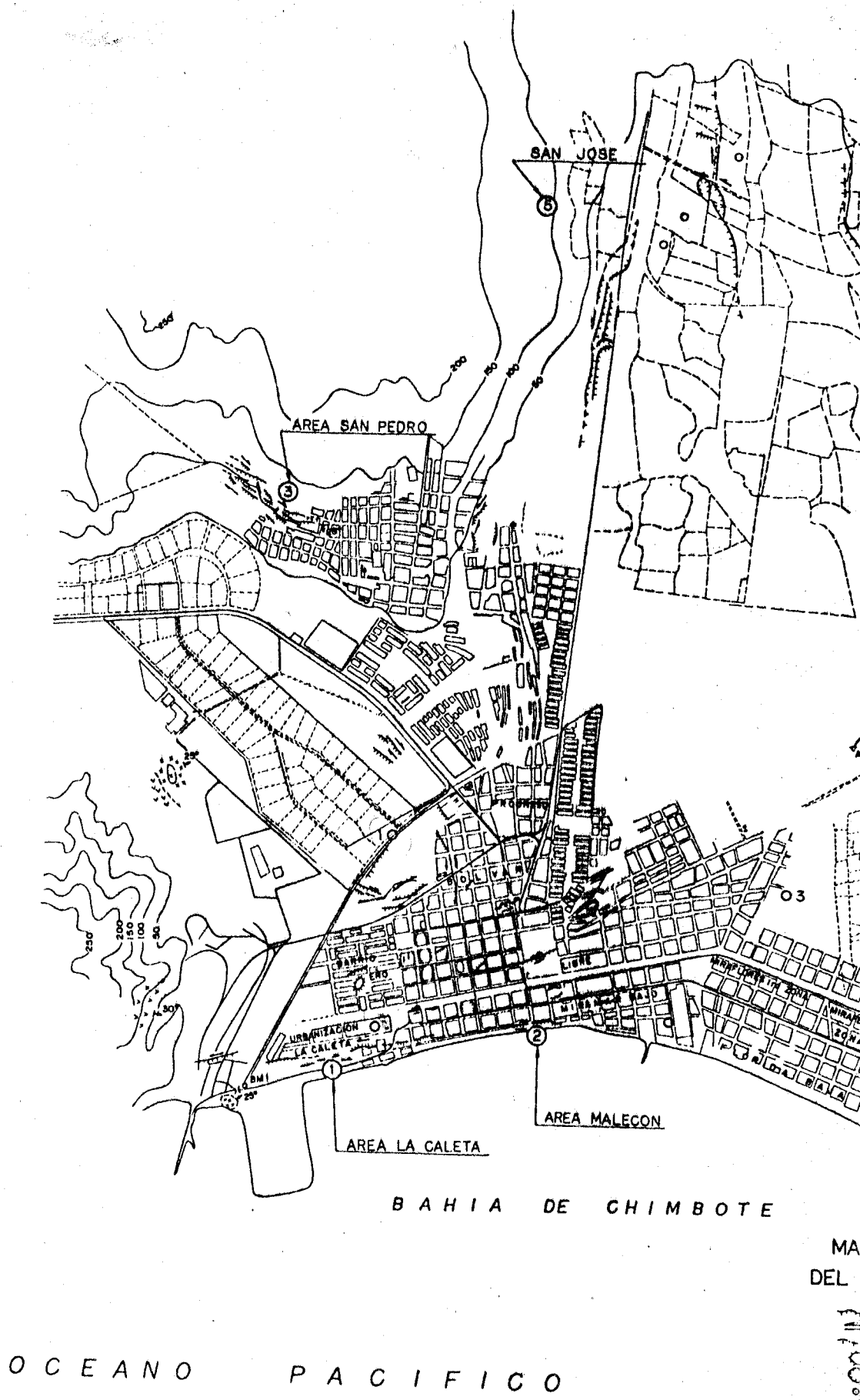



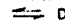
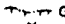




Fig. 8-1 DISTRIBUTION MAP OF GROUND CRACKS AND FORMED DURING MAY 31, 197

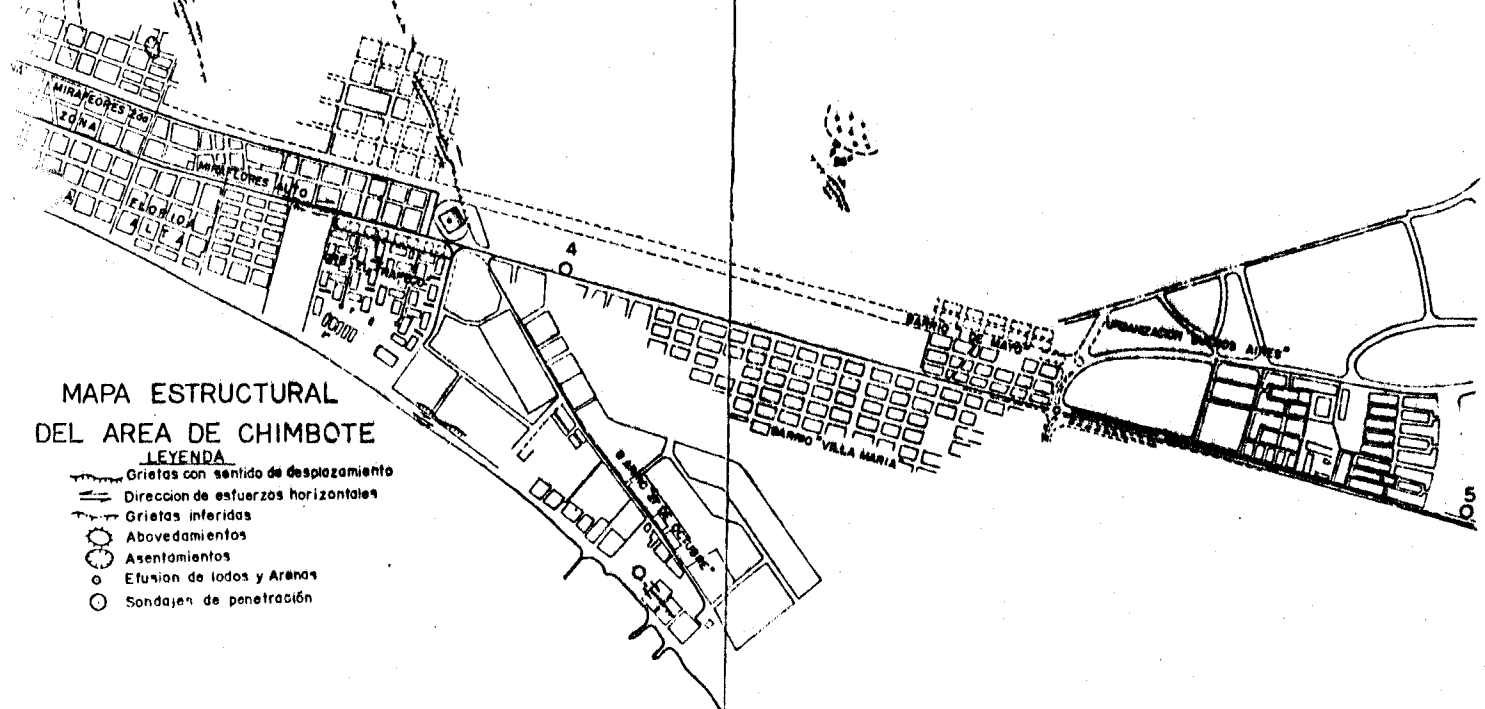
LA CLEMENCIA

AREA LAS CUCARDAS

MAPA ESTRUCTURAL  
DEL AREA DE CHIMBOTE

LEYENDA

-  Grietas con sentido de desplazamiento
-  Direccion de esfuerzos horizontales
-  Grietas inferidas
-  Abovedamientos
-  Asentamientos
-  Efusion de lodos y Aranas
-  Sondajes de penetración



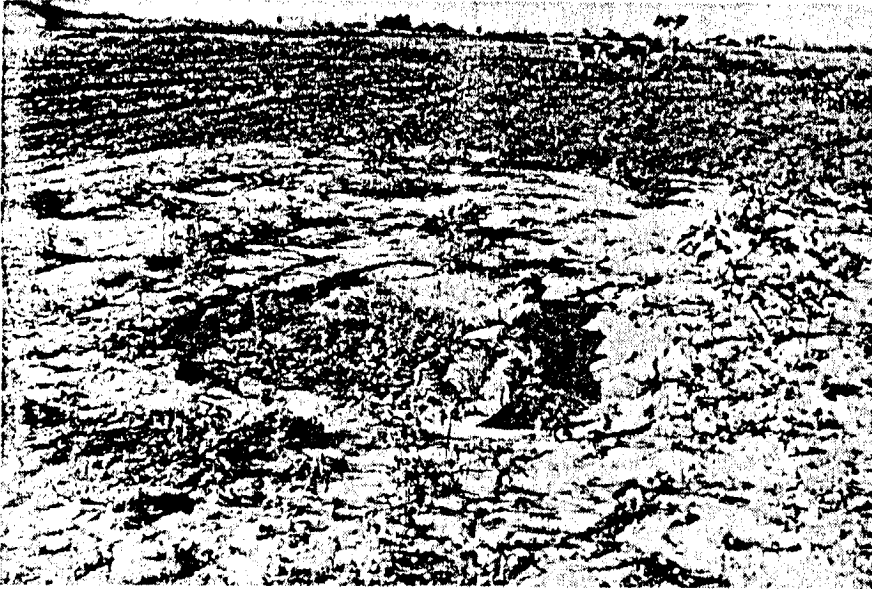
CRACKS AND SAND VOLCANOES IN THE CHIMBOTE AREA,  
31, 1970 EARTHQUAKE ( See Appendix 7 )



Fig. 8-2  
Sand volcanoes with  
open fissures on the  
Rio de Lacramarca  
alluvial plain (East  
of Hda. San Jose)



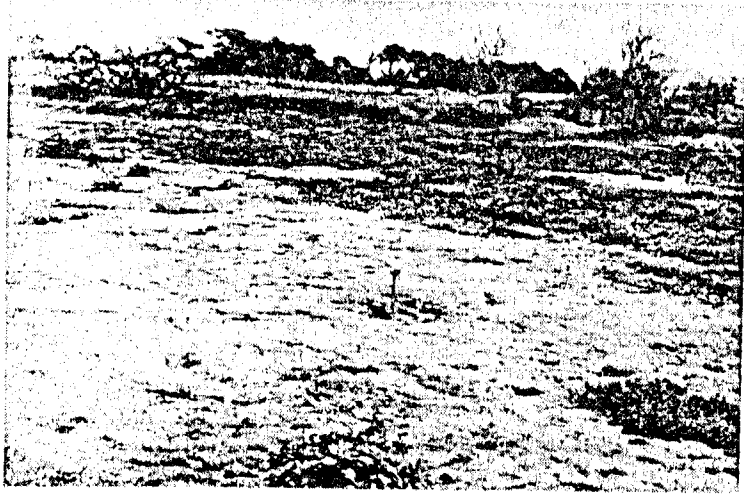
(a)



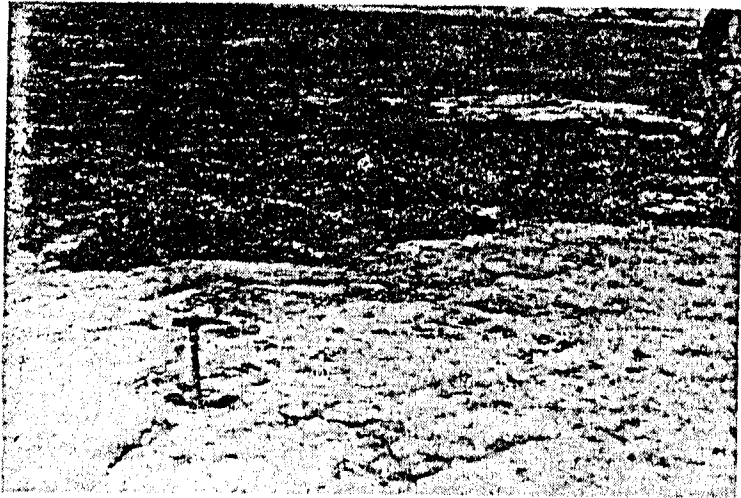
(b)



(c)



(a)



(b)



Fig. 8-4  
Open cracks associated with Sand volcanoes (Loc. same as Fig. 2 )

Fig. 8-5  
Ground cracks on the  
Rio de Lacramarca  
alluvial plain.  
(Hda. San Jose)



(a)



(b)



(c)

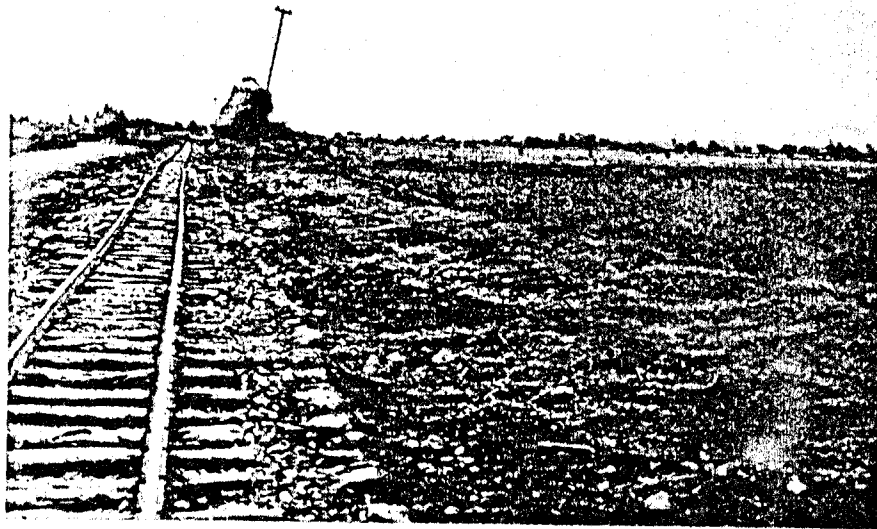


Fig. 8-6  
Damage due to sub-  
surface liquefaction on  
the Rio de Lacramarca  
alluvial plain.

a) damage to  
Chimbote-Huallanca  
railway near Hda. San Jose

(a) b) and c)  
damage to wells  
(subsidence and  
tilting)

(b: near Hda.  
San Jose

c: a restaurant  
along Camino Peru)

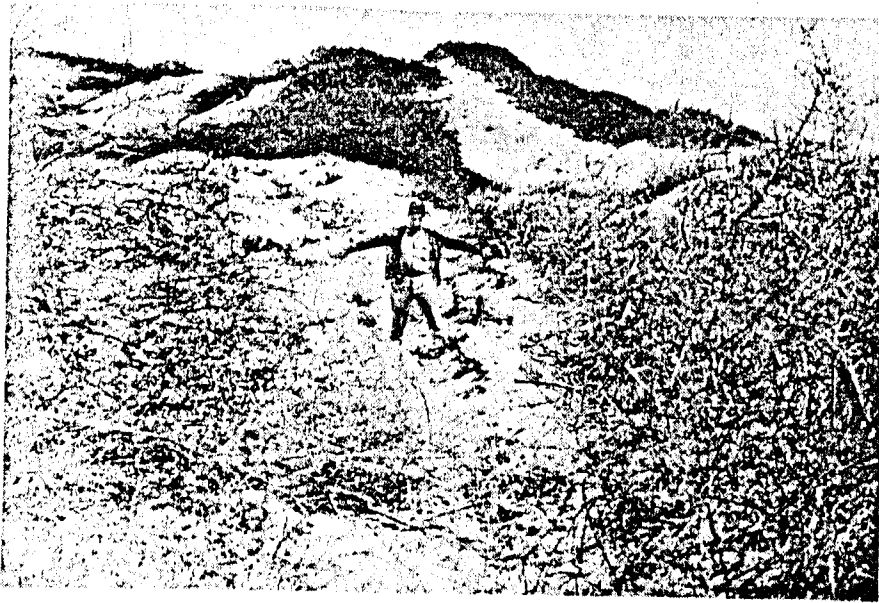


(b)

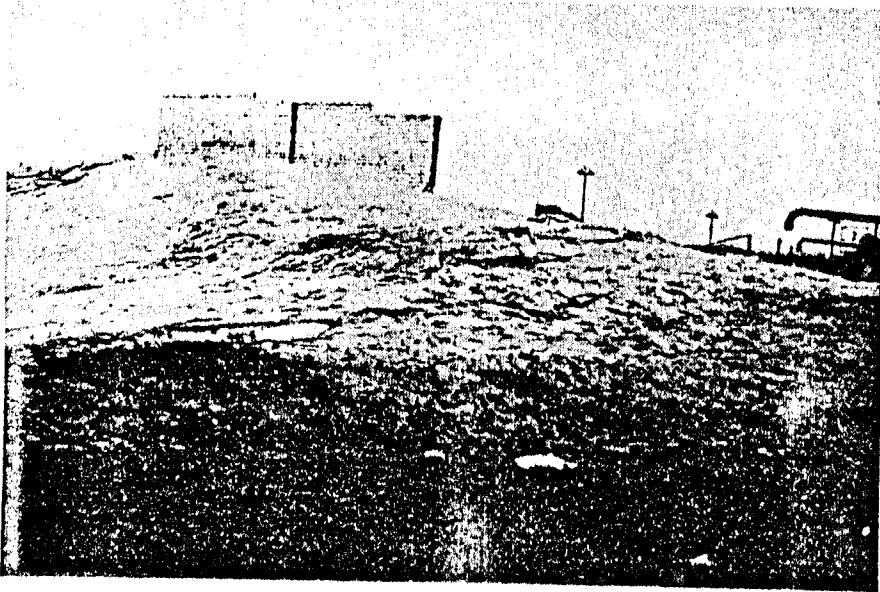


(c)

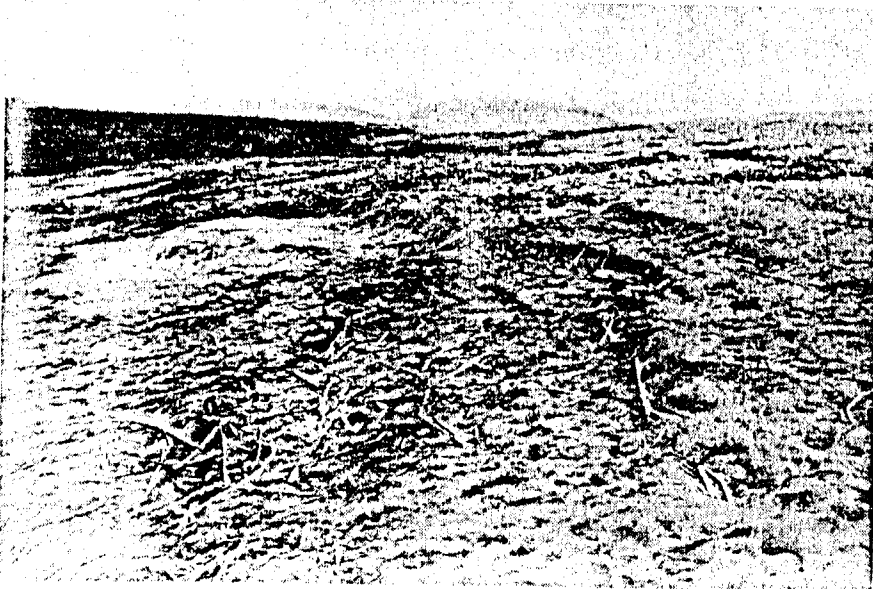
Fig. 8-7  
Cracks in sand dunes  
a: Cucardas  
b.c: north of Estadio  
Pensacola



(a)



(b)

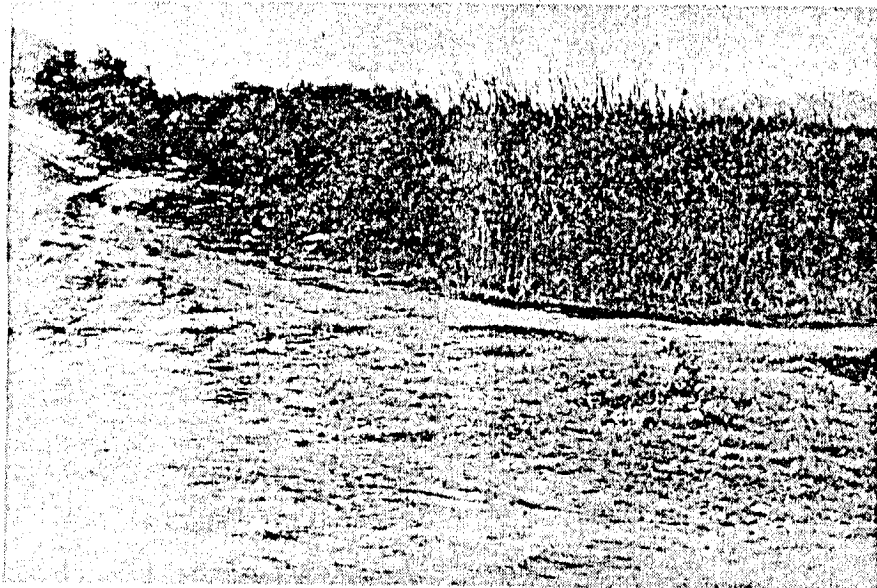


(c)



(a)

Fig. 8-8  
Cracks near the  
boundary between  
sand dune and  
backswamp  
(Tres Cabezas)

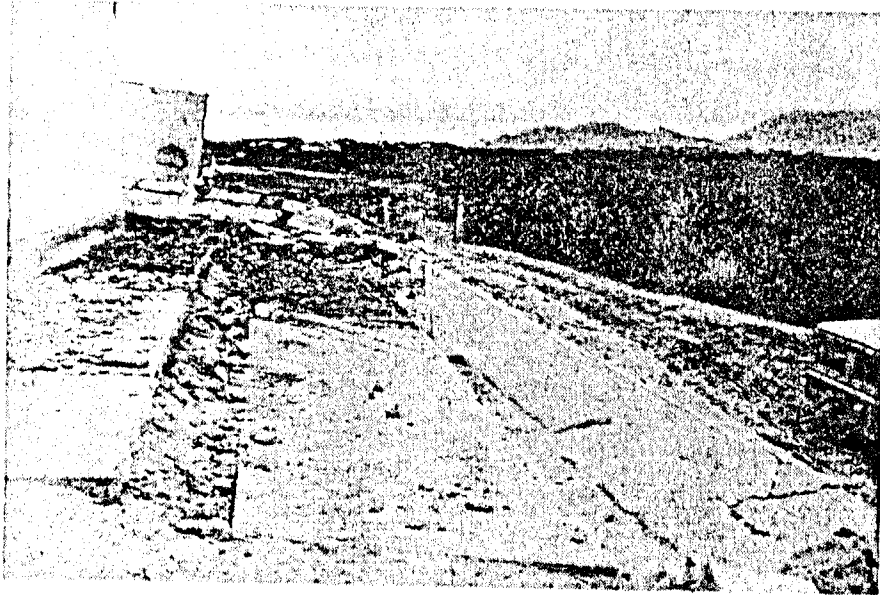


(b)



Fig. 8-9  
Cracks in the crust  
of semi-consolidated  
sand layers on the  
hill slope of San  
Pedro

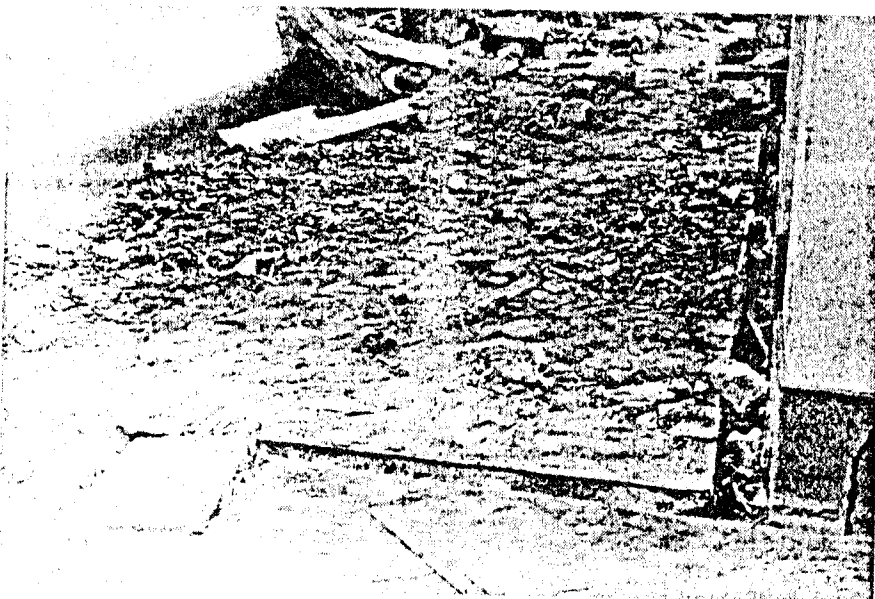
Fig. 8-10  
Damage due to  
differential subsidence  
and to  
opening of foun-  
dation at the  
edge of sand dune.  
(Tres Cabezas)



(a)



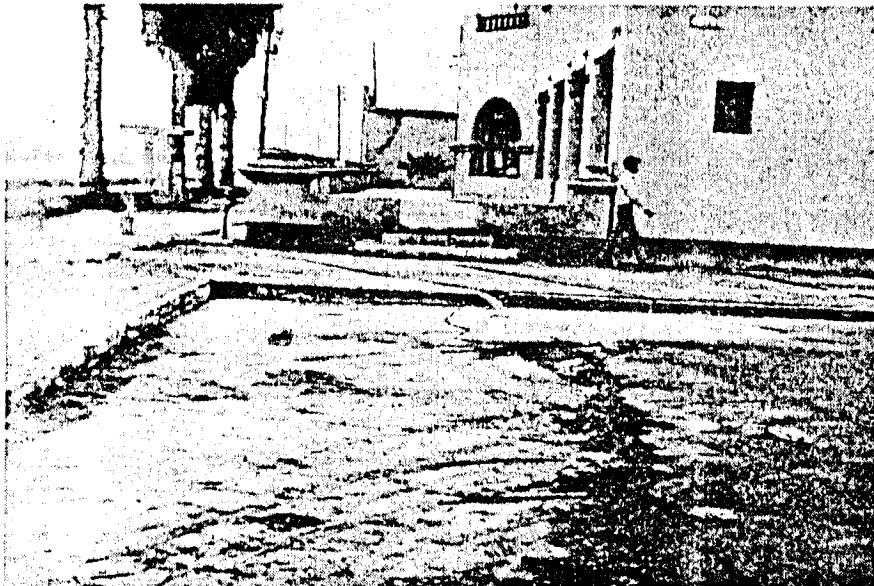
(b)



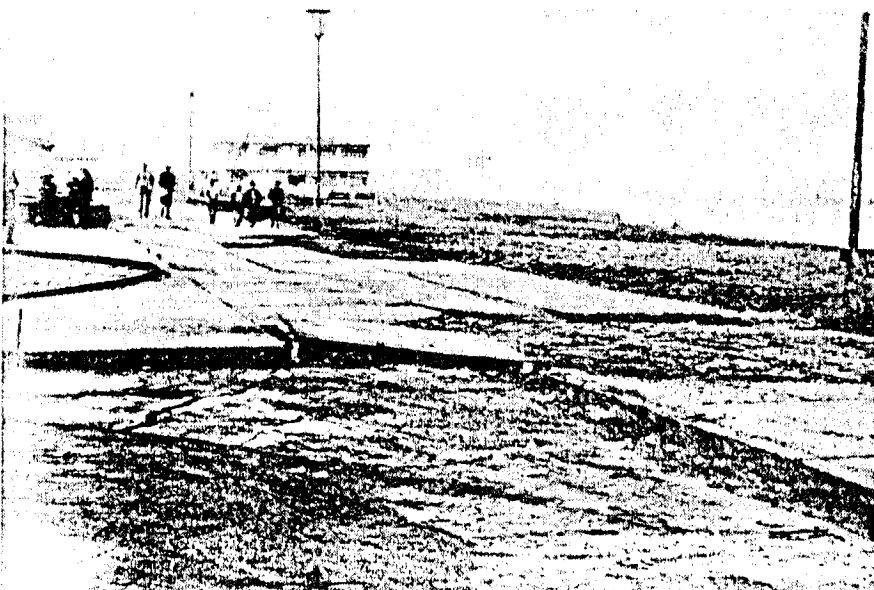
(c)



(a)



(b)



(c)

Fig. 8-11  
Differential sub-  
sidence of ground  
on beach ridge.  
(Coast near  
Hotel Chimú)



Fig. 8-12  
Differential sub-  
sidence of ground  
due to compaction.  
(Urbanizacion la  
Caleta)



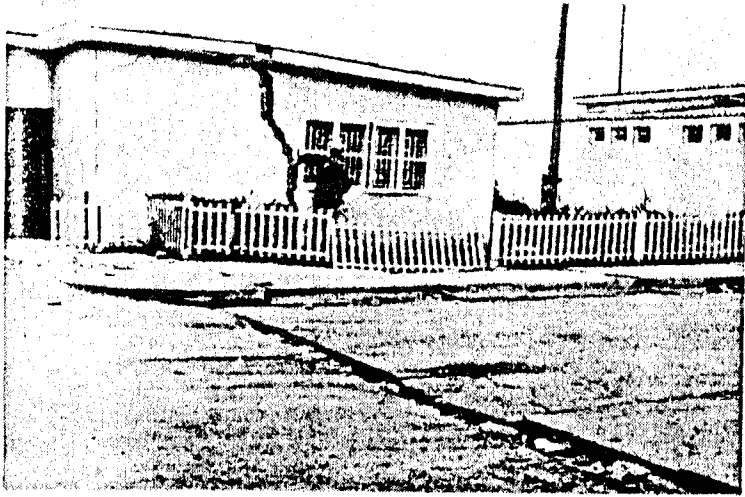
(a)



(b)



(c)

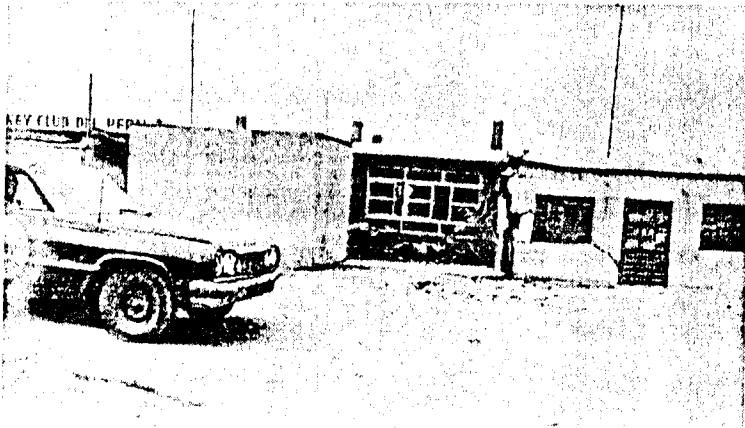


(a)

Fig. 8-13  
Damage to houses  
due to differential  
subsidence of the  
ground at the edge  
of beach ridge.  
(a, b: Urbanizacion  
la Caleta,  
c: Urb el Trapecio)



(b)



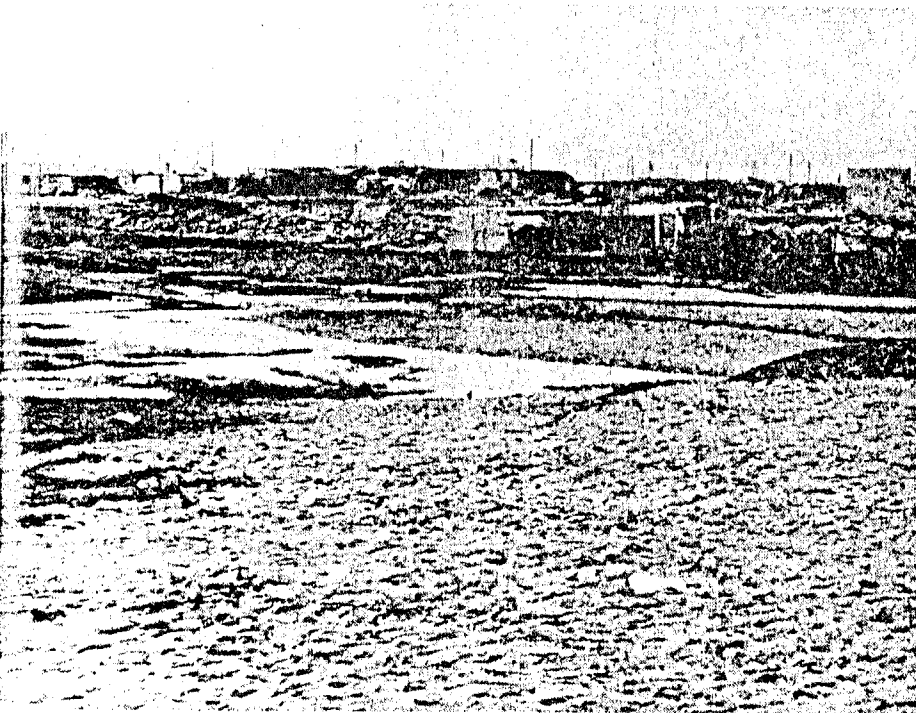
(c)

Fig. 8-14  
Ground settlement  
and rise of water table  
in the lowland along  
the valley dissecting  
the Rio de Lacramarca  
alluvial plain.

(Lowland between  
Miramar Bajo and  
Miraflores Baja)



(a)

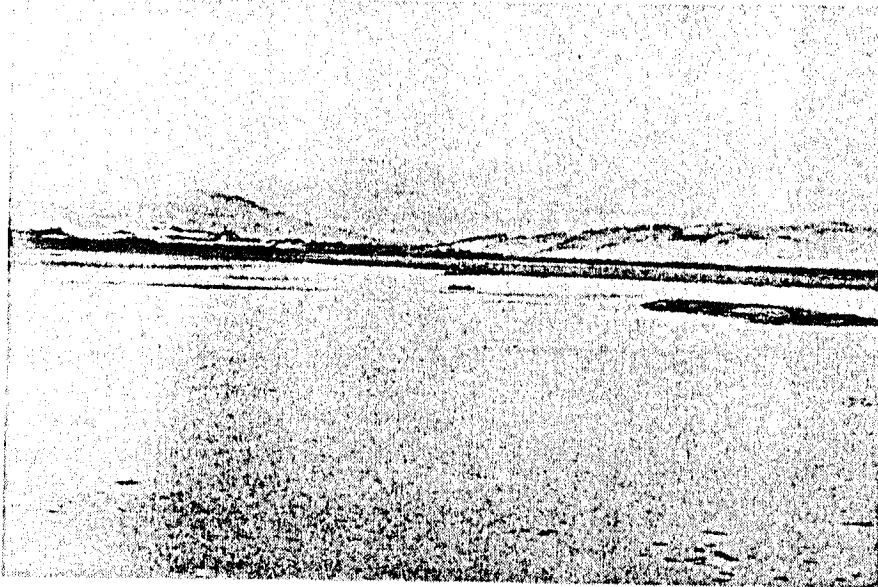


(b)

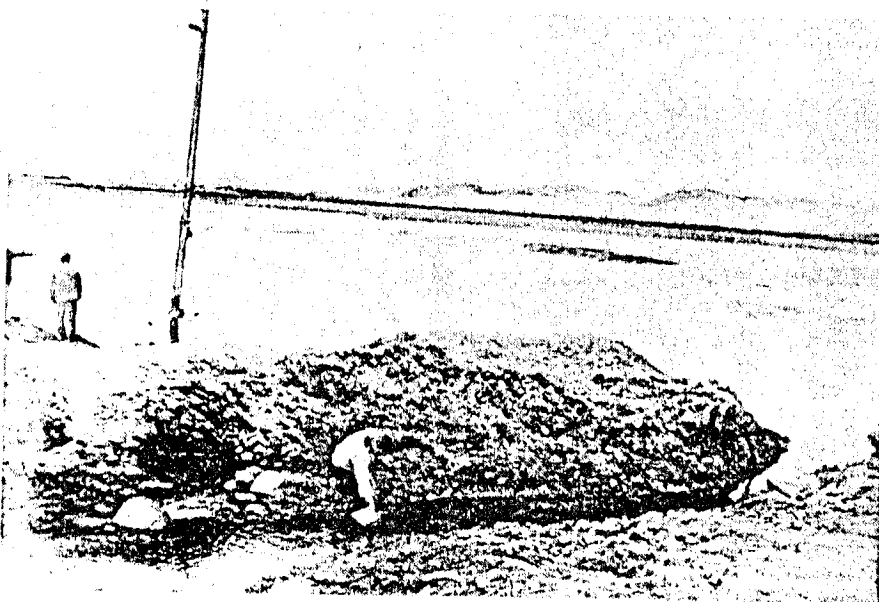
Fig. 8-15  
Flooded area  
due to ground  
settlement and  
uprise of water  
table.  
(Backswamp in  
southern Chimbote)



(a)

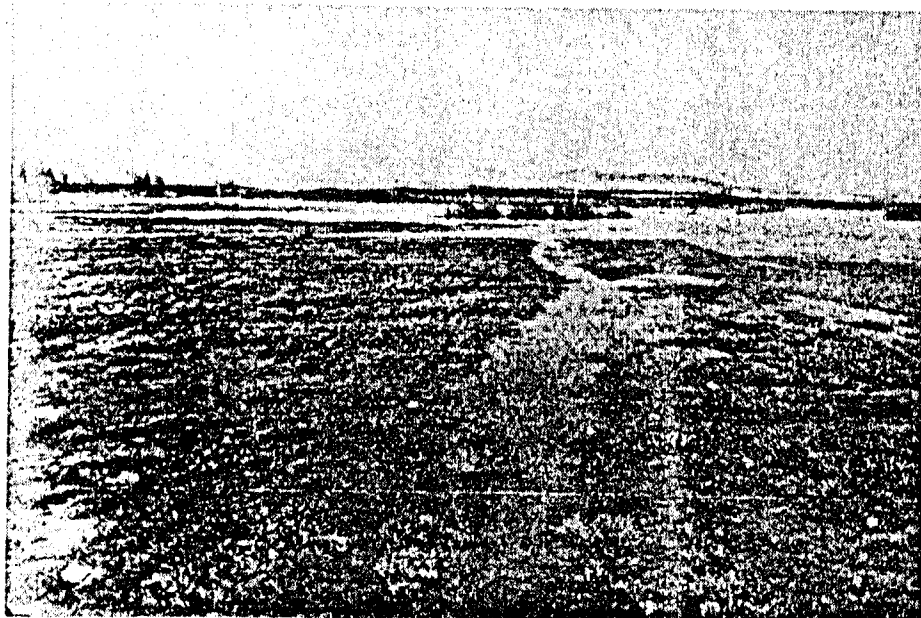


(b)

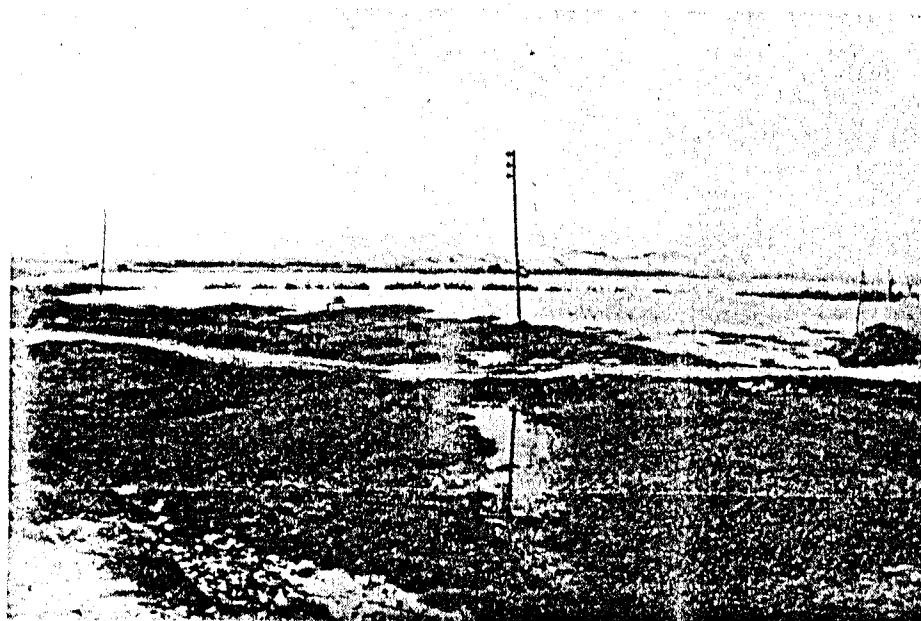


(c)

Fig. 8-16  
Flooded area due to  
ground settlement  
and rise of water  
table.  
(East of  
Miraflores Alto)

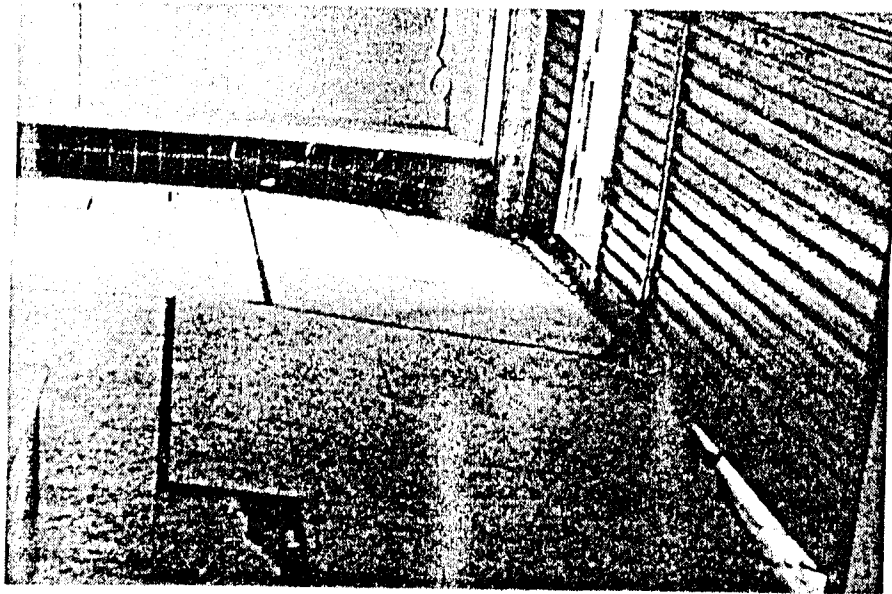


(a)

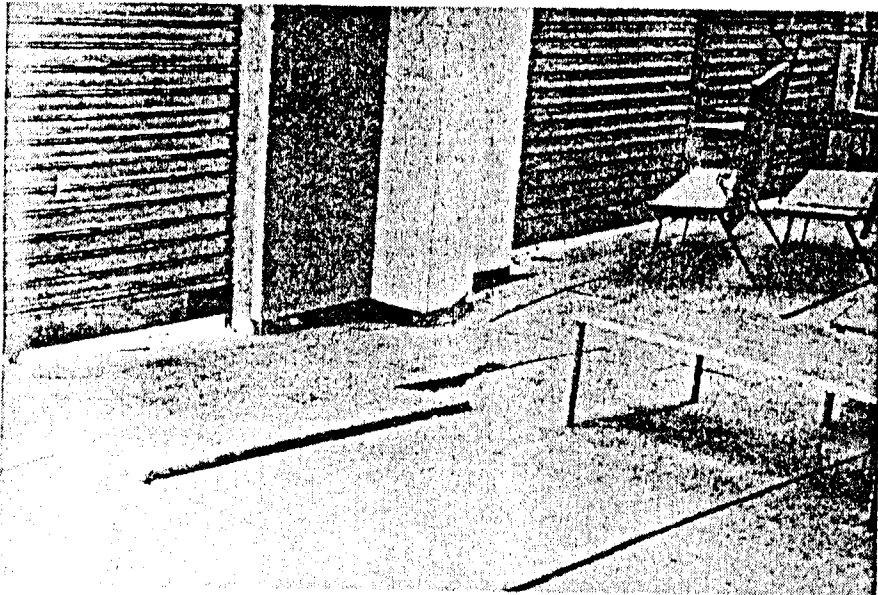


(b)

Fig. 8-17  
Damage due to  
differential sub-  
sidence of foun-  
dation of building  
(Casco Uabano)



(a)



(b)

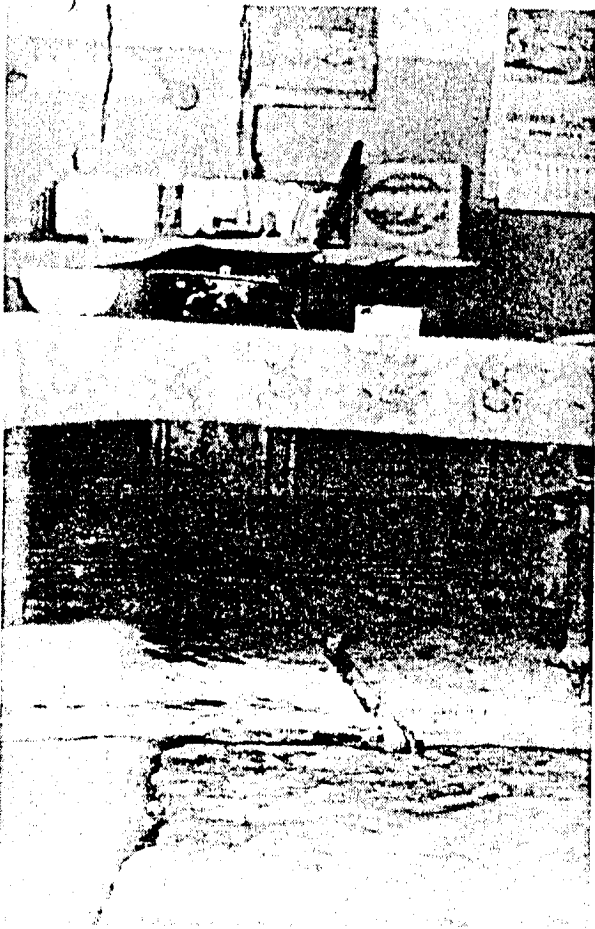


(c)

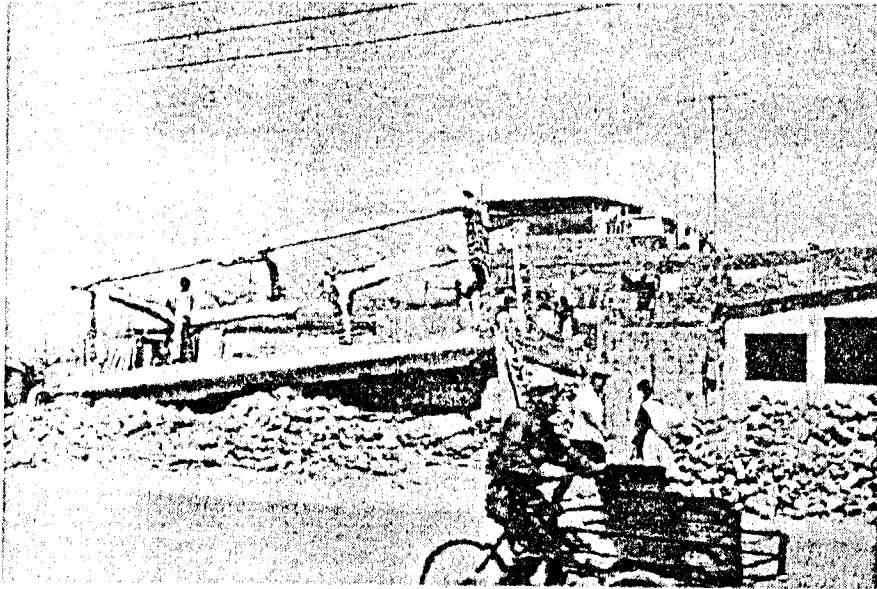
**Fig. 8-18**  
**Damage to house**  
**due to differential**  
**subsidence.**  
**(Casco Uabano)**



(a)



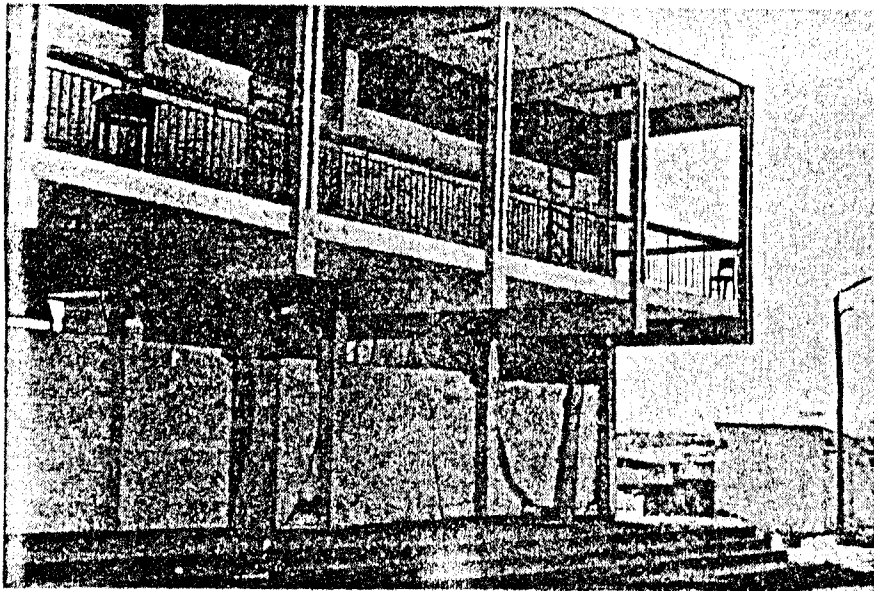
(b)



(a)

Fig. 8-19  
Damage to building  
due to earthquake  
shocks.

- (a: Miraflores,
- b: School
- building of G.U.E.
- Inmacu lada de la
- Merced,
- c: San Pedro)



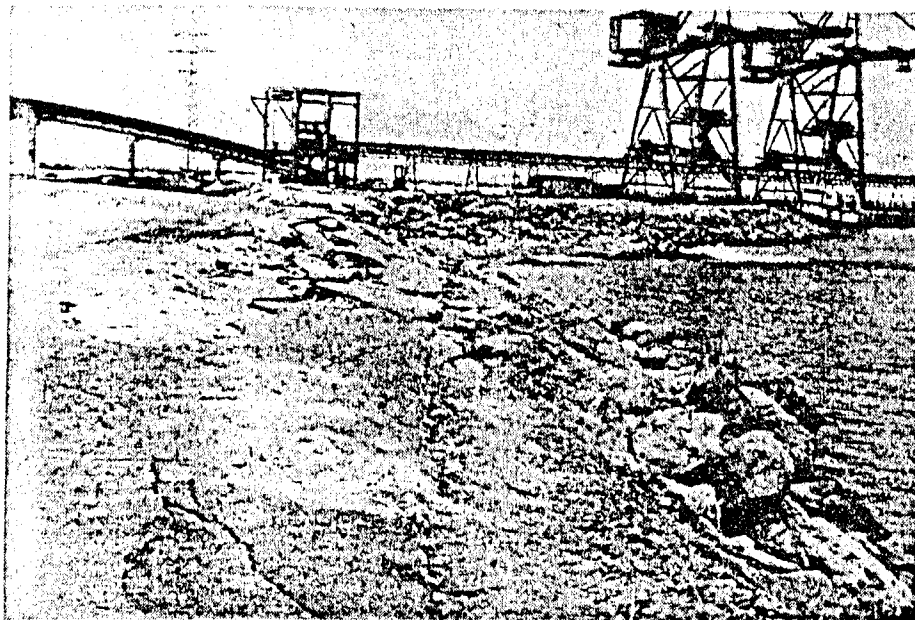
(b)



(c)



**Fig. 8-20**  
**Damage to Chimbote harbour**  
**a: slumping of paved road.**  
**b: ground settlement with cracks and sand volcanoes, due to liquefaction on the filled earth.**



(a)



(b)

## Chapter 9 Microzoning of Chimbote Area

Generally speaking, a ground movement and failure of structure due to an earthquake is essentially governed by the magnitude and epicentral distance. But when only a limited area is taken up there is a difference in the extent of damage depending on the locality, due to the difference of the local topography and of the subsoil condition.

The subsoil of the said area consists basically of a fluvial sandy deposit of Rio de Lacramarca and its upper part is loose to medium sand or sandy silt. This surface layer has a general trend to increase its thickness and to become finer in grain size towards the sea coast. The depth of the water table varies with topography.

Response of structures during an earthquake is affected greatly by the thickness of the surface layer, engineering properties of soils and the depth of the ground water table.

Effect of the ground condition on damage during an earthquake falls into two categories. The first category relates to failure conditions and the second is concerned with the dynamic response of intact soils. Failure condition of sandy soils is closely associated with the depth of the ground water table. Seismic force acting on a structure is affected not only by the rigidity of the ground, but also by the rigidity of the structure.

Based on the investigations stated in the previous chapters, the said area may be divided largely into four zones as shown in Fig. 9-1, from a view-point of land utilization, especially of the earthquake resistance design of structures.

The general feature of the zones and countermeasure necessary for the construction of structures will be as follows:

### ZONE I:

In zone I, the subsoil consists of dense gravels or rocks and the water table is at least 10 m deep below the ground surface. Most of this zone is located in the areas where the elevations are higher than 10 m. In this zone, there is practically no possibility of settlements in ordinary buildings and of the ground subsidence during an earthquake. However, the seismic force acting on these buildings may be a little stronger than in the other zones, from a view point of soil-structure interaction.

### ZONE II:

Zone II is an area covered by loose to medium-dense sand of several meters in thickness. Below this layer there is either dense sand or cemented compact sand formation. In most parts of this zone the water table is about 5 m below the ground surface. No appreciable settlement is expected in this zone for ordinary residential buildings (less than two stories), except on the outer edges of sand dunes. It is preferable that buildings of more than two stories are supported by piles reaching the dense sand.

When dune areas are turned into construction lots, filled sand should be compacted, for example, by means of vibrofloatation.

#### ZONE III:

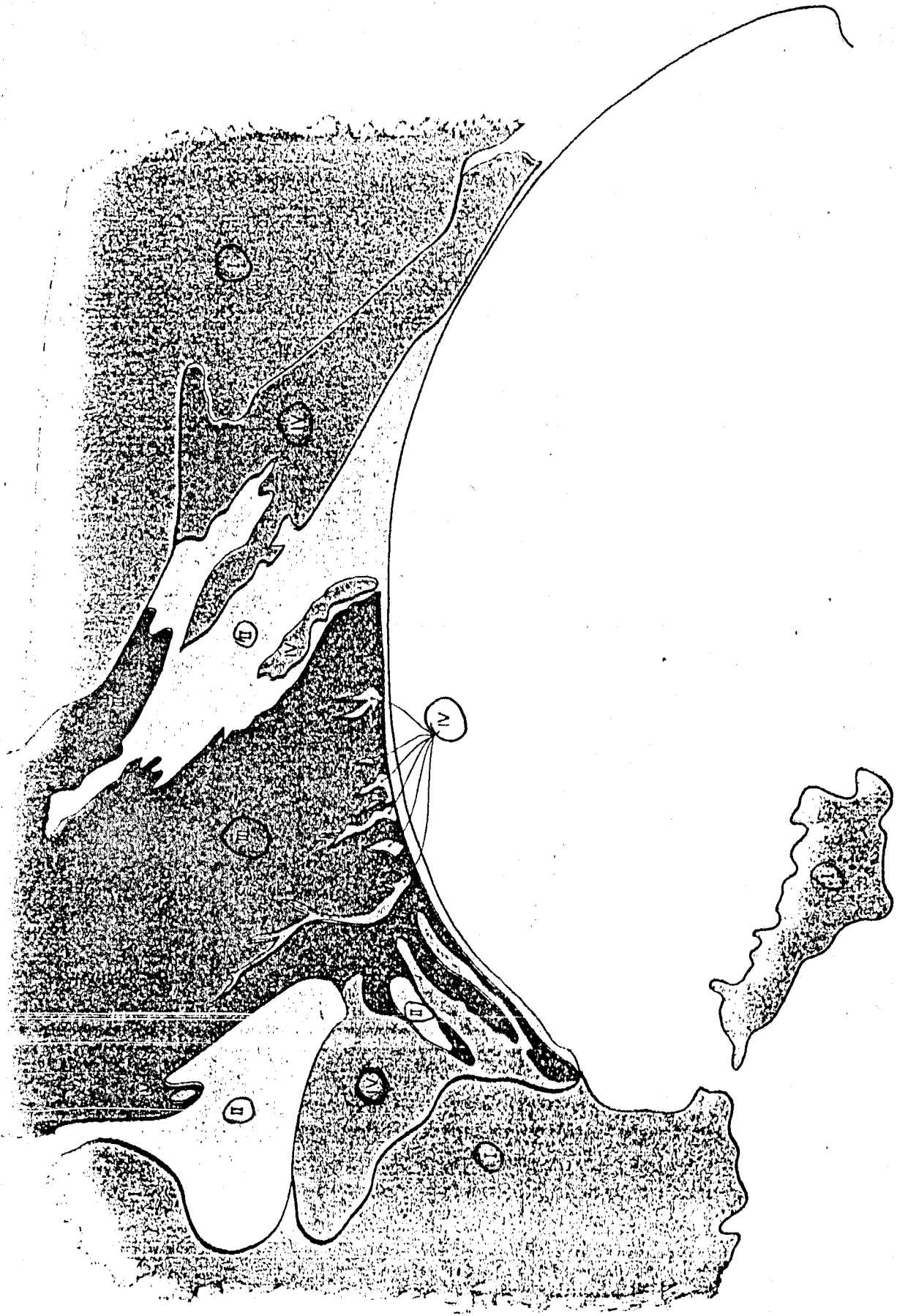
In zone III the subsoil consists mainly of a sandy soil covered by a thin agricultural soil. Gravel beds lie deeper than 10 m. The ground water-level is a few meters in depth.

Loose fine sand seating in some depths will liquefy during the earthquake. Therefore, there are possibilities of damage to structures due to local liquefaction of sands. Since the above mentioned liquefaction of sand will be generally limited to some range of depths below the ground surface, no appreciable settlement of buildings occurred, with a few exceptions. However, some considerations should be taken for the design of foundation of buildings higher than two stories.

#### ZONE IV:

Zone IV is characterized by high water-table, whose level is almost the same as the ground surface, hence, the most of the land is covered by water or swamps. Average elevation of zone IV is less than 5 m above sea level. The soil consists mainly of sands covered partially with a thin layer of organic silt.

The damage to buildings in this zone will be caused mainly by settlement and also partially by seismic force. There are some places where sand will liquefy up to the ground surface when the severe earthquake attacks. The buildings to be constructed in this zone should be supported by piles reaching the dense sand, otherwise, the soil should be improved by vibrofloating methods up to a certain depth.



MAPA DE MICROZONACION SISMICA DE LIMA

Fig. 9-1 SEISMIC MICROZONING MAP

## Chapter 10 General Recommendations

The territory of Peru extends over the seismic active region and the country has experienced destructive earthquakes many times since the ancient time, by which many human lives were lost and a huge amount of property damage was caused.

There are many approaches to prevent or at least to minimize the earthquake disasters. For this purpose, researches on the seismology and the earthquake engineering, including researches for prediction of earthquakes and of mud flow due to fall of ice-cap, must be made positively.

The expected research programs may be divided into the following groups:

- 1) Accurate observation of seismicity
- 2) Geodetic study for recent crustal movements
- 3) Study of geomagnetism
- 4) Seismotectonics including study of active faults
- 5) Topographic and geological study of seismic region
- 6) Research on adobe construction and on its material for strengthening against earthquakes
- 7) Research on dynamic behaviour of structures and of earth structure
- 8) Research on soil dynamics
- 9) Research on dynamic behaviour of foundations

Items 1) to 5) will contribute greatly to the prediction of the imminent earthquakes and saving of many human lives. However, even if an earthquake can be predicted, it will be impossible to prevent the occurrence of an earthquake. It is very important, therefore, to know how to construct appropriate structures which can withstand the forthcoming earthquakes (Item 6 to 9).

As it takes long time and a huge amount of money is required to implement these recommendations, the Government is expected to start the projects as soon as possible.

The establishment of a kind of Composite Research Institute for Disaster Prevention of Earthquake, participated by scientists and engineers specializing the above-mentioned fields, will greatly facilitate the implementation of the projects.

It is also recommended that the exchange of scholars and students between Peru and Japan or with other countries be promoted for this purpose.

Besides the above-mentioned research items, it is very important to prepare the seismic microzoning maps for major cities, following the procedures used for the Chimbote area.

## **Appendix 1**

### **Comparison of the Two Penetration Tests**

## Appendix

### Appendix 1. Comparison of the two penetration tests.

The two types of the penetration tests were performed in the two boreholes two meters far from each other, respectively. The test site is located at Inage City, Chiba Prefecture of Japan, where a thick sand deposit exists.

One of the penetration tests (type A) was as the same as adopted in the investigation in the Chimbote area. Drilling was advanced by jetting fresh water from a bit attached to the lower end of the drilling rod of 2 in. in diameter, lowering casing of 3 in. in an inner diameter to support the walls of the hole. The penetration test was performed at the bottom of the cased hole. An outer diameter of a spoon sampler of 2.5 in., a weight of 220 lb and a height of fall of 20 in. were used.

The another borehole was made by rotary drilling without casing, using the circulating mud water. The penetration test consisted of a 2 in. spoon sampler, a weight of 140 lb, and a falling height of 30 in. as used commonly as a standard (type B). The drilling rod was 1.6 in. in diameter.

The results of the two tests are shown in Figs. A-1 and A-2. It is found that the fairly good linear relationship exist as follow,

$$N = 0.88 N'$$

where N and N' represent number of blows per foot for the test B and A, respectively,

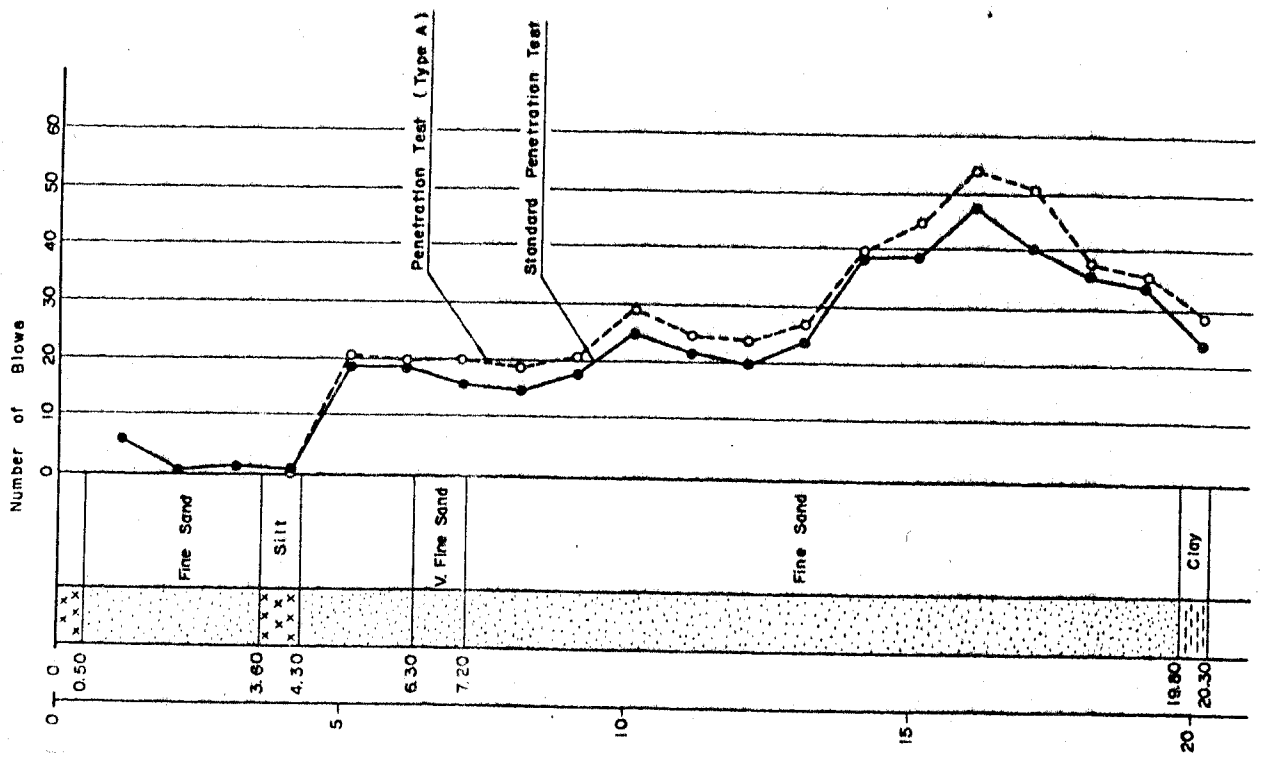


Fig. A-1-1 RESULT OF THE TWO PENETRATION TESTS

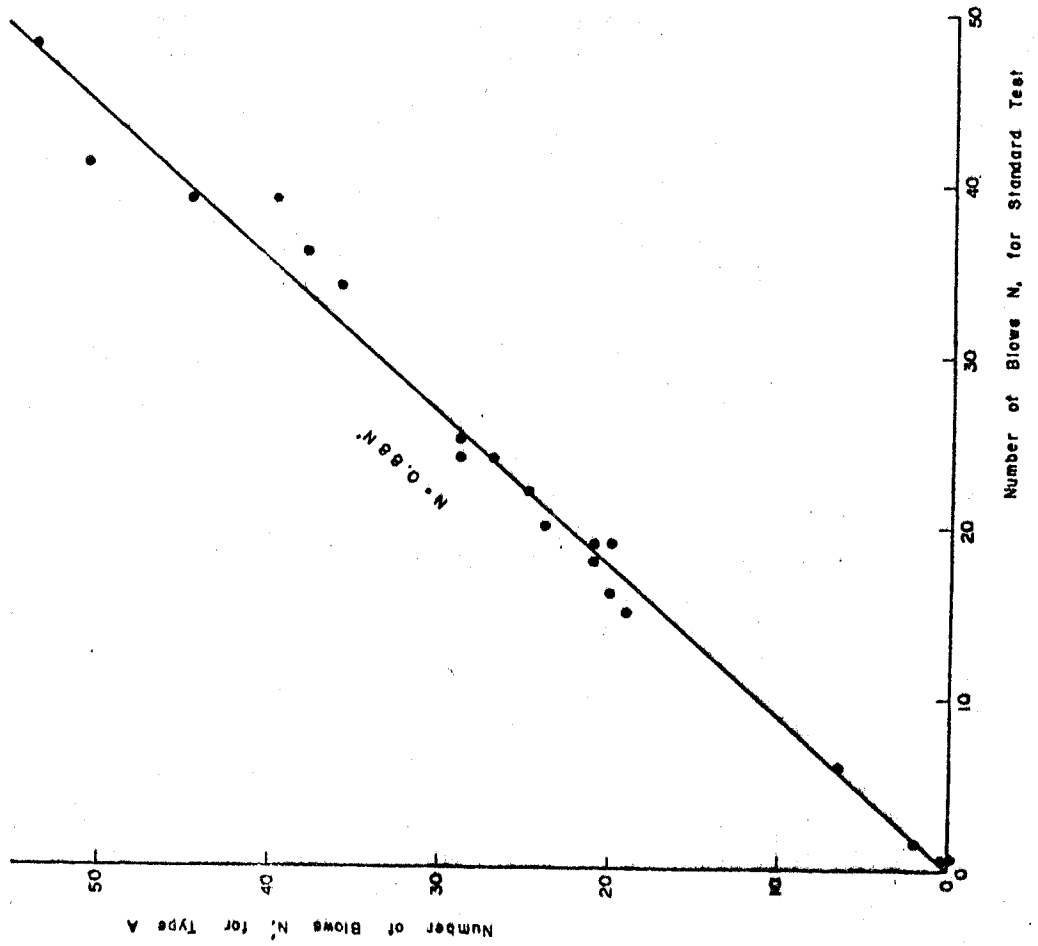


Fig. A-1-2 CONFARISON OF PENETRATION RESISTANCE VALUES



## **Appendix 2**

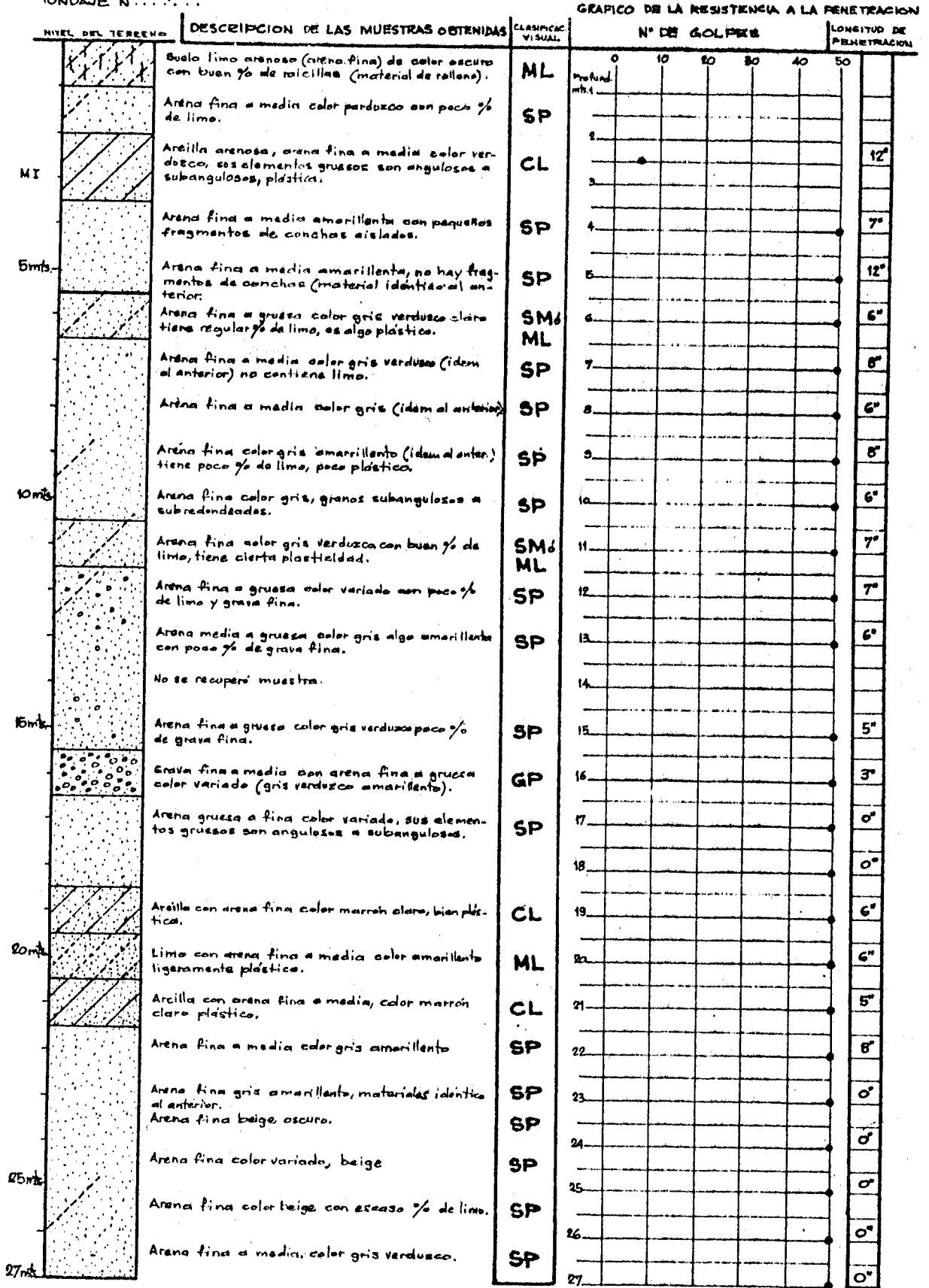
### **Field Record of Borings and Penetration Tests**

Fig. A-2-1

PROYECTO CHIMBOTE

INVESTIGACIONES DEL SUB-SUELO DE CHIMBOTE

UBICACION: AV. Industrial COTA: NIVEL DE AGUA: Superficial...  
 BONDADJE N° 1

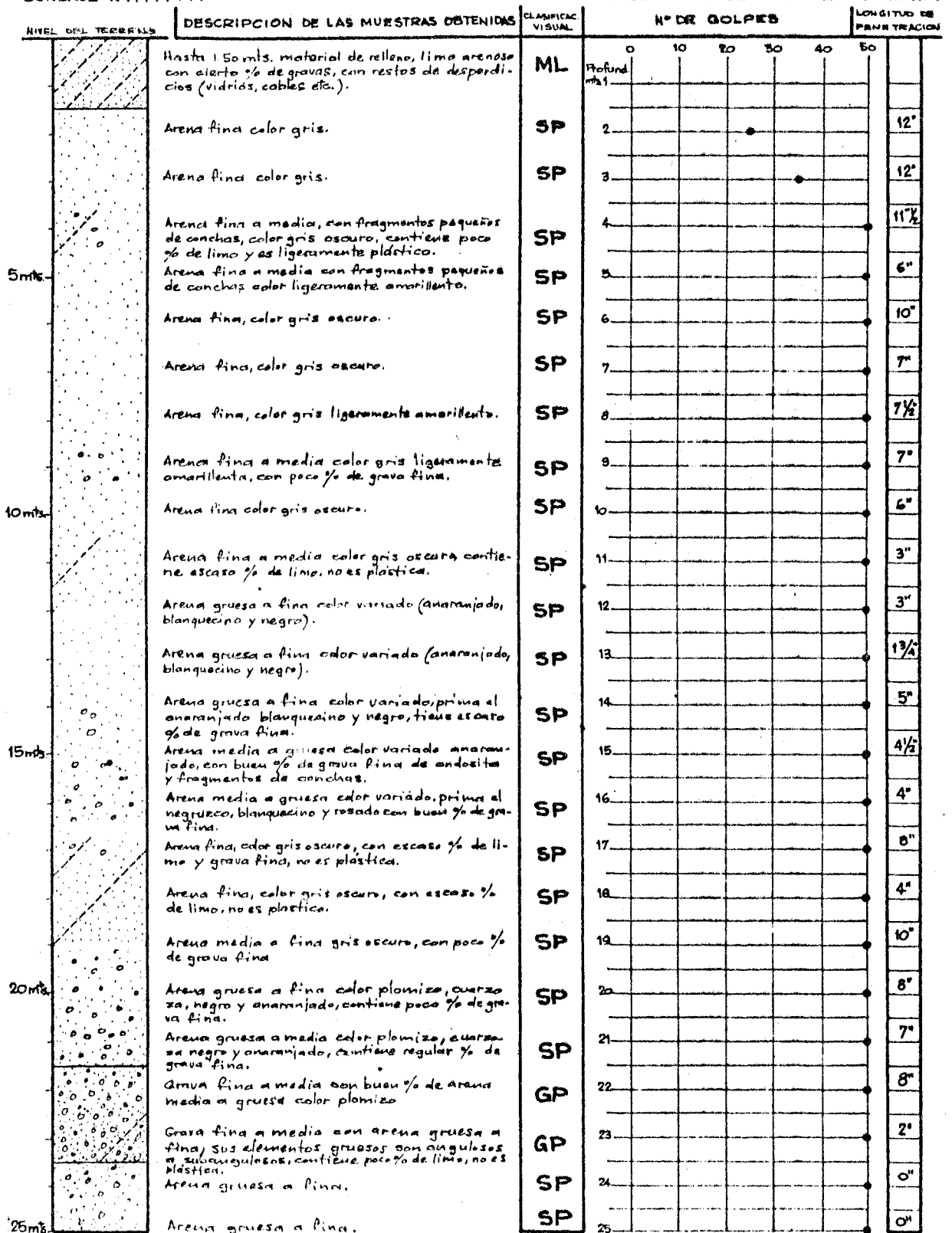


# Fig. A-2-2 PROYECTO CHIMBOTE

## INVESTIGACIONES DEL SUB-SUELO DE CHIMBOTE

UBICACION: Calle Inca Garcilaso de la Vega (Atacado) COTA: ..... NIVEL DE AGUA: ... 3.25 mts.  
 SONDAJE N°... 2 ...

GRAFICO DE LA RESISTENCIA A LA PENETRACION



NOTA: Los elementos gruesos de las arenas son angulares y subangulares, existiendo en la mayoría de las muestras en mayor porcentaje, cuarzo, plagioclasas, ortoclasas y basicas (ferromagnesianas, hematitas, andositas etc.).

# Fig. A-2-3 PROYECTO CHIMBOTE

## INVESTIGACIONES DEL SUB-SUELO DE CHIMBOTE

UBICACION: Zona Alta Perú ..... COTA: ..... NIVEL DE AGUA: 0.70 mts.  
 SONDAJE Nº 3

GRÁFICO DE LA RESISTENCIA A LA PENETRACION

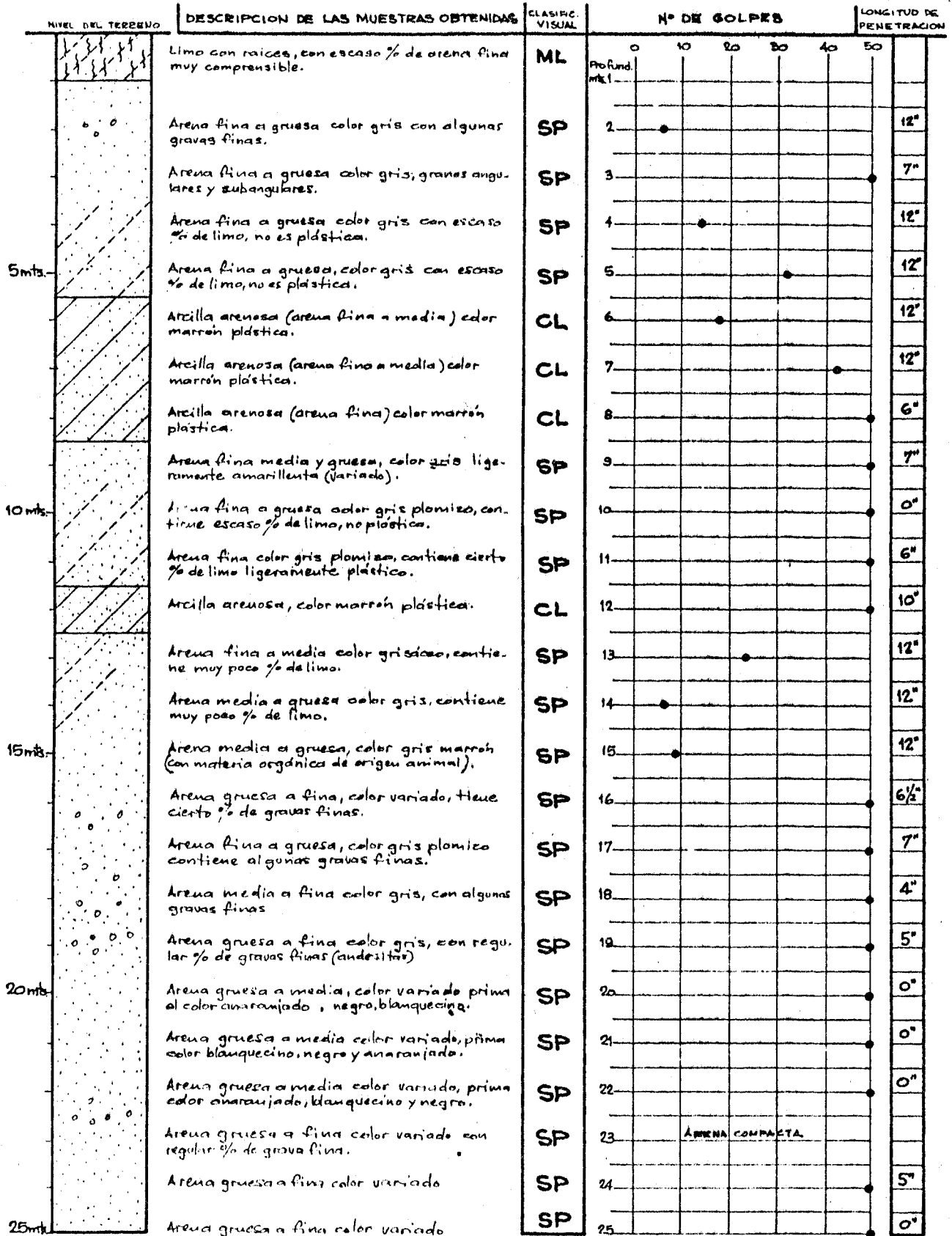


Fig. A-2-4

PROYECTO CHIMBOTE

INVESTIGACIONES DEL SUB-SUELO DE CHIMBOTE

UBICACION: Carretera Intermediana Sur

COTA: .....

NIVEL DE AGUA: Superficial 1.045

SONDAJE N° 4

NIVEL DEL TERRENO	DESCRIPCION DE LAS MUESTRAS OBTENIDAS	CLASIFICACION VISUAL	GRAFICO DE LA RESISTENCIA A LA PENETRACION					FUNDACION DE PUNTERON	
			N° DE GOLPES						
0.70	Limo arenoso con grava fina a gruesa, material de relleno, traido de la carretera.	ML	0	10	20	30	40	50	
	Arena fina a media, color oscuro.	SP							11"
	Arena fina a media, color ligeramente verdusco.	SP							10"
	Arena gruesa a fina, color amarillento, con regular % de grava media a gruesa, los gruesos son angulosos a planos, tiene buen % de fragmentos de conchas, tiene regular % de arcilla, es ligeramente plastica.	SP							6"
5m	Arena fina a gruesa color ligeramente verdusco con escaso % de limo, no es plastica.	SP							7"
	Arena fina a gruesa, color ligeramente verdusco con escaso % de limo, no es plastica.	SP							12"
	Arena fina color verde oscuro con escaso % de limo, no es plastica.	SP							8"
	Arcilla con arena fina, color verde amarillento bien plastica.	CL							10"
	Arcilla con arena fina, color verde amarillento bien plastica.	CL							8"
10m	Arena fina limosa, color verde amarillento ligeramente plastica.	SM							10"
	Arena fina a media, color verde amarillento con tiene escaso % de limo, no es plastica.	SP							8"
	Arena gruesa a fina, color verdusco con escaso % de arcilla, no es plastica, sus elementos gruesos son angulosos a subangulosos (Cuorras, ortos, micos, basires) se recupera grava gruesa.	SP							6"
	Arena gruesa a fina, con regular % de grava fina con regular % de arcilla, es ligeramente plastica.	SC <sup>o</sup> SP							9"
	Arena gruesa a fina, con regular % de grava media color verdusco amarillento, con regular % de arcilla es ligeramente plastica.	SC <sup>o</sup> SP							7"
15m	Arena fina color verde amarillento con escaso % de arcilla no plastica, con grava fina y gruesa.	SP							5 1/2"
	Arena fina color verde oscuro, con escaso % de limo no es plastica.	SP							4 1/2"
	Arena fina a media color verde amarillento con escaso % de limo, no es plastica.	SP							5"
	Arena fina a media color amarillento con escaso % de arcilla, contiene grava fina, no es plastica.	SP							8"
	Arena fina a media, color amarillento, con escaso % de arcilla, no es plastica.	SP							10"
20m	Arena fina a media color verdusco, con escaso % de arcilla, no es plastica.	SP							6"
	Arena fina a media color verdusco amarillento, con regular % de arcilla ligeramente plastica.	SC <sup>o</sup> CL							12"
	Arena fina color verde amarillento con escaso % de arcilla, no es plastica.	SP							11 1/2"
	Arena fina a gruesa color verde amarillento con escaso % de arcilla, con cierto % de grava fina, no es plastica.	SP							7"
25m	Arcilla con arena fina color marron, plastica.	CL							3"
	Arena fina a gruesa, color café oscuro con escaso % de limo, no es plastica.	SP							3 1/2"
26m	Arena fina color café oscuro, con escaso % de limo, no es plastica.	SP							
			no se hizo prueba						

Fig. A-2-5

PROYECTO CHIMBOTE  
INVESTIGACIONES DEL SUB-SUELO DE CHIMBOTE

UBICACION: Zona Buenos Aires, frente calle Huaraz. COTA: .....  
SONDAJE N° 5

NIVEL DE AGUA: 16.15 mts.

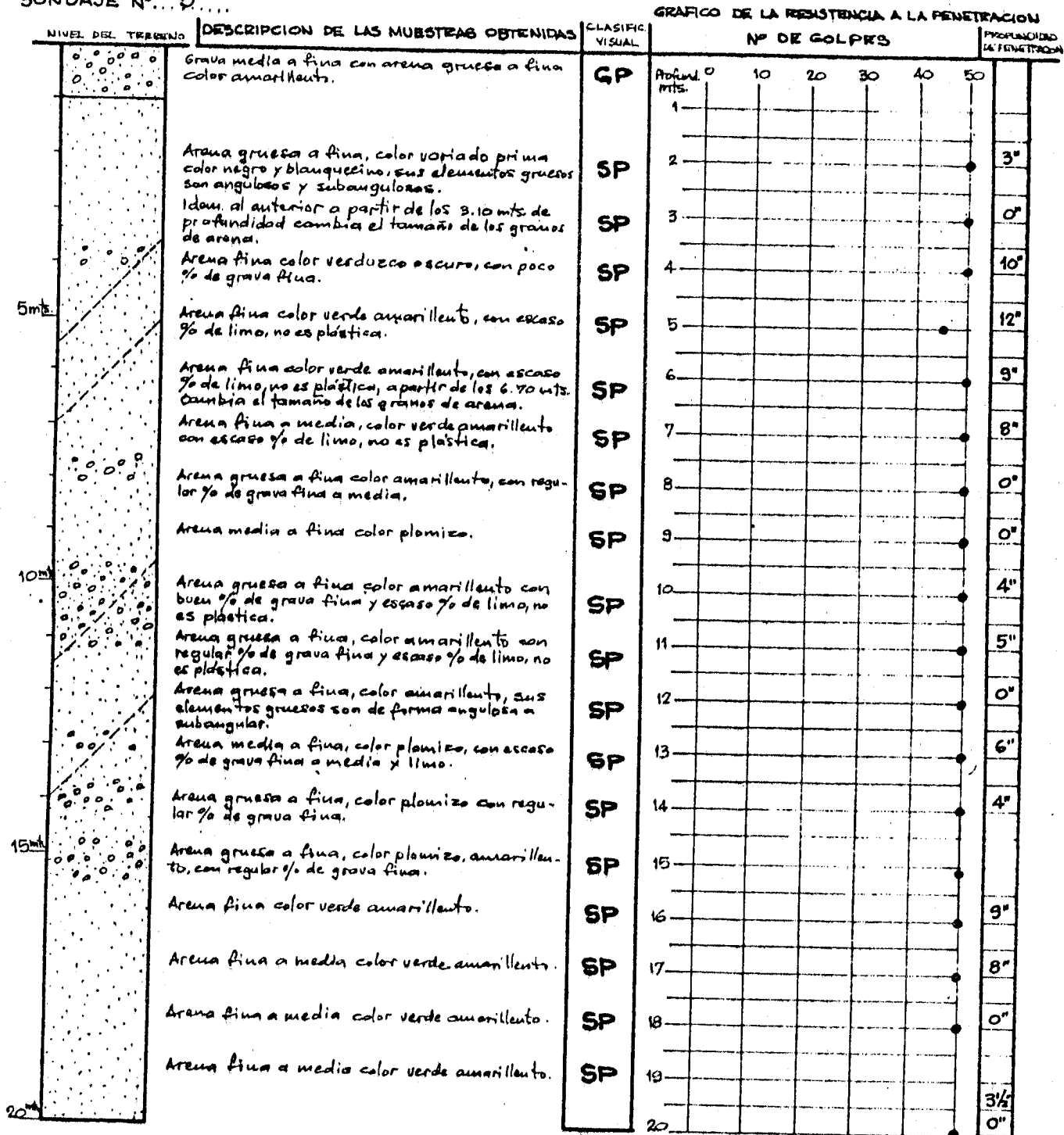


Fig. A-2-6

PROYECTO CHIMBOTE  
INVESTIGACIONES DEL SUB-SUELO DE CHIMBOTE

UBICACION: Zona Miramar Bajo-frente al Instituto Industrial COTA: .....  
SONDAJE N° 7

NIVEL DE AGUA: ± 4.25 mts.

GRAFICO DE LA RESISTENCIA A LA PENETRACION

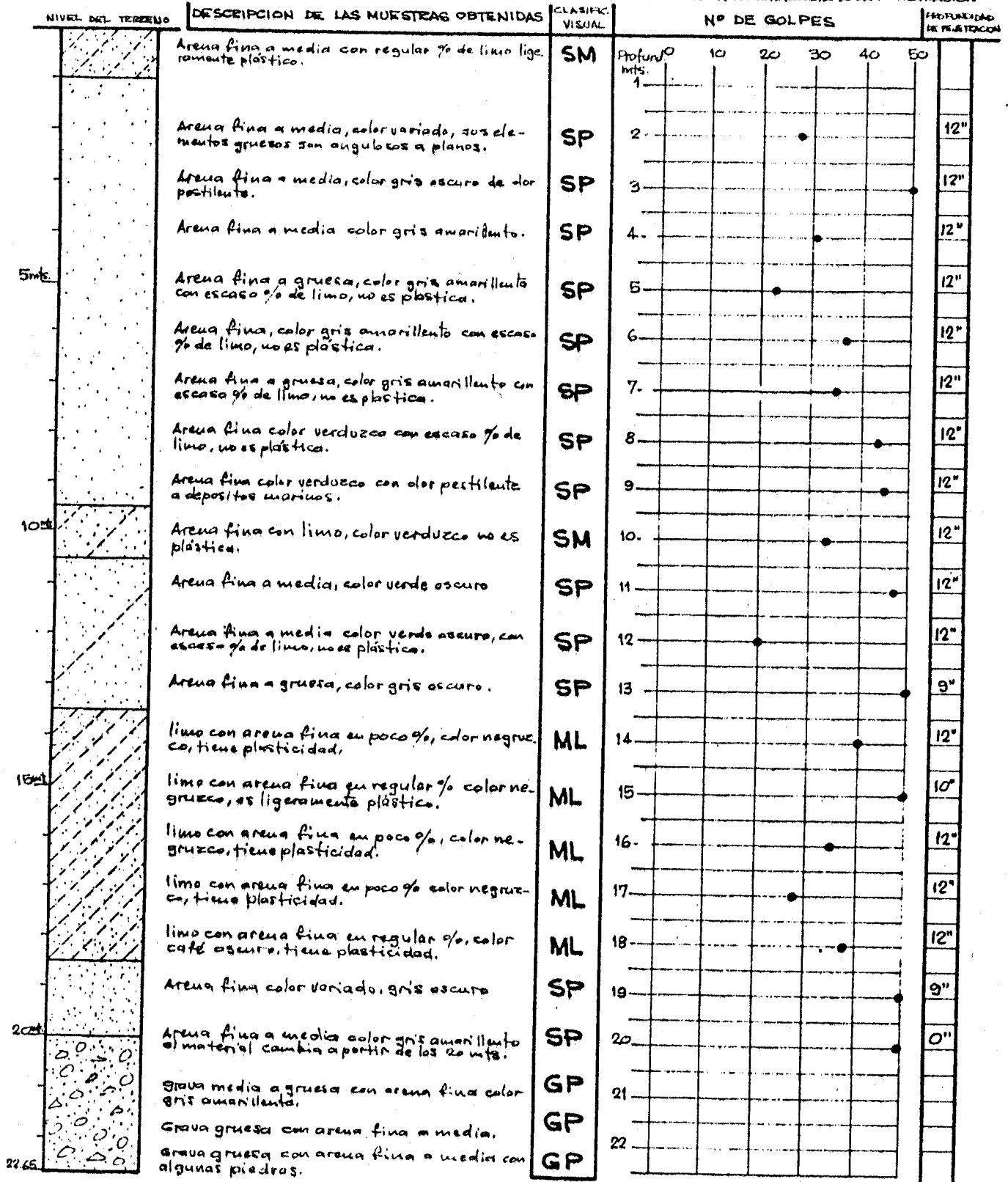


Fig. A-2-7

PROYECTO CHIMBOTE

INVESTIGACIONES DEL SUB-SUELO DE CHIMBOTE

UBICACION: Zona "La Caleta", Marítima, Esquina "Planta B"

COTA: ..... NIVEL DE AGUA: 1.67 mts.

SONDA Z N° B

GRAFICO DE LA RESISTENCIA A LA PENETRACION

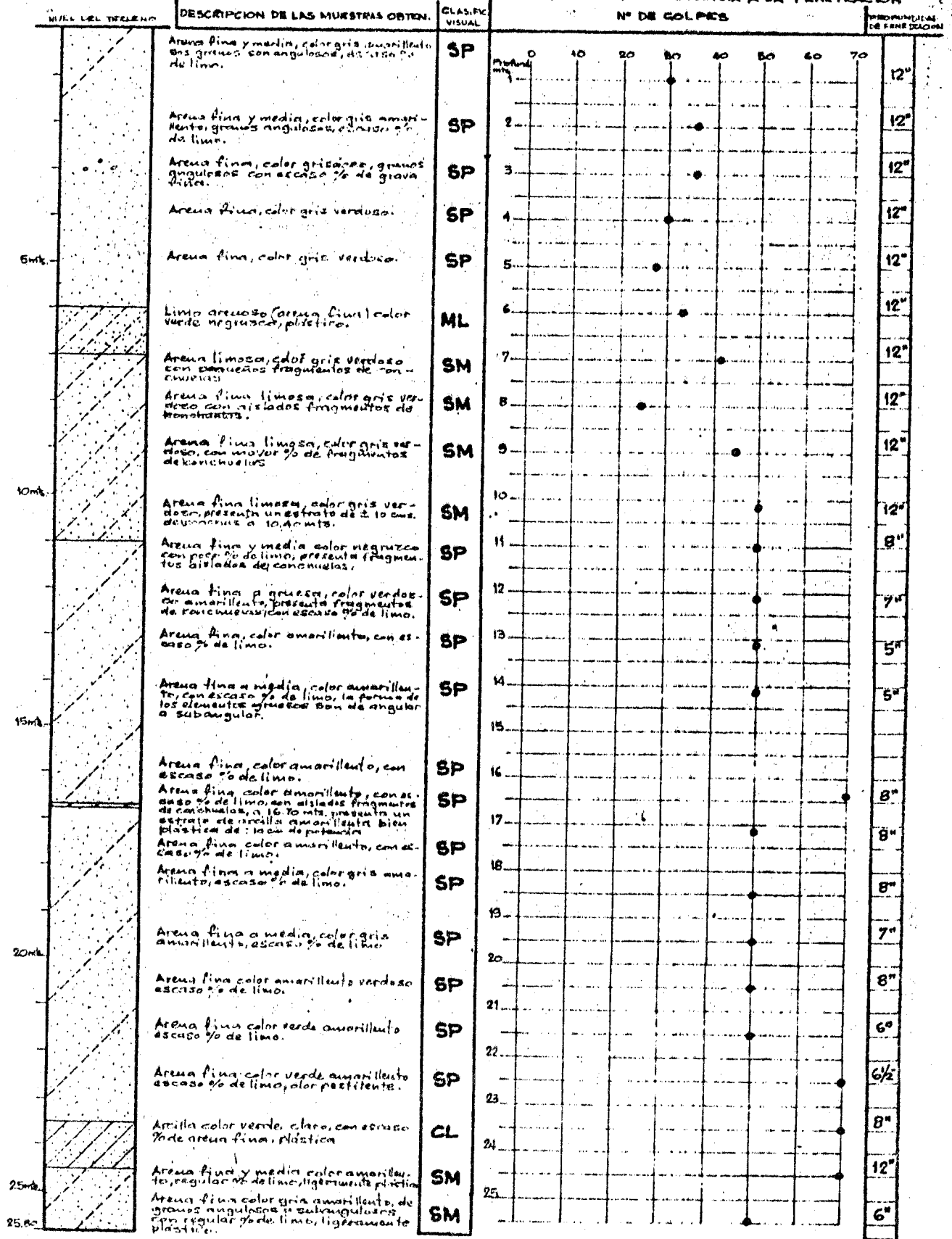




Fig. A-2-8

PROYECTO CHIMBOTE

INVESTIGACIONES DEL SUB-SUELO DE CHIMBOTE

UBICACION: Zona 2da Miraflores, Esq. Jr. Callao y Av. Ferrocarril

COTA: ..... NIVEL DE AGUA: 1.40 mts.

SONDAJE N° 10

GRAFICO DE LA RESISTENCIA A LA PENETRACION

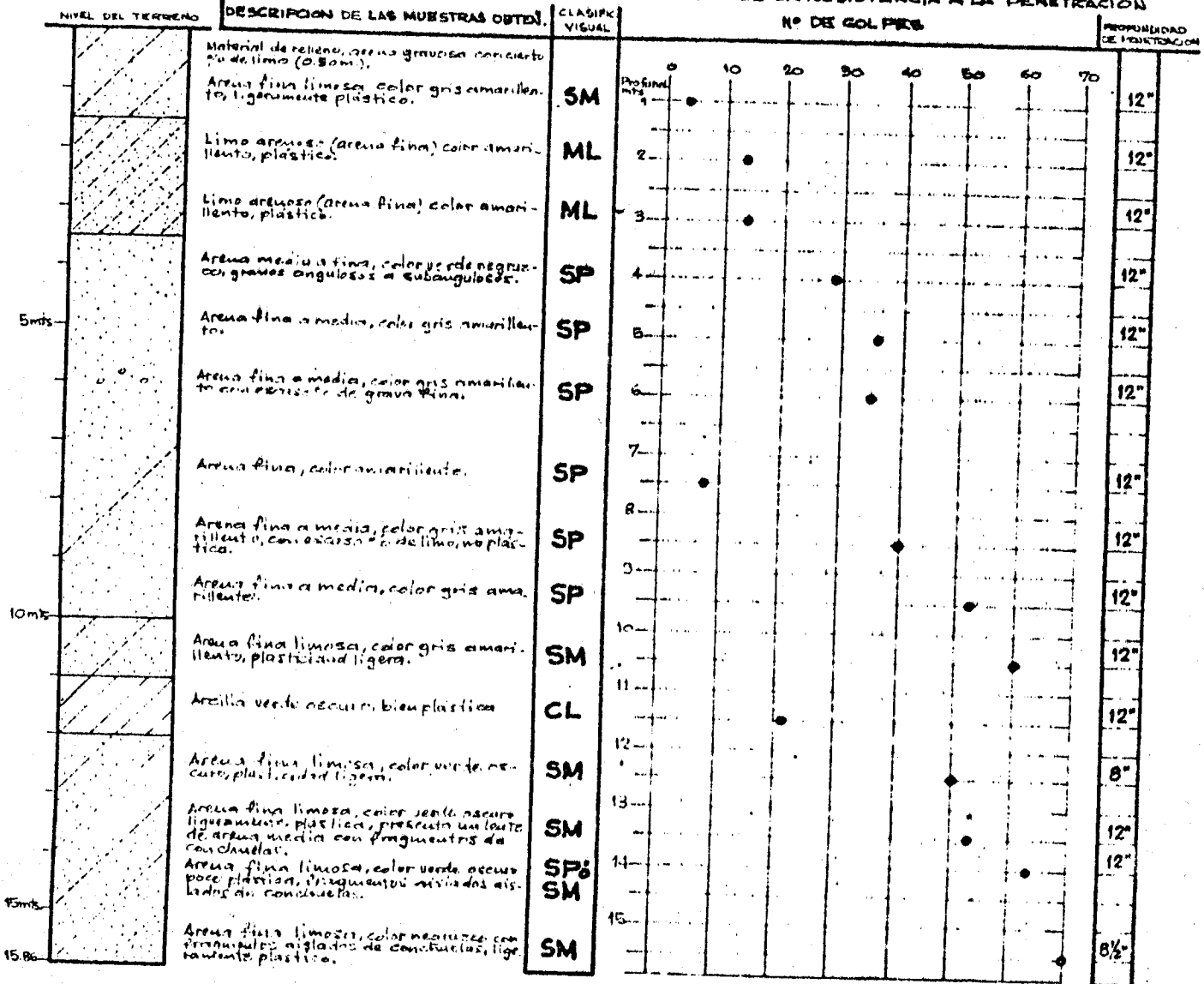


Fig. A-2-9

PROYECTO CHIMBOTE

INVESTIGACIONES DEL SUB-SUELO DE CHIMBOTE

UBICACION: Zona 27 de Octubre, Av. los Resplandores (Extram. Huanan) cota: ..... NIVEL DE AGUA: ± 1.00mts.

SONDAJE Nº 11

GRAFICO DE LA RESISTENCIA A LA PENETRACION

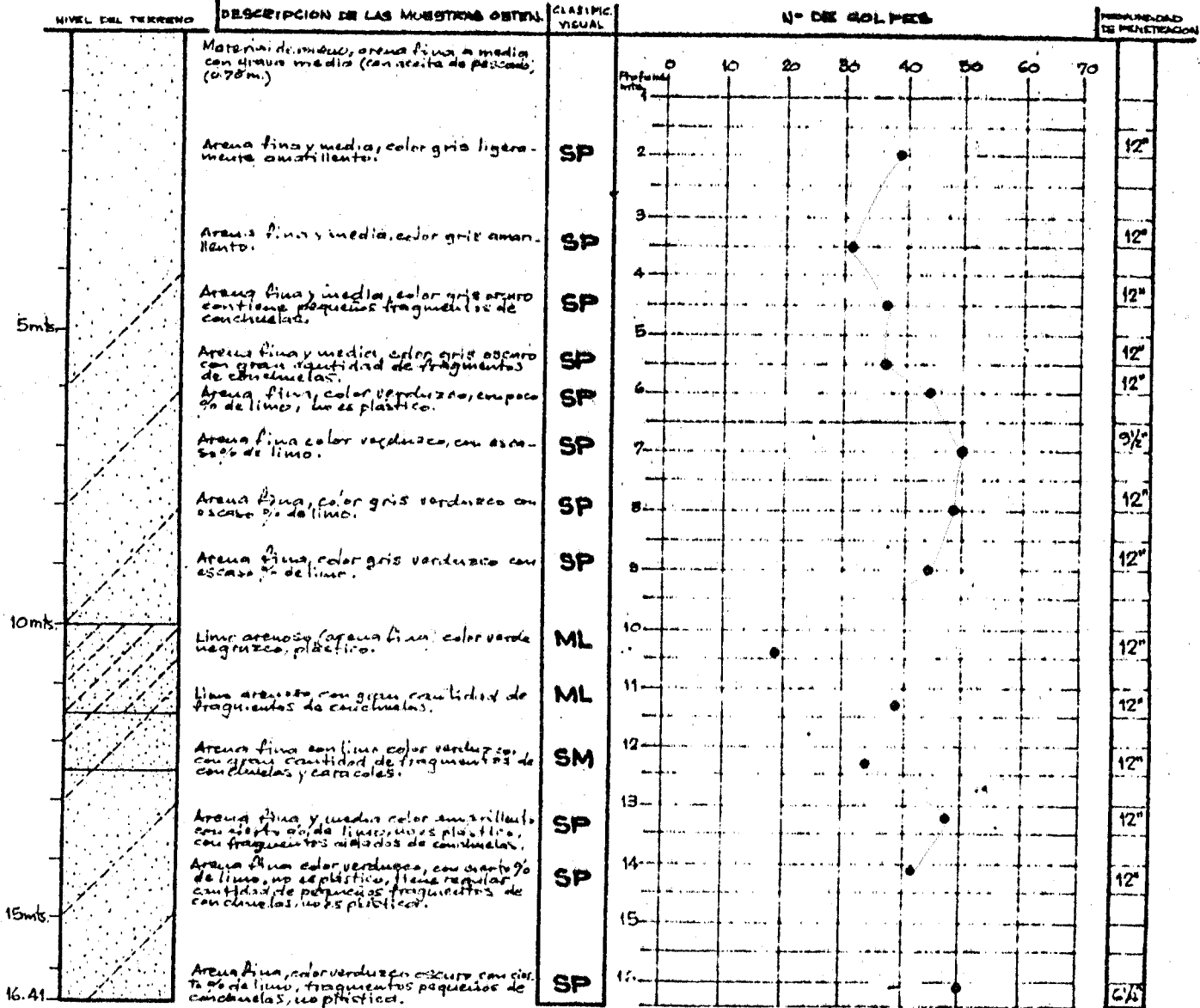


Fig. A-2-10

PROYECTO CHIMBOTE

INVESTIGACIONES DEL SUB-SUELO DE CHIMBOTE

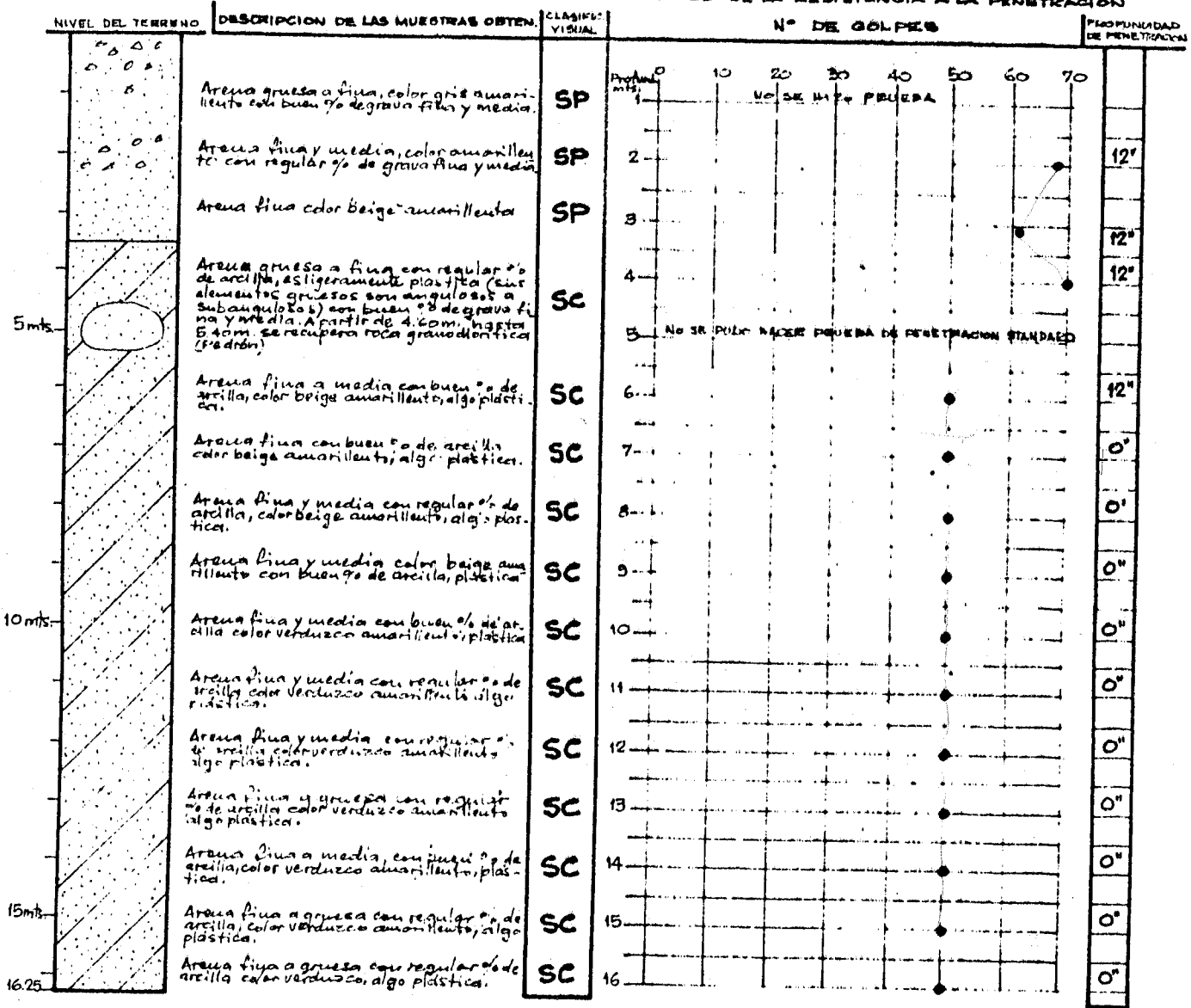
UBICACION: Zona Alta "Buenos Aires"

COTA:

NIVEL DE AGUA: No se encontro

SONDAJE N° 12

GRAFICO DE LA RESISTENCIA A LA PENETRACION



# Fig. A-2-11 PROYECTO CHIMBOTE

## INVESTIGACIONES DEL SUB-SUELO DE CHIMBOTE

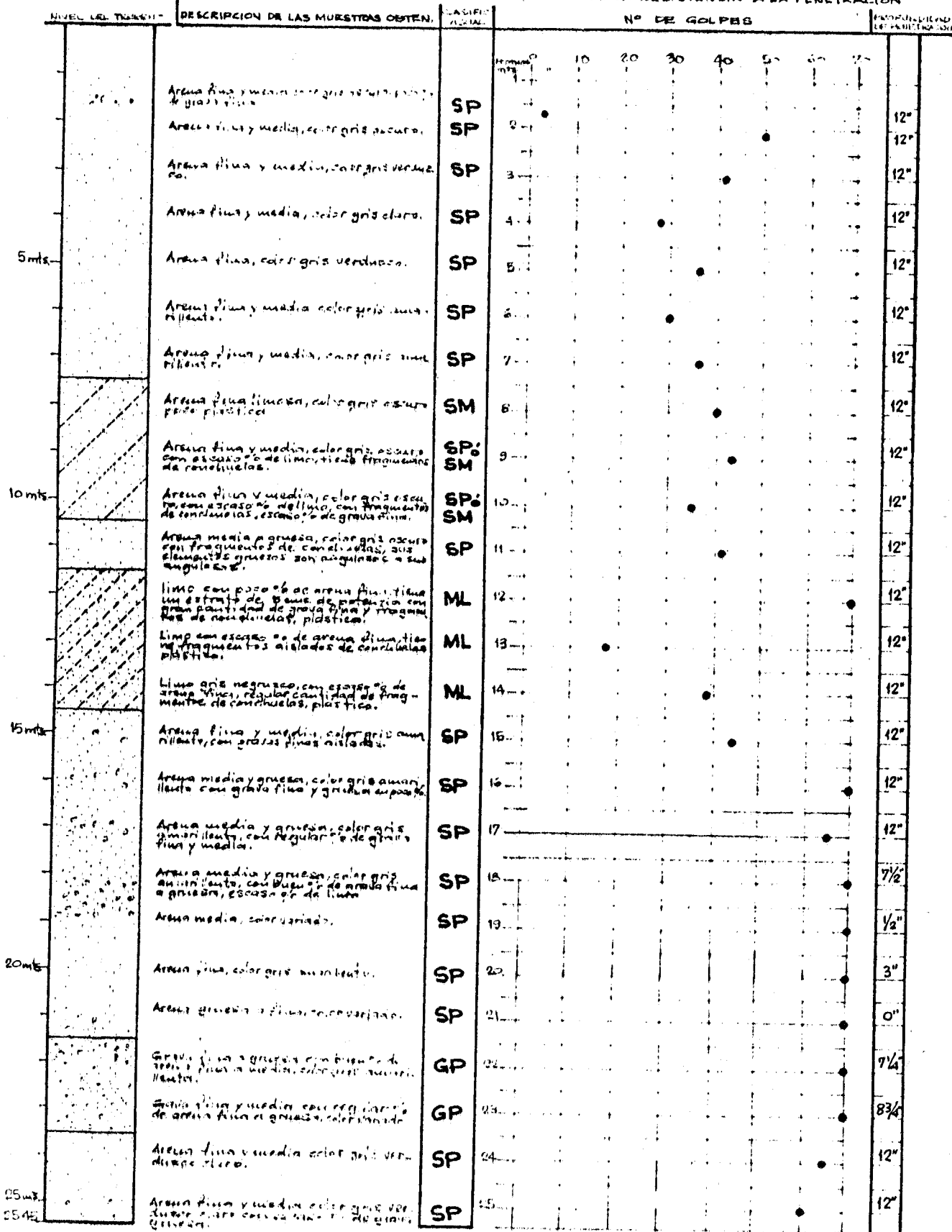
UBICACION: 200 M. al sur de Bajo - Escuela, República de Perú

COTA:

NIVEL DEL AGUA: 0.70 mts.

SONDAJE N° 13

### GRÁFICO DE LA RESISTENCIA A LA PENETRACION



# Fig. A-2-12 PROYECTO CHIMBOTE

## INVESTIGACIONES DEL SUB-SUELO DE CHIMBOTE

UBICACION: Urb. "Unidad", Calle 100, Lima

COTA: Nivel LA AGUA: ± 4.60 mts.

SONDAJE N° 15

GRAFICO DE LA RESISTENCIA A LA PENETRACION

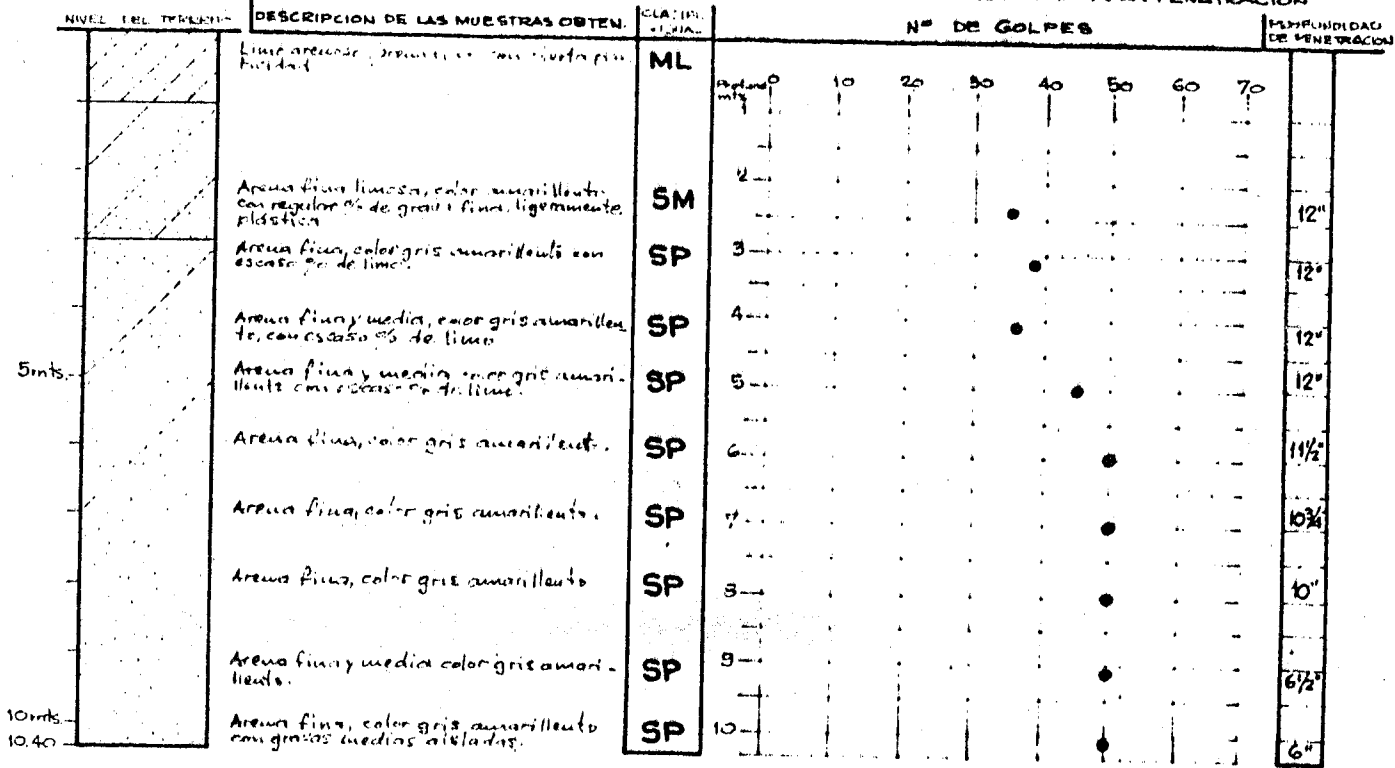


Fig. A-2-13

PROYECTO CHIMBOTE

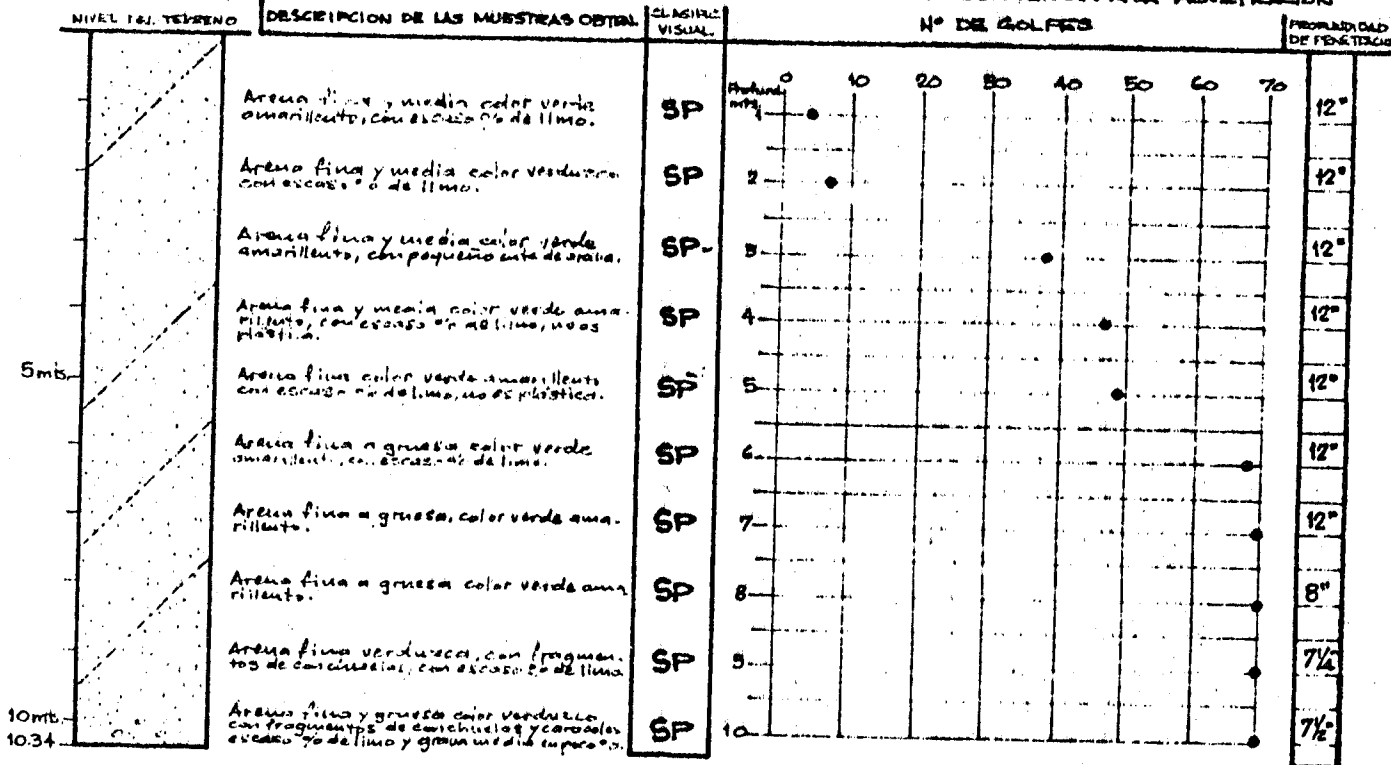
INVESTIGACIONES DEL SUB-SUELO DE CHIMBOTE

UBICACION: Zona "Miraflores Alto" Av. Hards

COTA: ..... NIVEL DEL AGUA: ..... 0.80 mt.

SONDAJE Nº 17

GRAFICO DE LA RESISTENCIA A LA PENETRACION



## **Appendix 3**

### **Results of Grain Size Analysis**

Fig. A-3-1

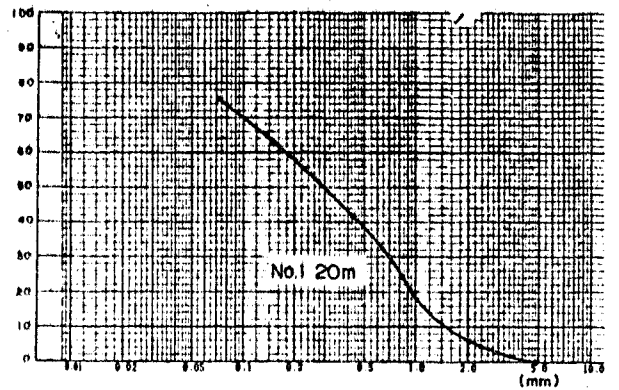
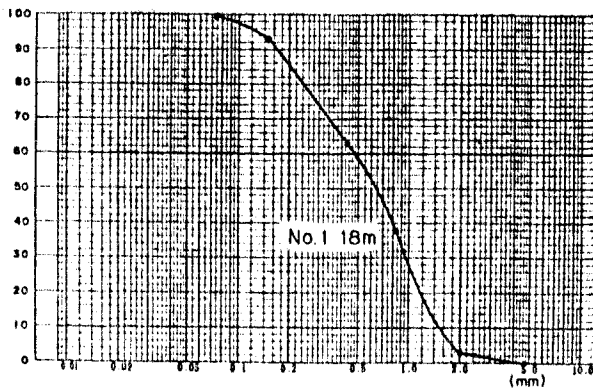
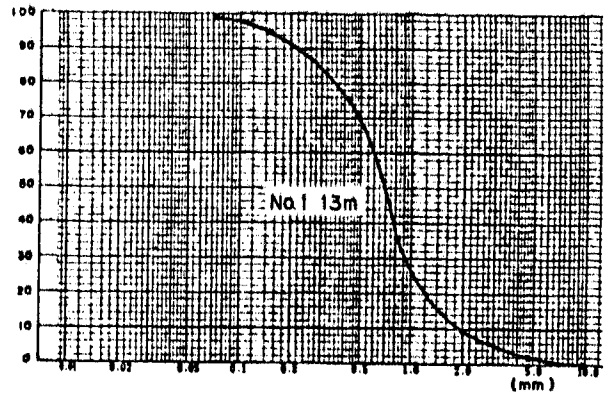
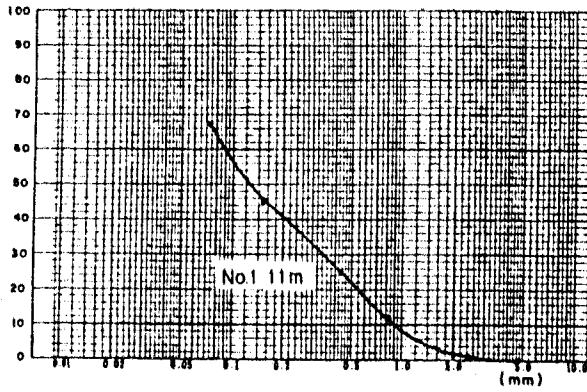
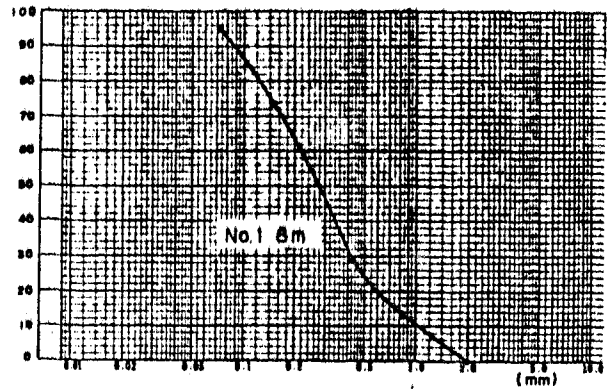
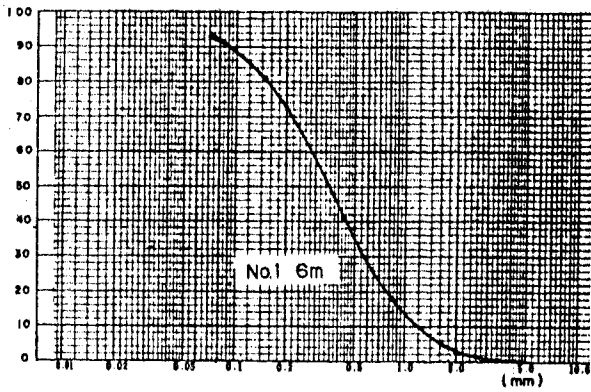
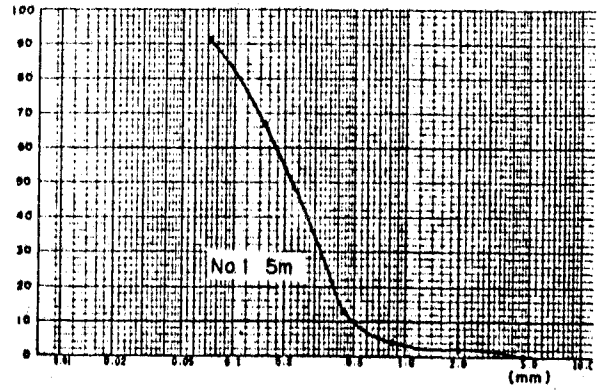
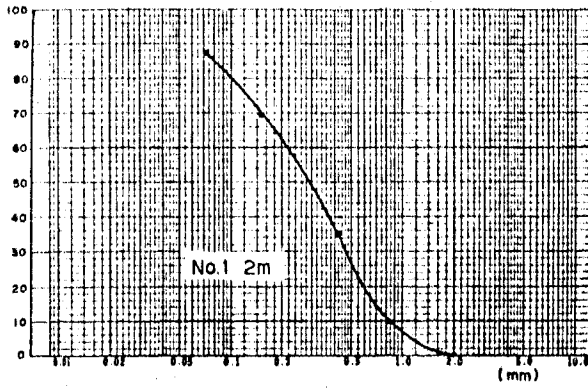




Fig. A-3-2

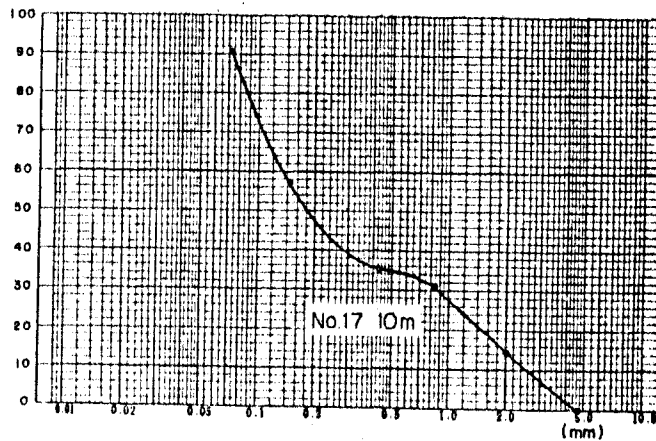
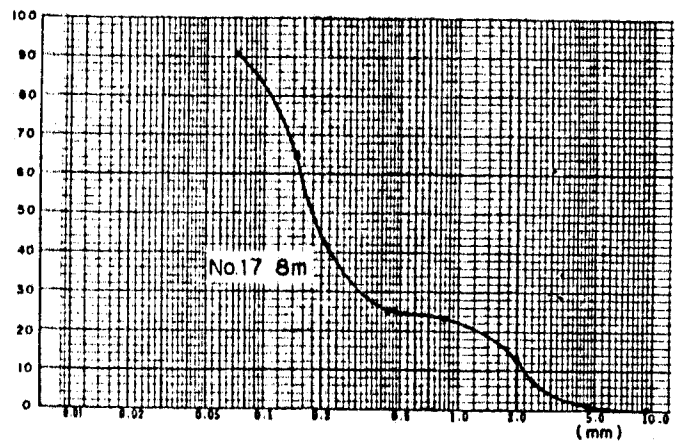
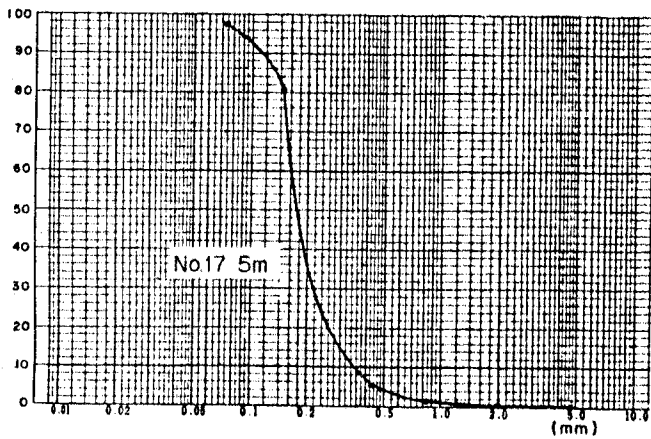
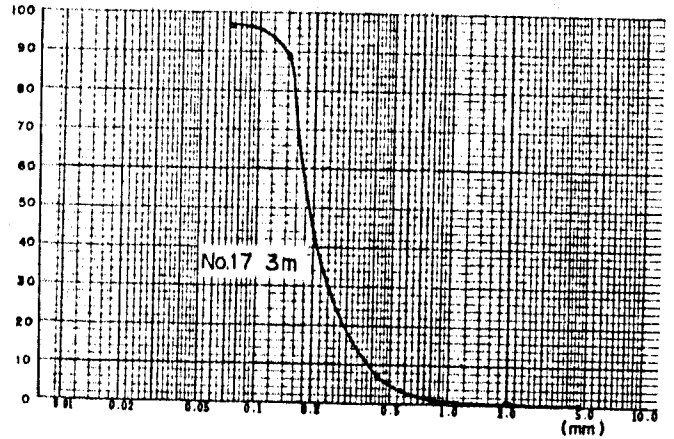
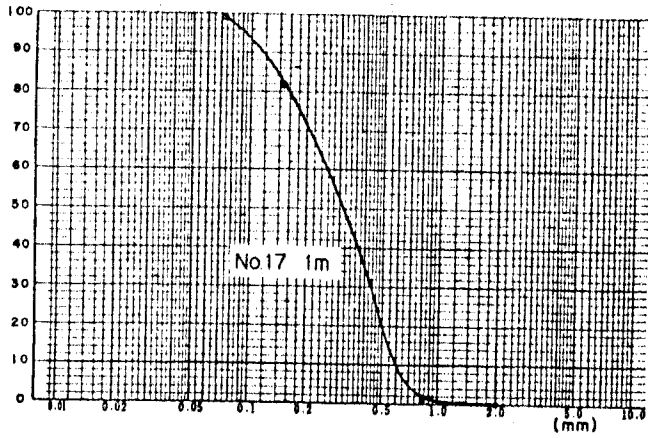


Fig. A-3-3

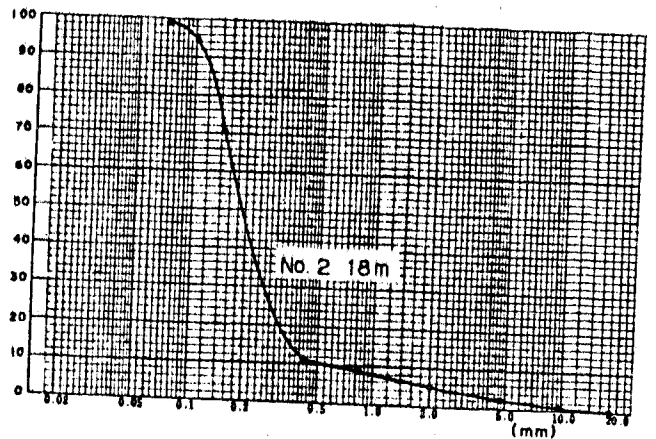
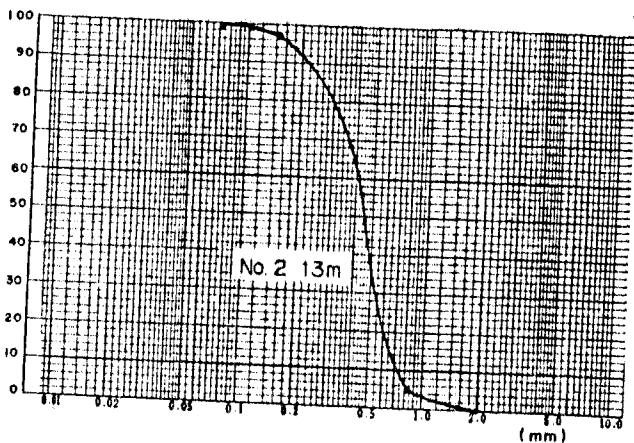
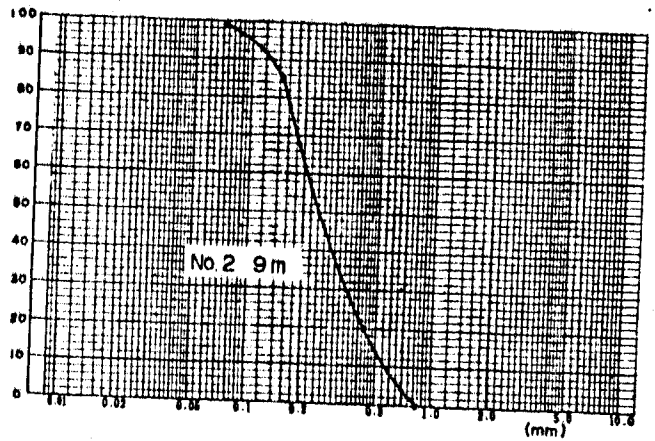
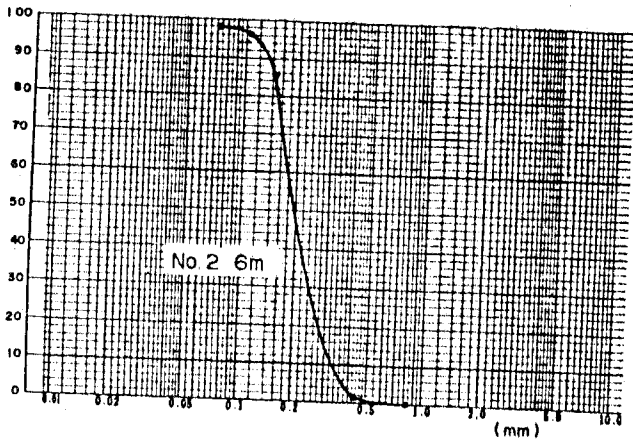
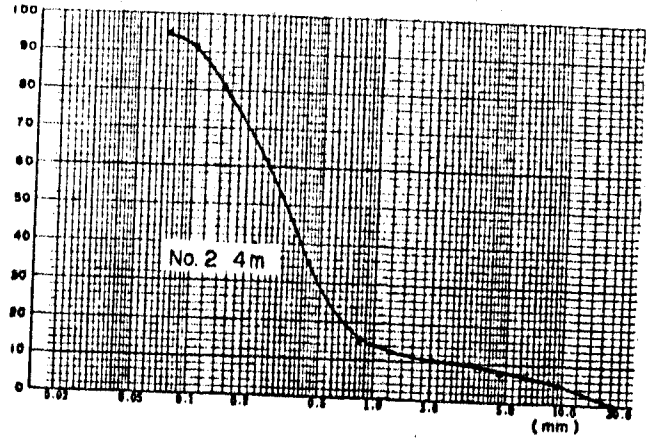
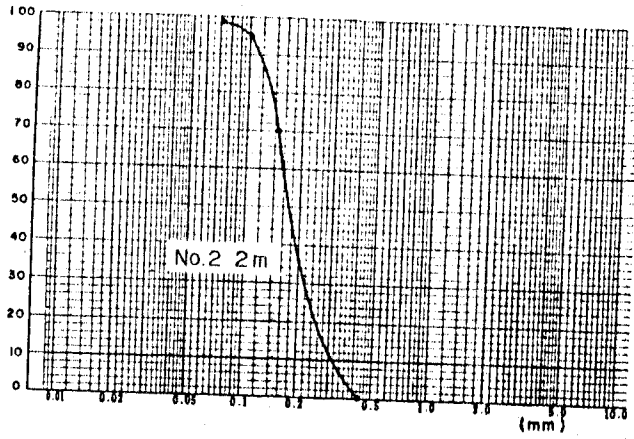


Fig. A-3-4

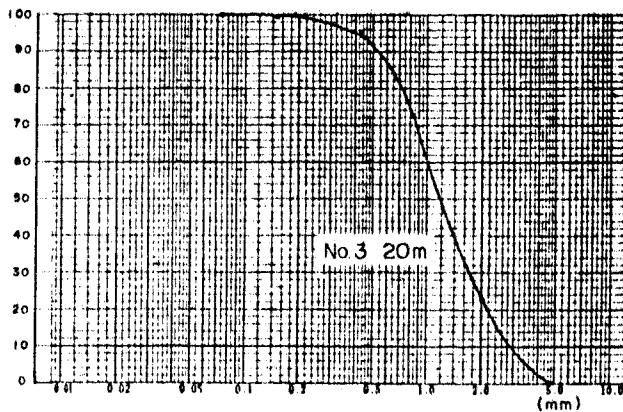
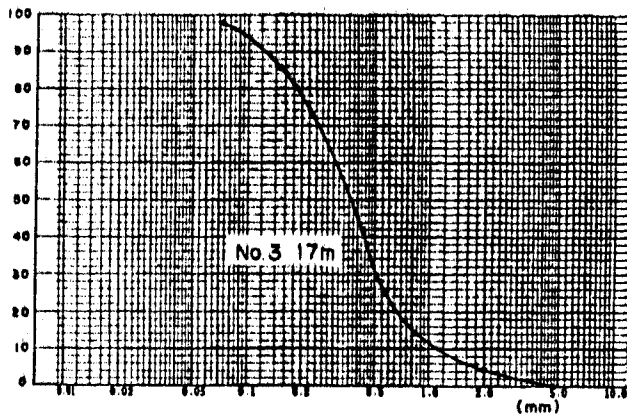
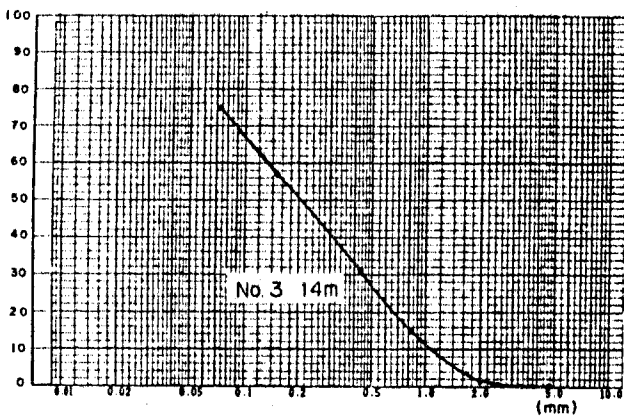
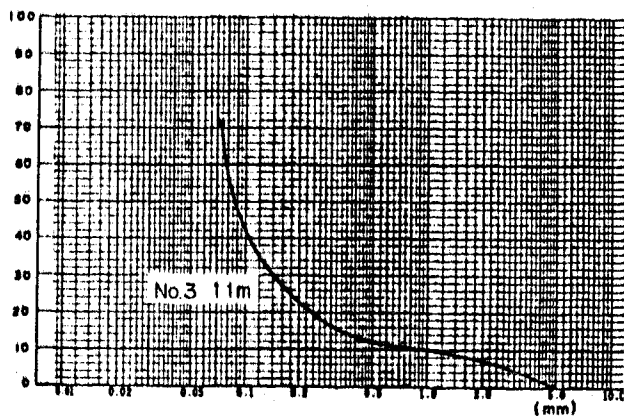
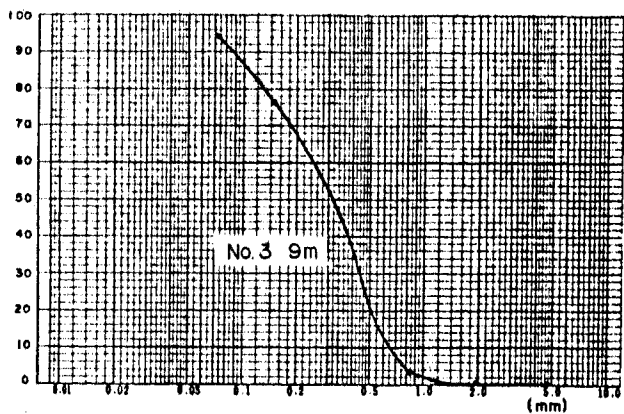
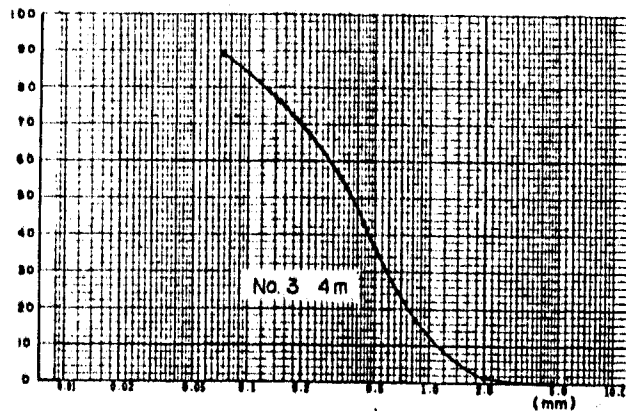
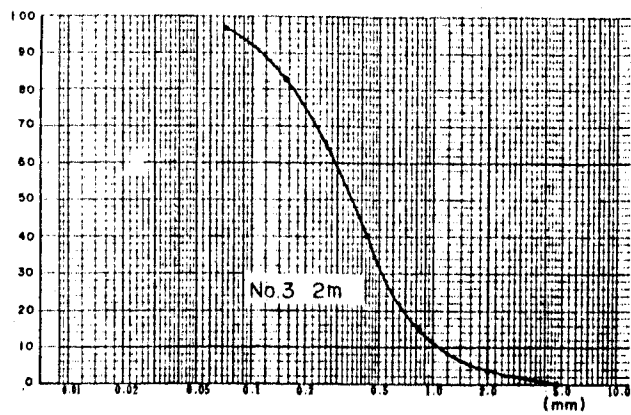


Fig. A-3-5

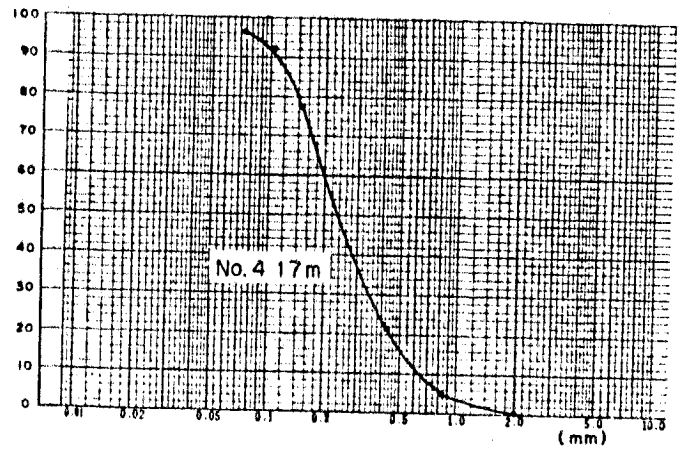
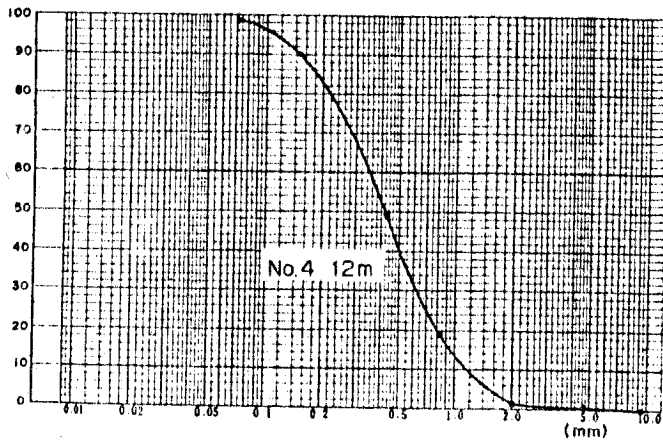
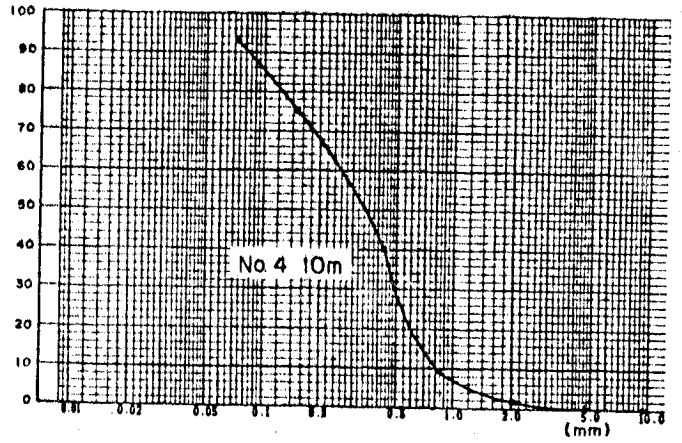
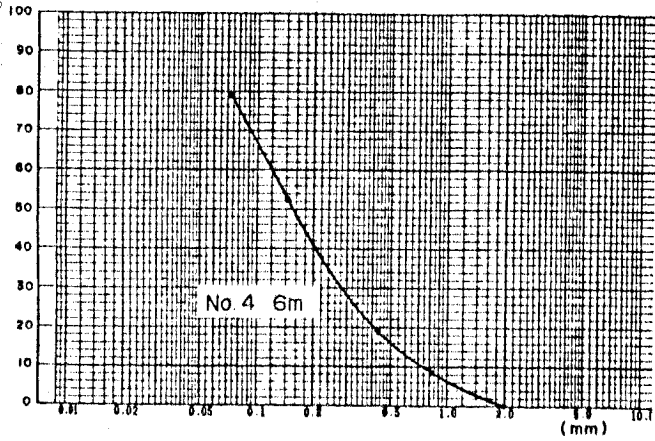
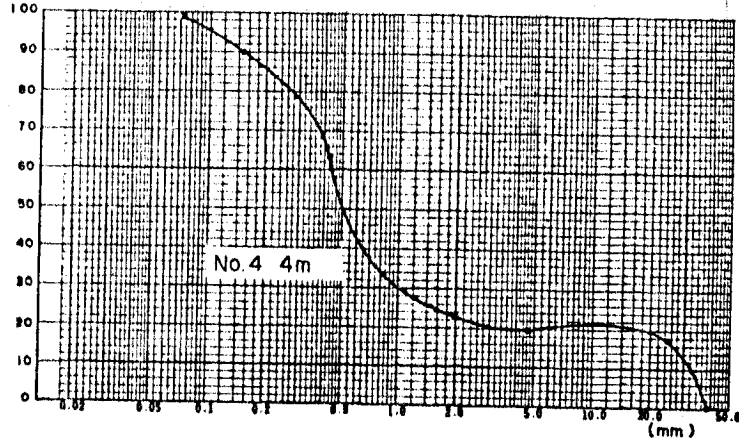
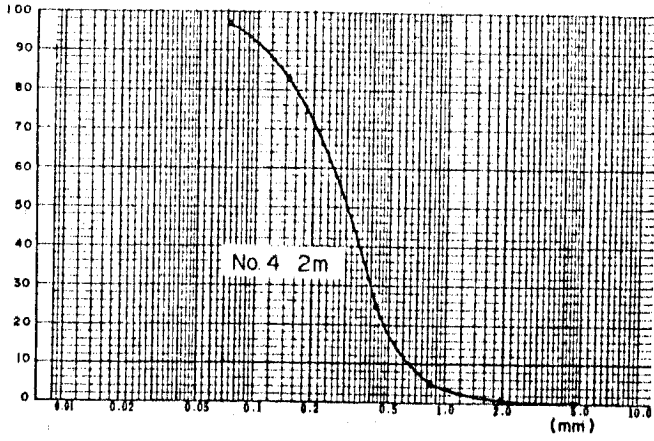


Fig. A-3-6

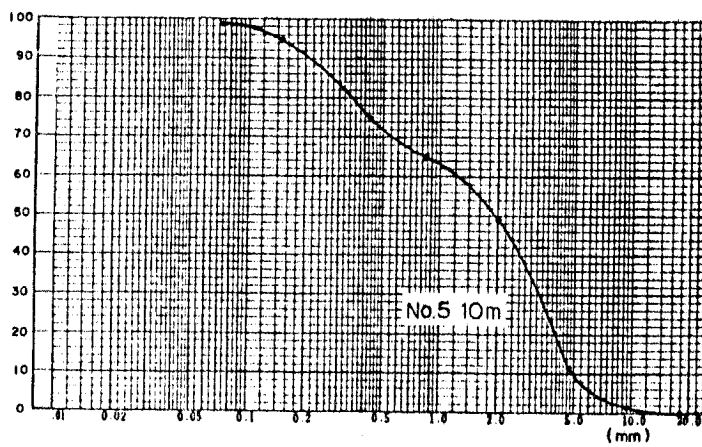
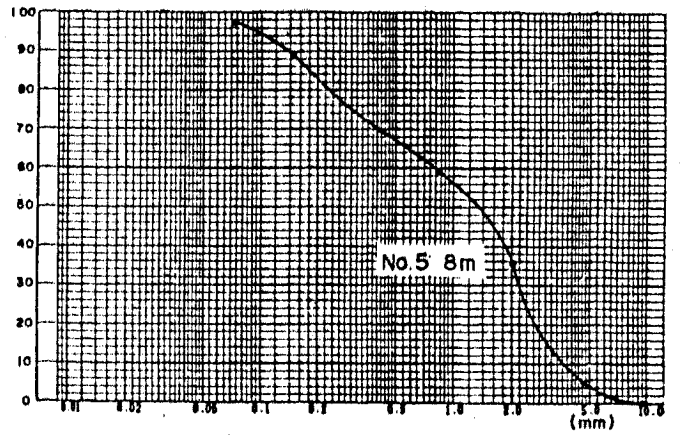
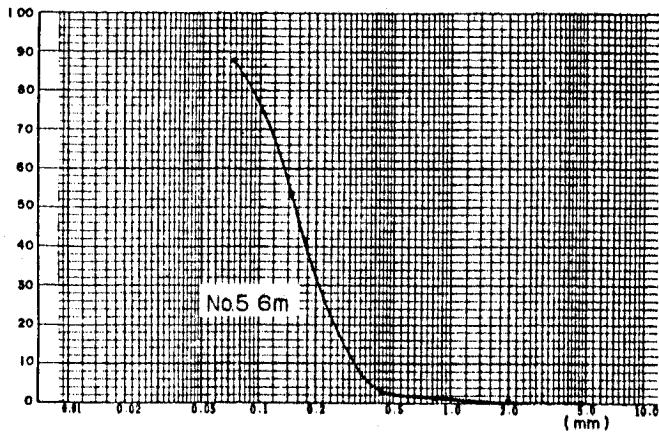
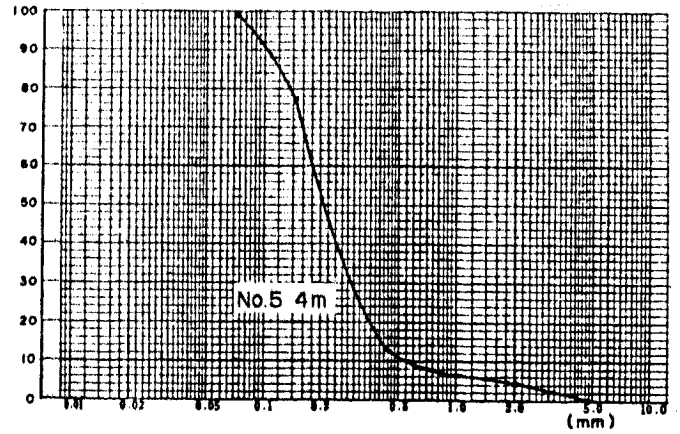
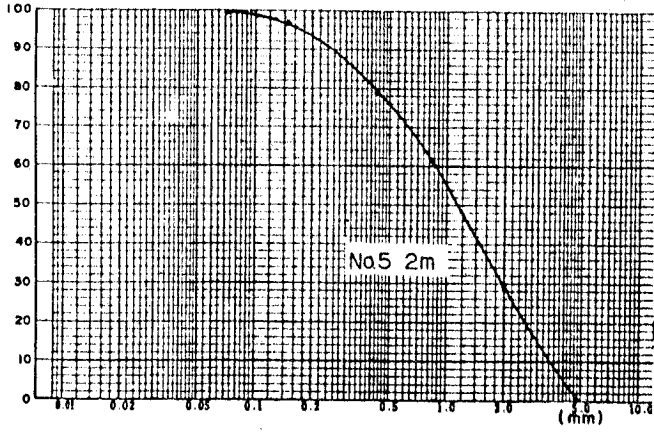


Fig. A-3-7

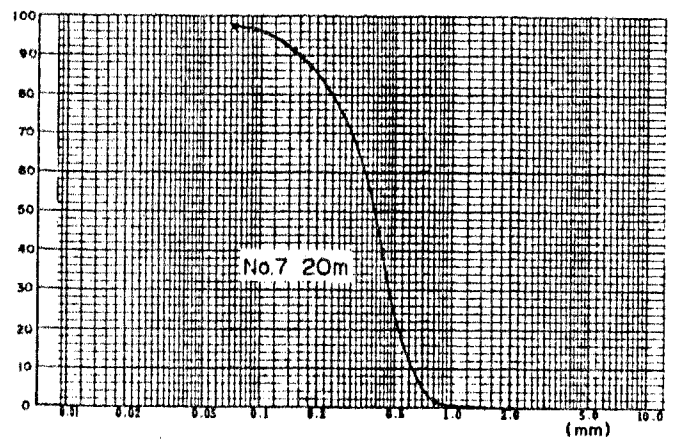
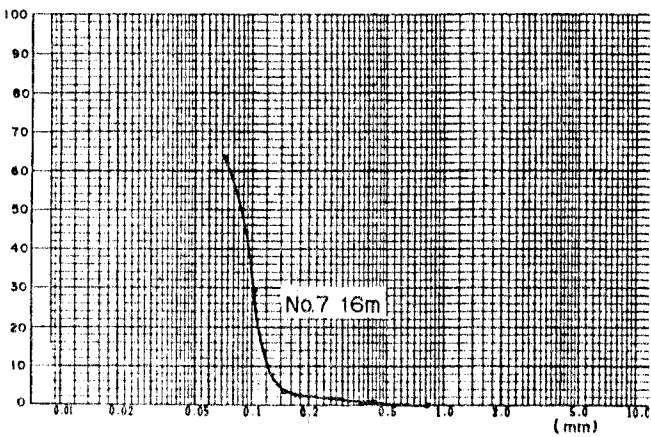
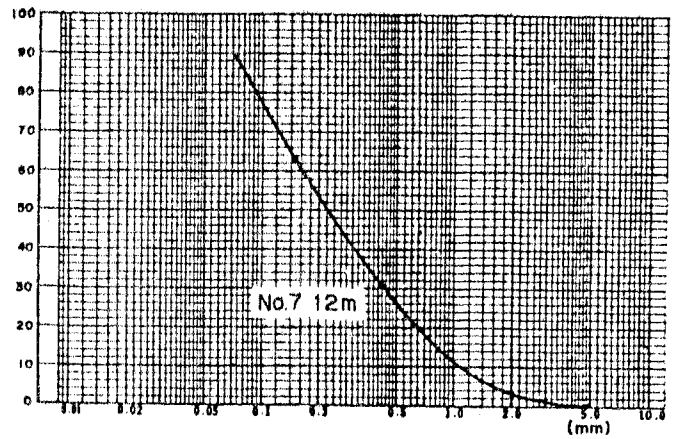
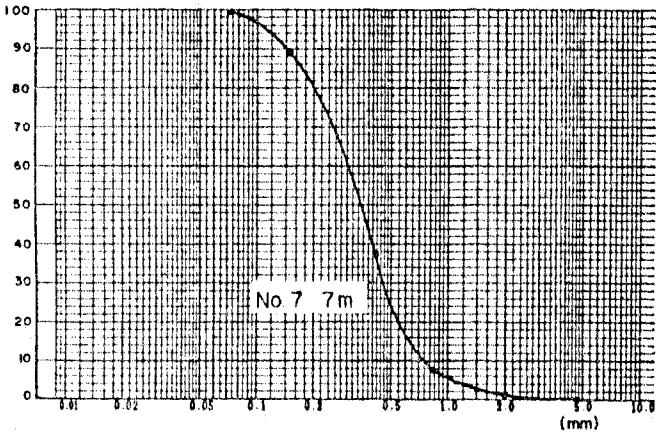
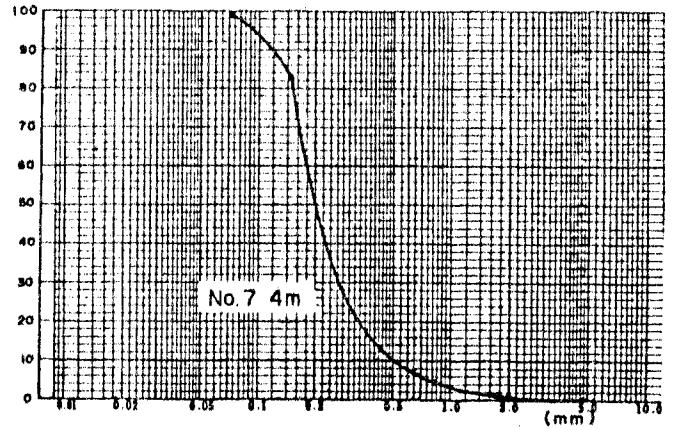
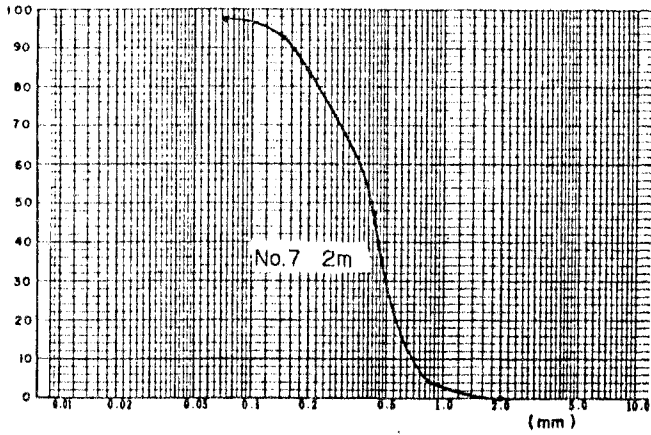


Fig. A-3-8

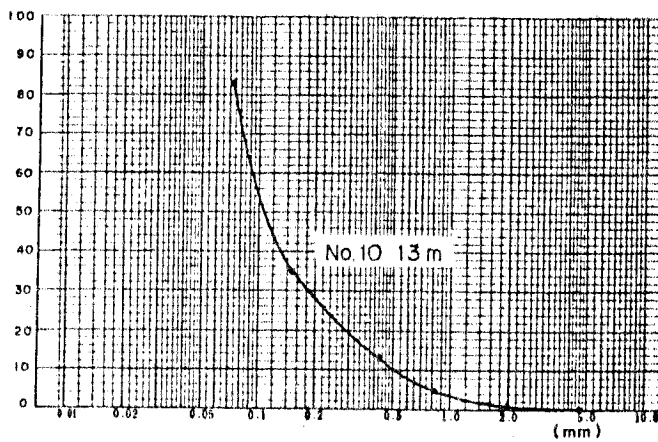
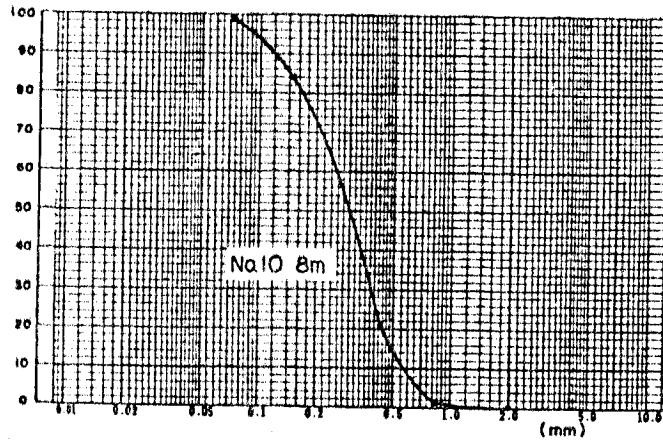
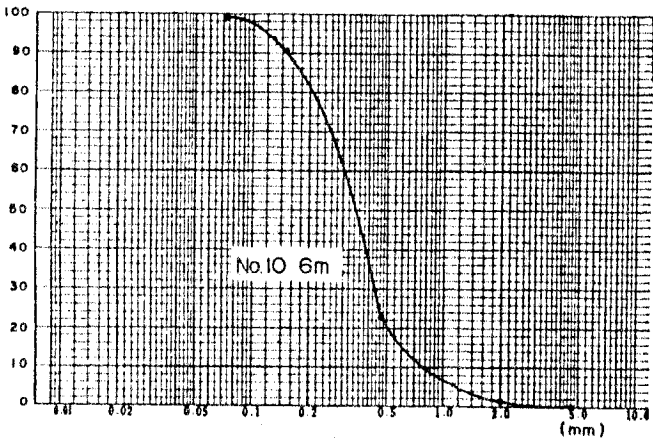
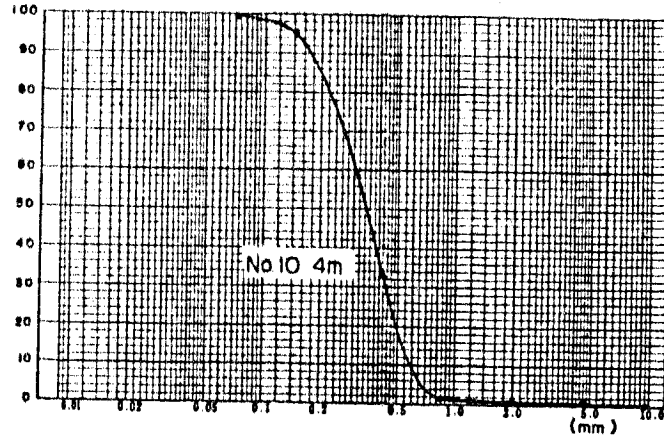
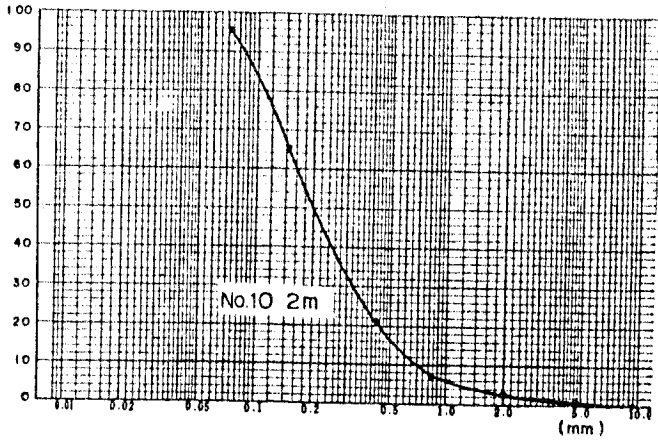
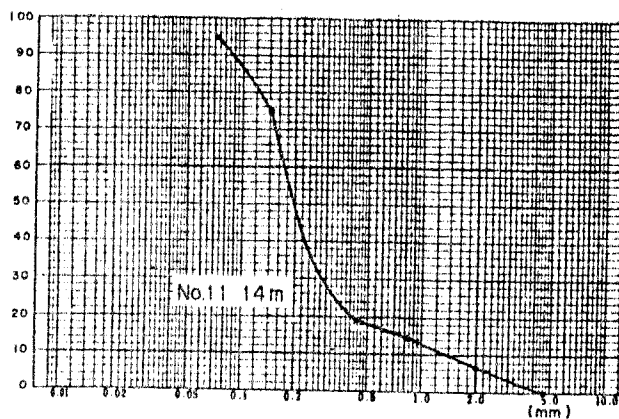
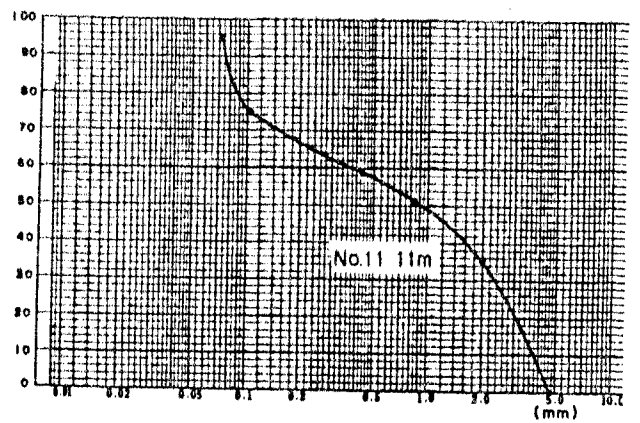
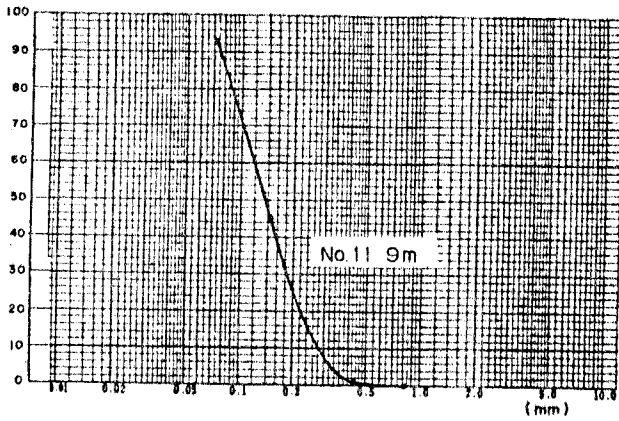
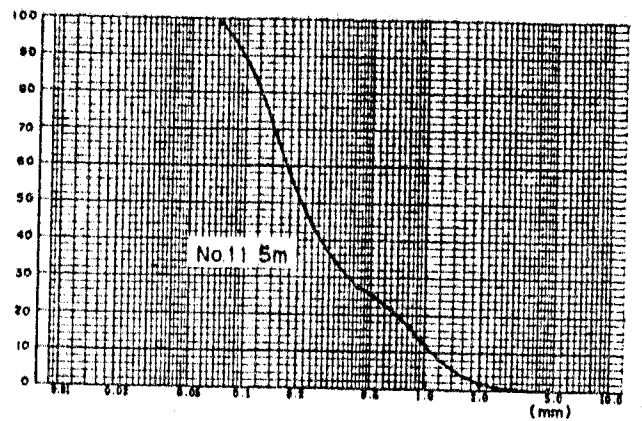
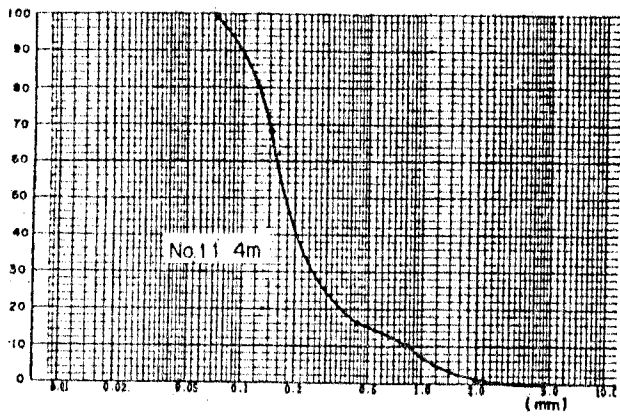
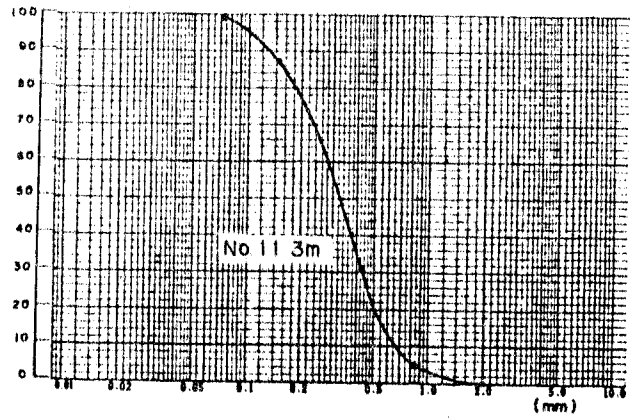
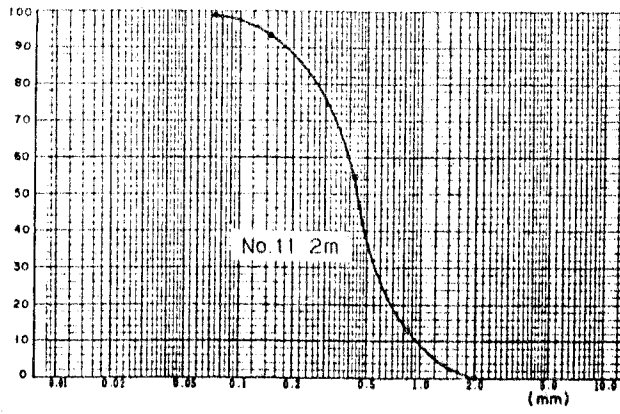


Fig. A-3-9

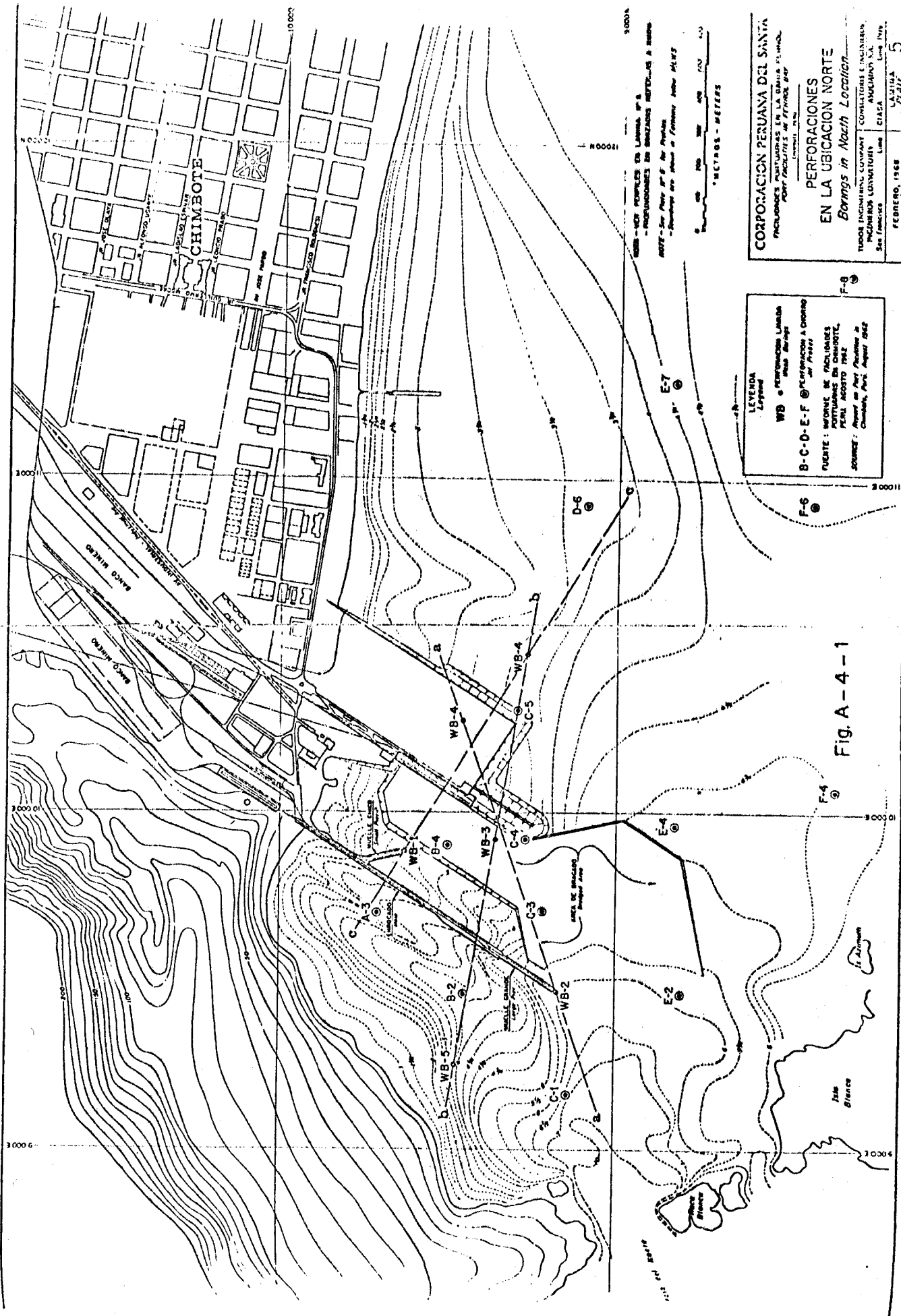




## **Appendix 4**

### **Pre-existing Data of Water-wells and Borings**

- I. From Report on Port Facilities in Chimbote  
Perú August 1962**
  
- II. From Report of Ministerio de Fomento  
y Obras Publicas Sub Direccion de Obres  
Sanitaris**



3000  
 3500  
 4000  
 4500  
 5000

0 100 200 300 400  
 METROS - METERS

**CORPORACION PERUANA DEL SANTA**  
 INVESTIGACIONES EN LA ZONA MINERA  
 PARA FACILITAR EL TRAFICO DE  
 COQUE EN LA ZONA

**PERFORACIONES EN LA UBICACION NORTE**  
*Boreholes in North Location*

TRUSS ENGINEERING COMPANY CONSULTING ENGINEERS  
 INCORPORATED SAN FRANCISCO CALIFORNIA U.S.A.  
 FEBRERO, 1968

LAZARUS  
 FALIZ 5

**LEYENDA**  
 Legend

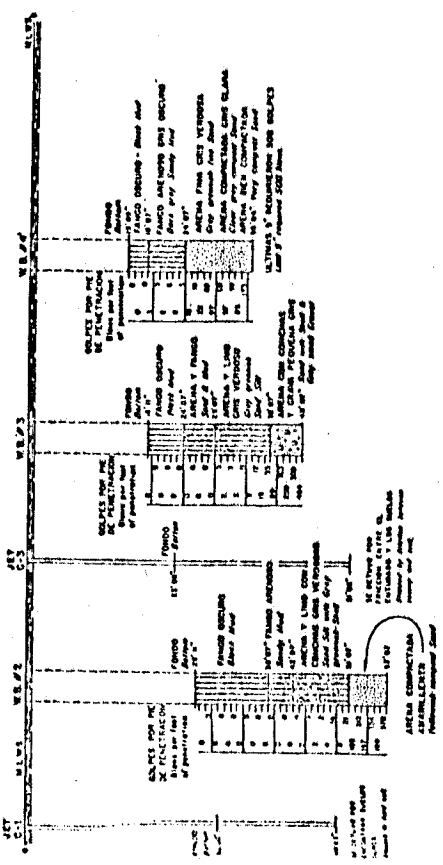
WB = PERFORACION LINDA  
 (Borehole)

B-C-D-E-F = PERFORACION A COQUE  
 (Borehole)

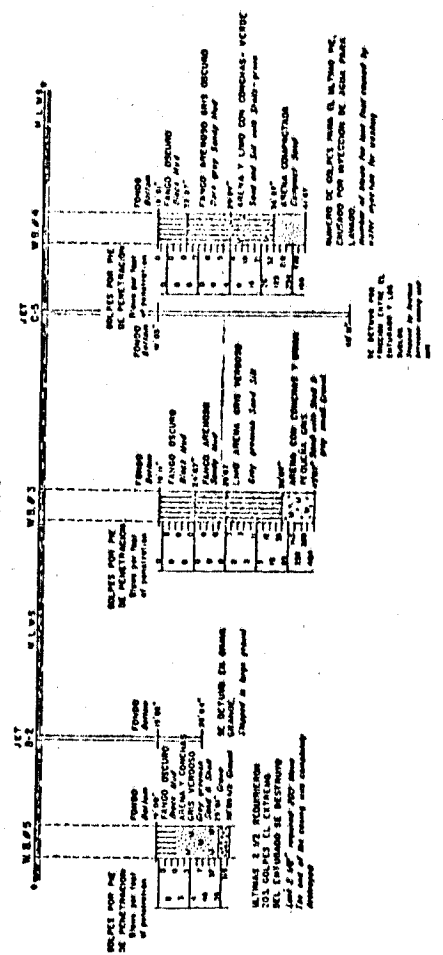
**FUENTE:** INFORME DE PERFORACIONES POTAMICAS EN CHIMOTE, PERU AGOSTO 1962  
**SCALES:** Report on Pot. Boreholes in Chimote, Peru August 1962

Fig. A-4-1

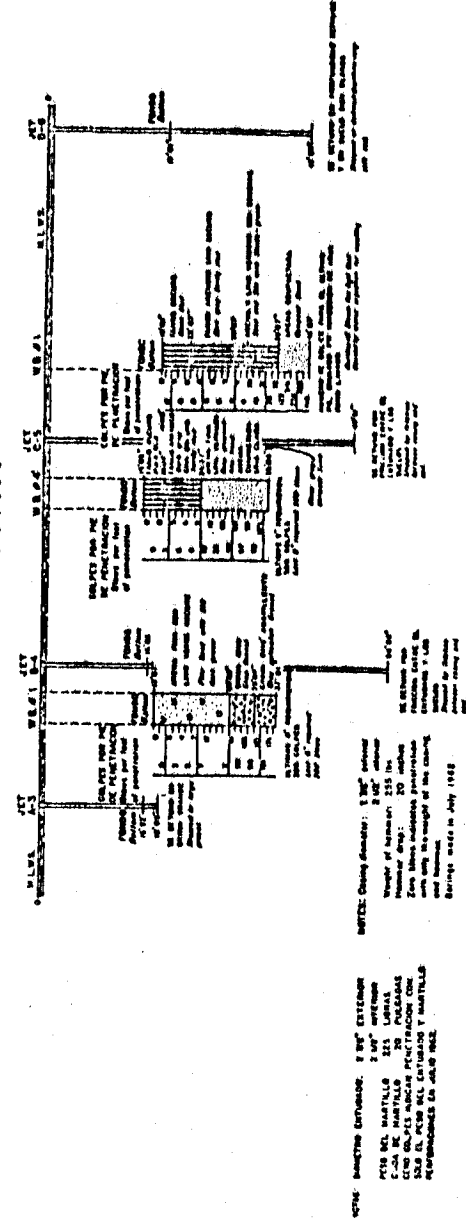
**PERFIL 8-B**  
*Profile*



**PERFIL b-b**  
*Profile*



**PERFIL 8-C**  
*Profile*



**SÍMBOLOS**  
*Symbols*

	TIPO DE SUELO	Soil Type
	RESULTADO DE LA PRUEBA	Test Result
	PRUEBA DE PENETRACION	Penetration Test
	PRUEBA DE RESISTENCIA AL CIZALLADO	Shear Strength Test
	PRUEBA DE CONTENIDO DE HUMEDAD	Moisture Content Test
	PRUEBA DE LIMITE LIQUIDO	Liquid Limit Test
	PRUEBA DE INDICE DE PLASTICIDAD	Plasticity Index Test
	PRUEBA DE CONSOLIDACION	Consolidation Test
	PRUEBA DE COMPRESION	Compression Test
	PRUEBA DE COMPRESION SIN CONFINAMIENTO	Unconfined Compression Test
	PRUEBA TRIAXIAL	Triaxial Test
	PRUEBA DE CAJA DE CIZALLADO	Shear Box Test
	PRUEBA DE CIZALLADO DIRECTO	Direct Shear Test
	PRUEBA DE CIZALLADO CICLO	Cyclic Shear Test
	PRUEBA DE CAMINO DE TENSION	Stress Path Test
	PRUEBA DE PERMEABILIDAD	Permeability Test
	PRUEBA DE CONSOLIDACION	Consolidation Test
	PRUEBA DE COMPRESION	Compression Test
	PRUEBA DE COMPRESION SIN CONFINAMIENTO	Unconfined Compression Test
	PRUEBA TRIAXIAL	Triaxial Test
	PRUEBA DE CAJA DE CIZALLADO	Shear Box Test
	PRUEBA DE CIZALLADO DIRECTO	Direct Shear Test
	PRUEBA DE CIZALLADO CICLO	Cyclic Shear Test
	PRUEBA DE CAMINO DE TENSION	Stress Path Test
	PRUEBA DE PERMEABILIDAD	Permeability Test

**CORPORACION PERUANA DEL SANTA**  
INGENIEROS PORTUENAS DE LA BANCA FERROVIA  
PERFILES DE PERFORACIONES  
UBICACION NORTE  
*Barrings Profiles in North Location*

PERUANA INGENIERIA CONSULTORES Y CONSTRUCTORES S.A.  
AV. SAN JUAN DE LOS RIOS 1000  
LIMA, PERU

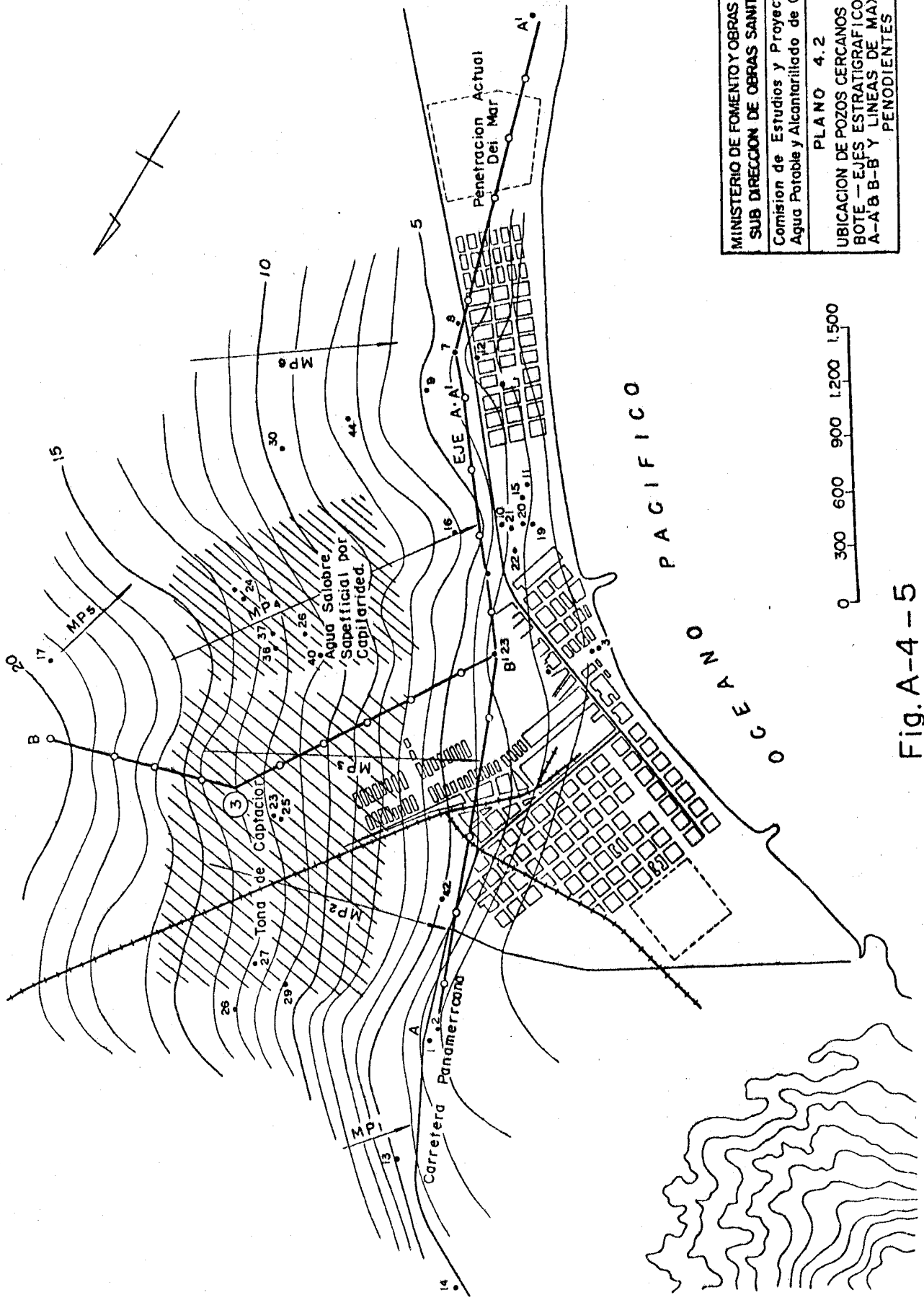
FEBRERO, 1968

Fig. A-4-2

FIGURE: INFORME FACILITADO POR PERUANA DE INGENIERIA PORTUENAS DE LA BANCA FERROVIA  
SOURCE: Report on Soil Profiles in North Location, Peru August 1968.

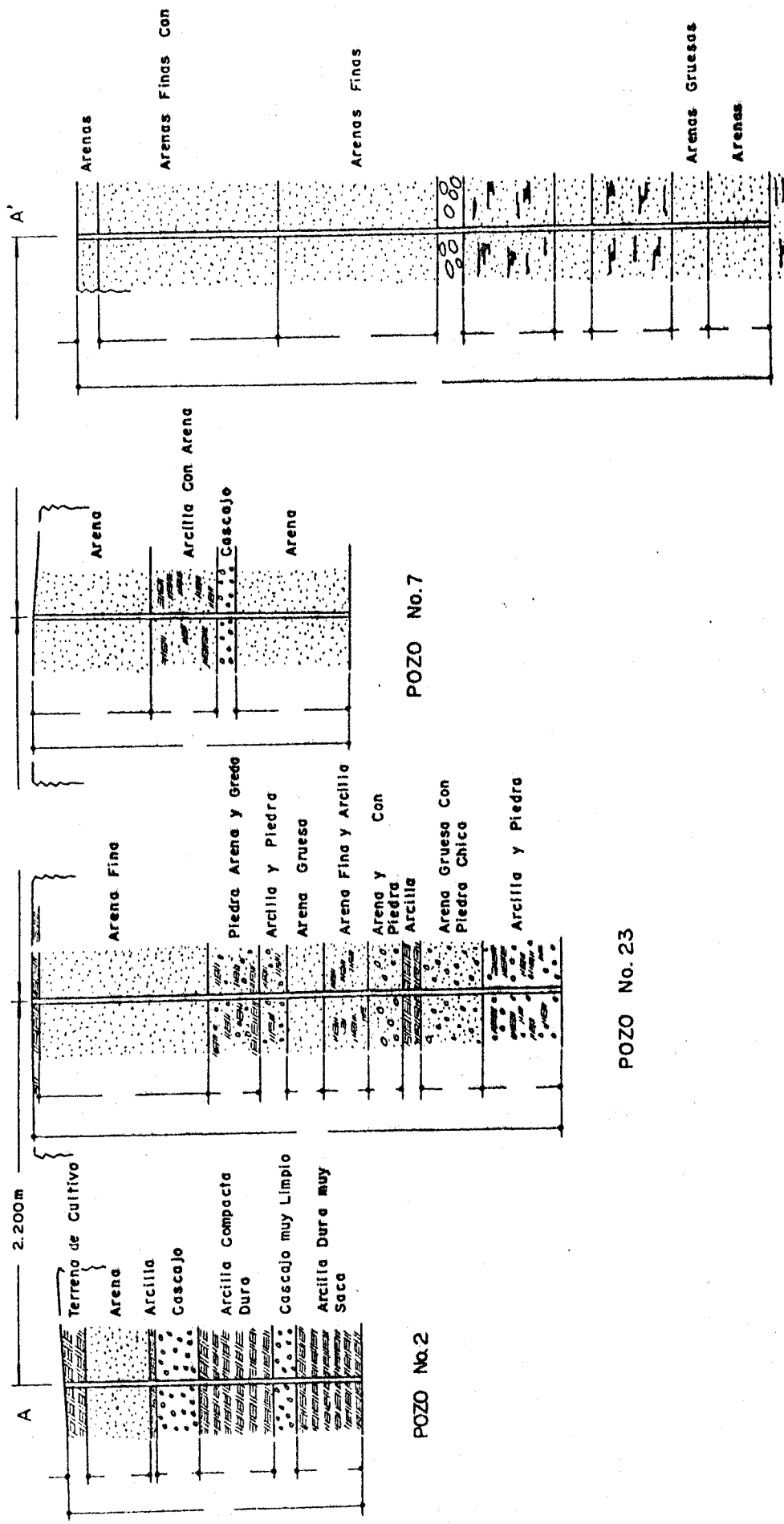






MINISTERIO DE FOMENTO Y OBRAS PUBLICAS SUB DIRECCION DE OBRAS SANITARIAS Comision de Estudios y Proyectos de Agua Potable y Alcantarillado de Chimboe PLANO 4.2
UBICACION DE POZOS CERCANOS A CHIM- BOTE - EJES ESTRATIGRAFICOS A-A & B-B Y LINEAS DE MAXIMA PENODIENTES

Fig. A-4-5



POZO No.45

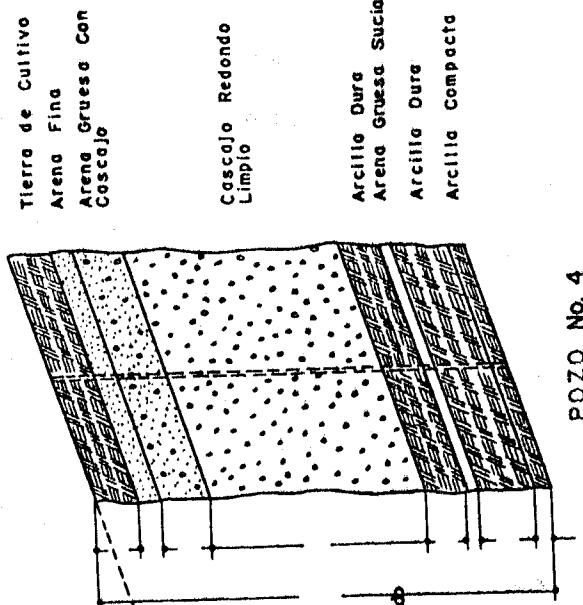
POZO No. 23

POZO No. 7

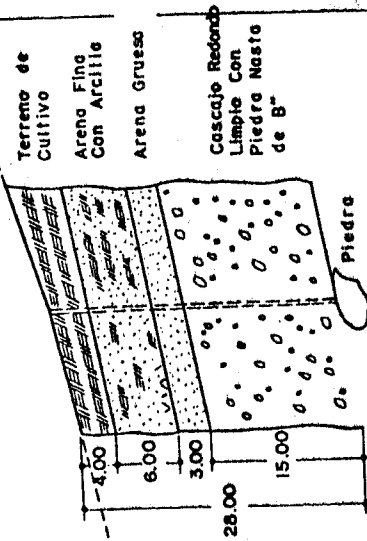
POZO No. 2

MINISTERIO DE FOMENTO Y OBRAS PUBLICAS  
 SUB DIRECCION DE OBRAS SANITARIAS  
 Comision de Estudios y Proyectos de  
 Agua Potable y Alcantarillado de Chimbofe  
 GRAFICO 4.2  
 CORTES ESTRATIGRAFICOS DEL  
 SUB-SUELO DE CHIMBOTE SECON  
 EL CORTE A-A'

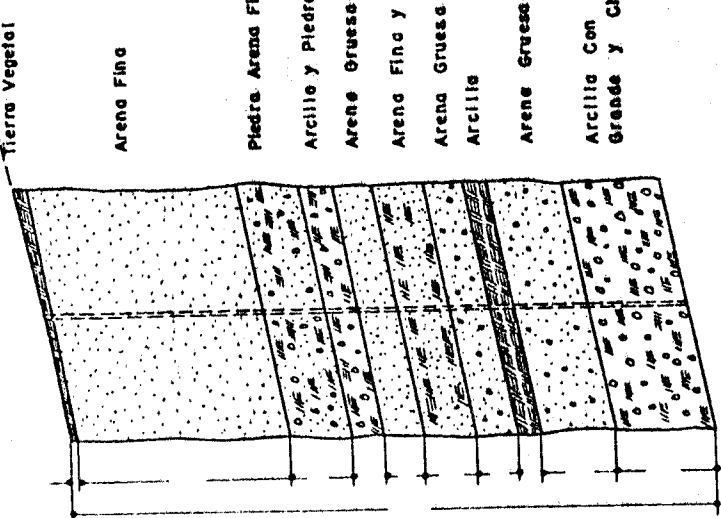
Fig. A-4-6



POZO No. 4



POZO No. 3



POZO No. 23

MINISTERIO DE FOMENTO Y OBRAS PUBLICAS  
SUB DIRECCION DE OBRAS SANITARIAS  
Comision de Estudios y Proyectos de Agua Potable y Alcantarillado de Chimbo  
GRAFICO 4.3  
CORTES ESTRATIGRAFICOS DEL SUB-SUELO DE CHIMBOTE SECON EL EJE B-B'

Fig. A-4-7



## **Appendix 5**

### **Micro-Tremor Records in Chimbote Area**

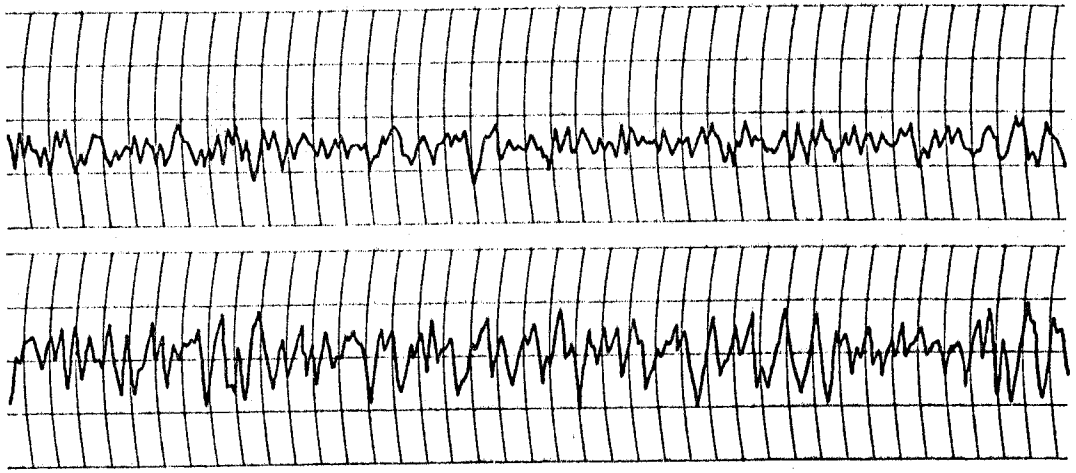


FIG. A-5-1 No.1 PLAZA DE ARMAS

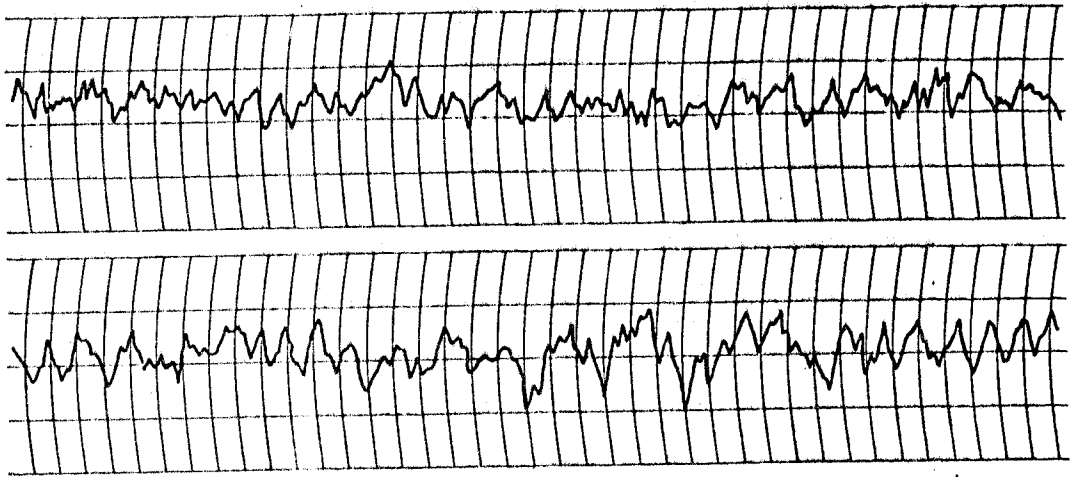


FIG. A-5-2 No.5 URBANIZACION LA CALERA

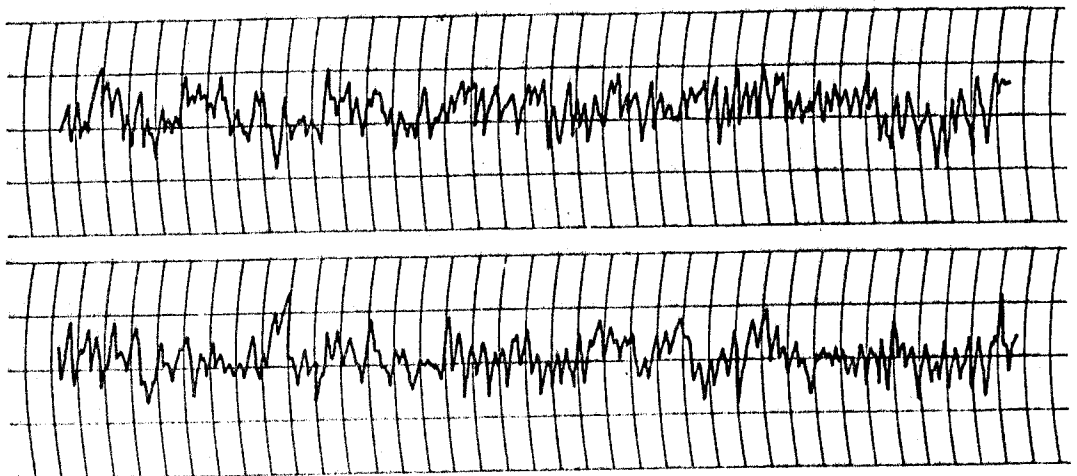


FIG. A-5-3 No.13 SAN PEDRO

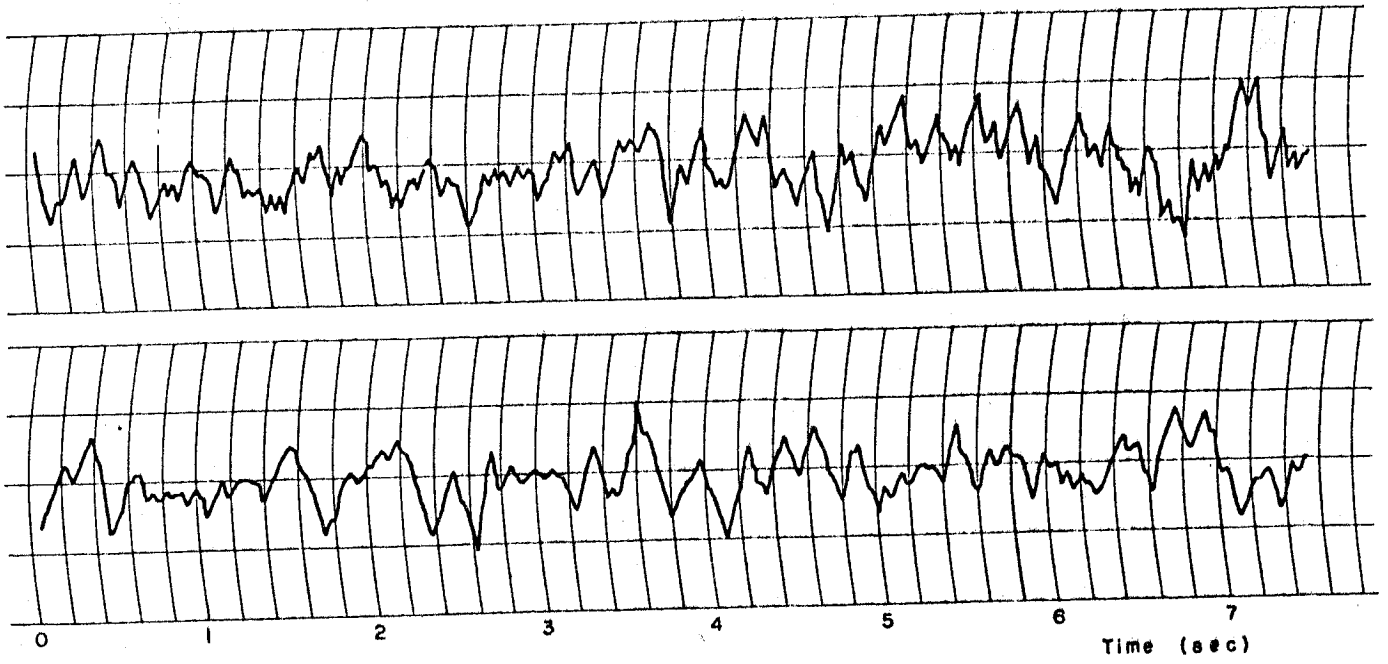


Fig. A-5-4 No.7 NEAR T. V. ANTENNA

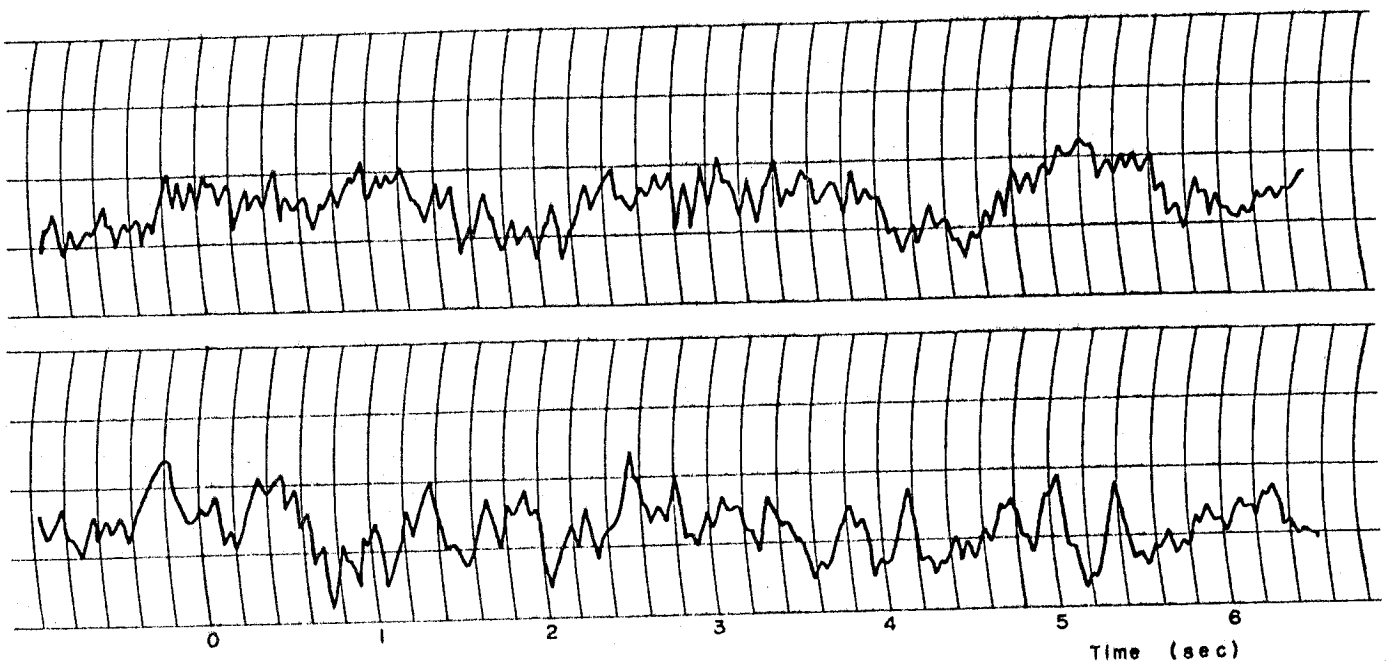


Fig. A-5-5 No.14 URB. 21 DE ABRIL

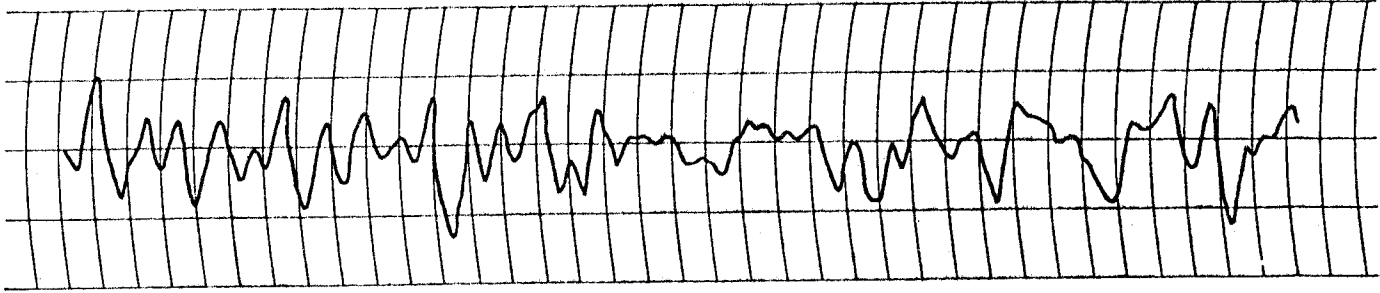
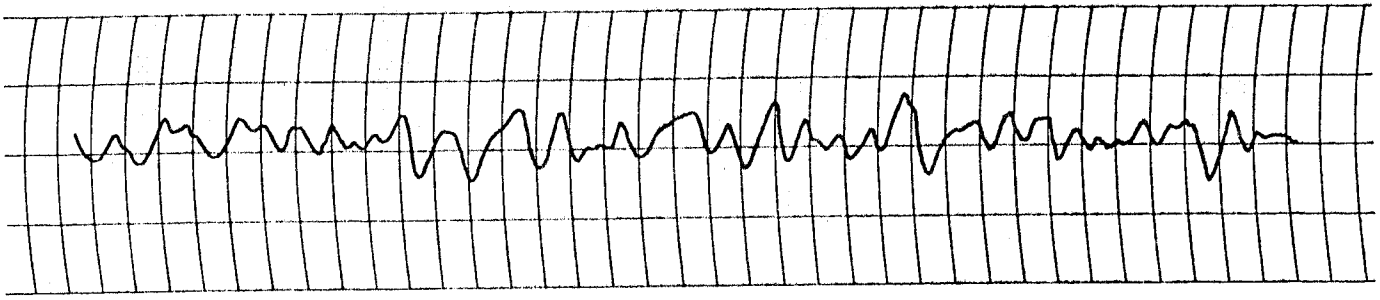


Fig. A-5-6 No.15 JIRON UNION- CUADRA 8 FINAL

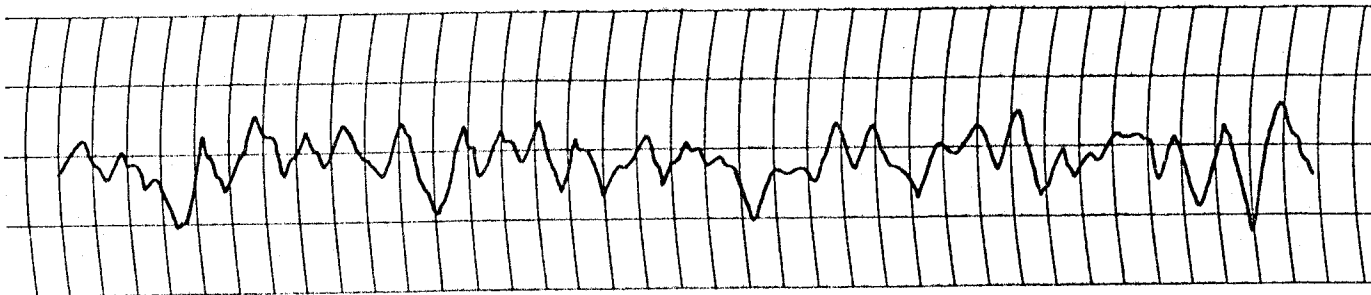
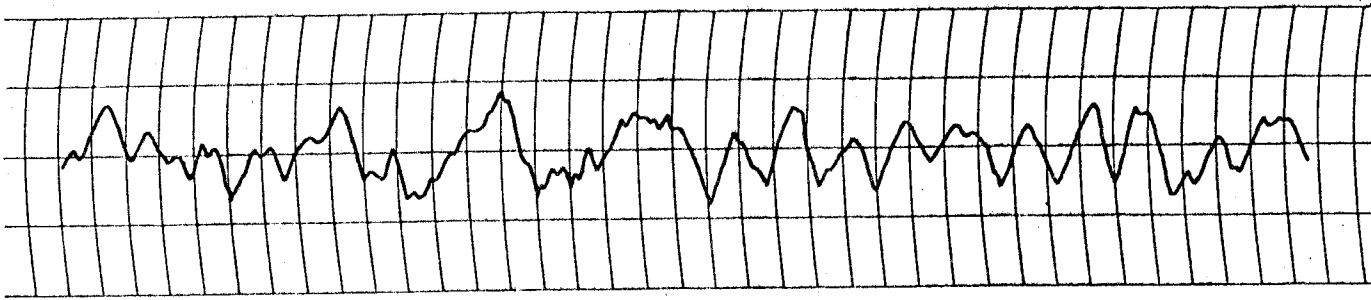


Fig. A-5-7 No. 20 PERFORACION JIRON ICA

## **Appendix 6**

### **Frequency—Periods Curve of Micro— Tremor Records in Chimbote Area**

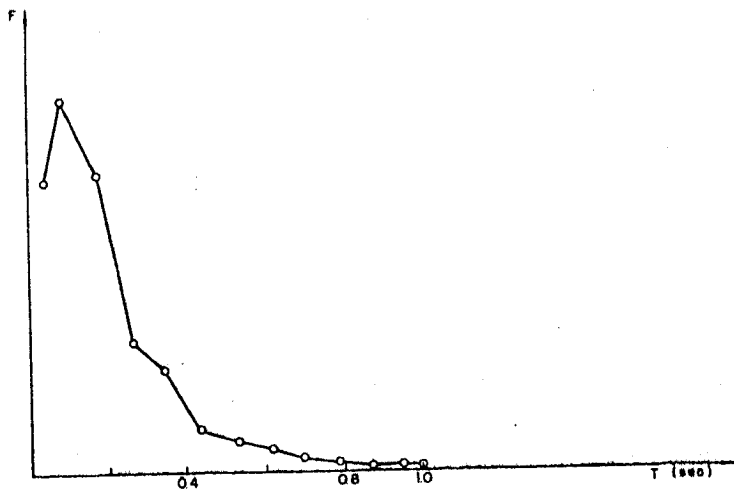


Fig. A-6-1  
MULTI-LAYERED GROUND SURFACE

POINT No. 13 San Pedro  
Pick No. 1

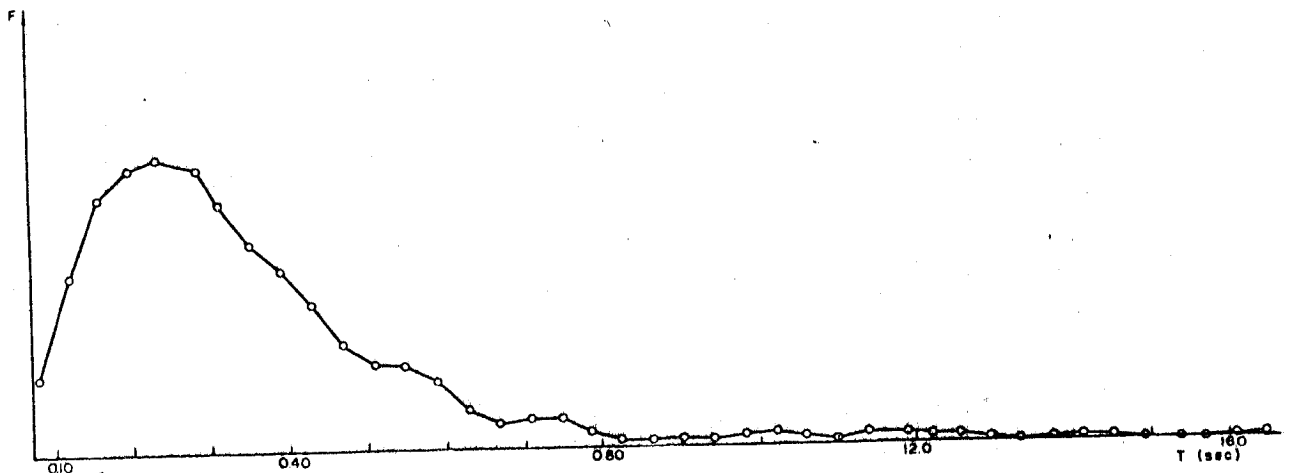


Fig. A-6-2

POINT No. 16  
JF. Union Cuadra 1  
Pick No. 1 (1 A. La. Calle)  
Tp = 0.23 Fp = 80  
T Mayor = 1.64

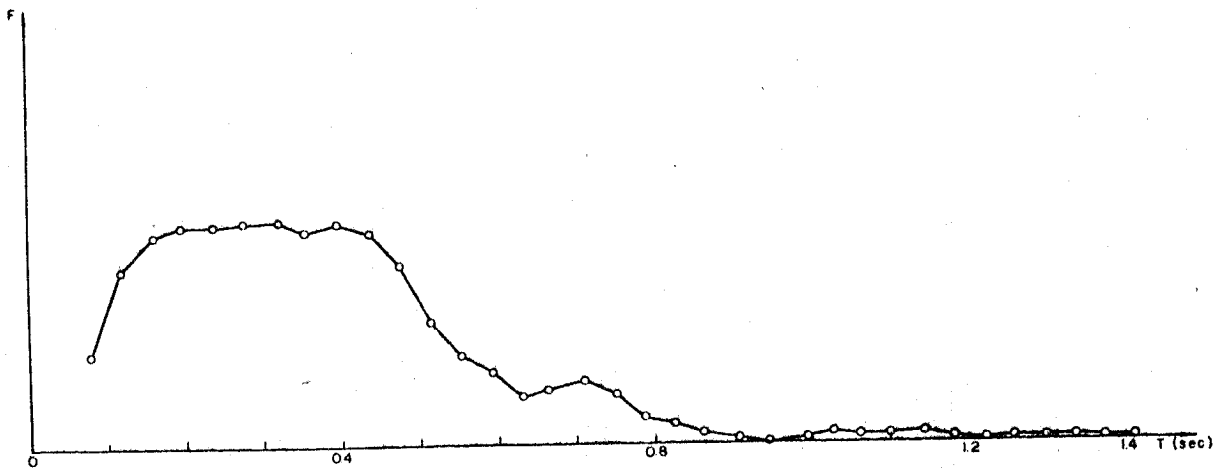


Fig. A-6-3

POINT No. 18  
JF. Union Cuadra 1  
Pick No. 2 (En El Suelo)  
T Mayor = 1.4

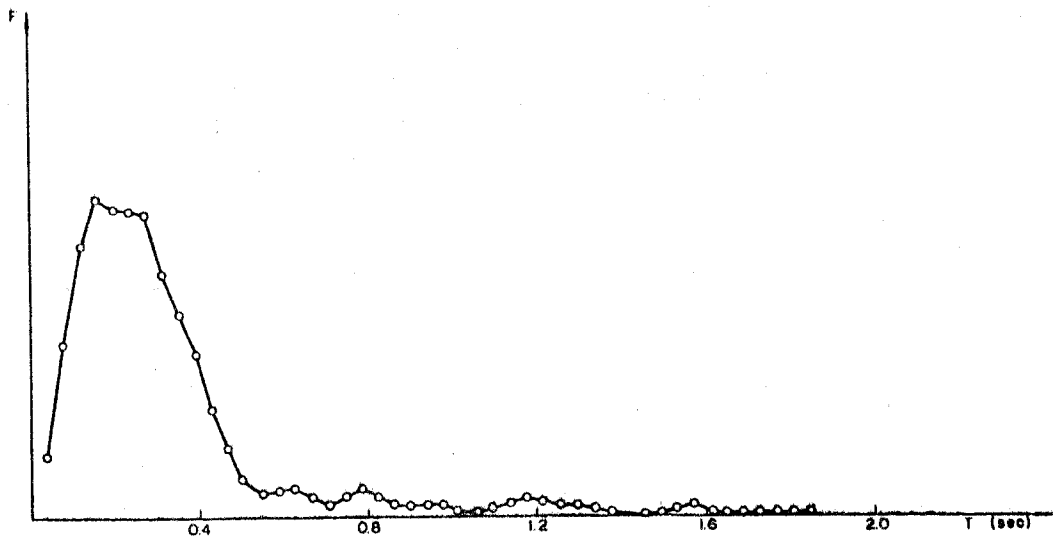
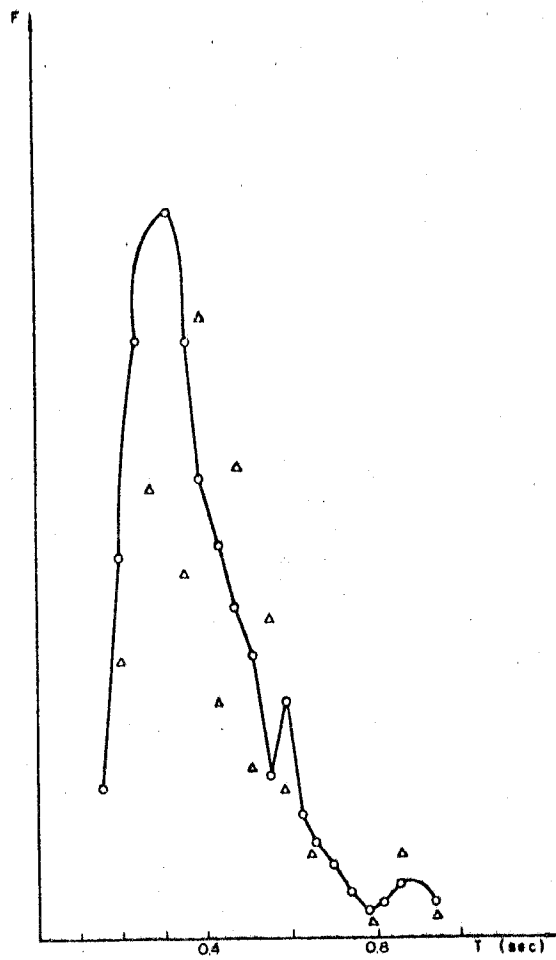


Fig. A-6-4

POINT No. 24  
 Barrio Villa Maria  
 Pick No. 1



POINT No.

- △ Point de F
- Point de F'
- Pick No. 2

Fig. A-6-5

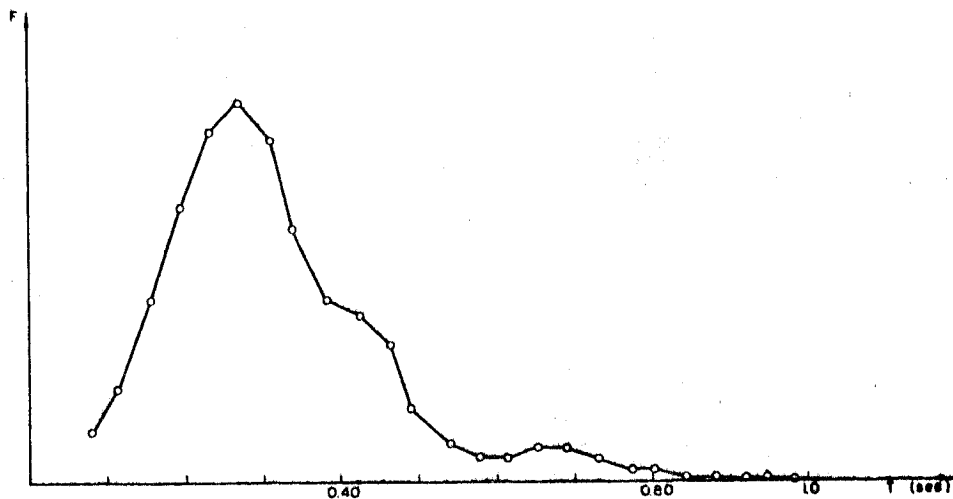


Fig. A-6-6

POINT No. 19  
 Pozo No. 4  
 Pick No. 2 (En. El. Suelo)  
 T Mayor  $\frac{F-1}{F_0-0.8}$   
 Tp = 0.27

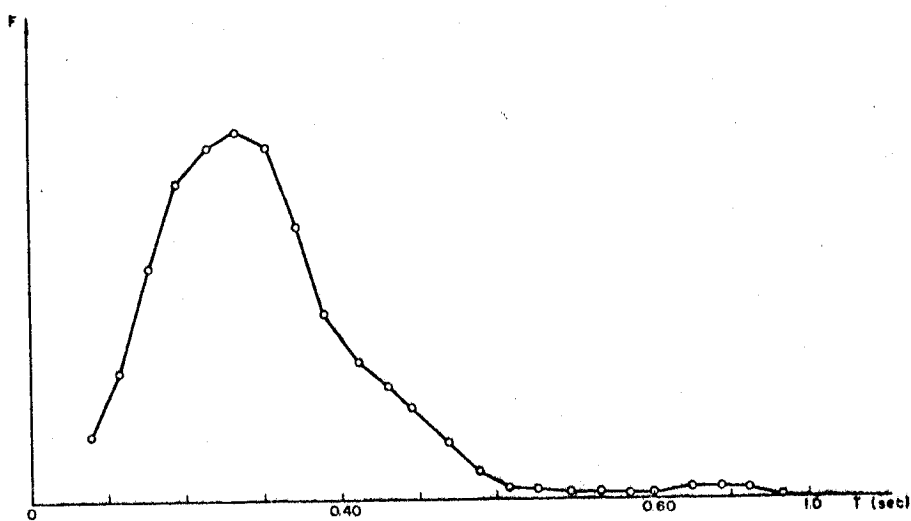


Fig. A-6-7

POINT No. 19  
 Pozo No. 4  
 Pick No. 1 (En. El. Suelo)  
 T Mayor = 1.18  $\frac{F-1}{F_0-0.8}$

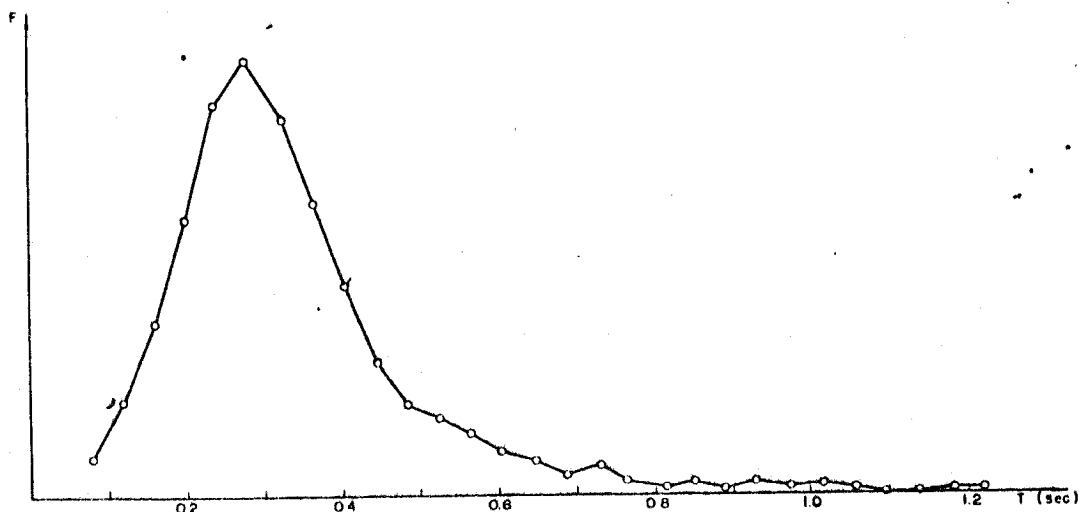


Fig. A-6-8

POINT No. 20  
 Pozo No. 3 (Jr. Ica)  
 Pick No. 2 (En. El. Suelo)  
 T Mayor = 1.22 sec



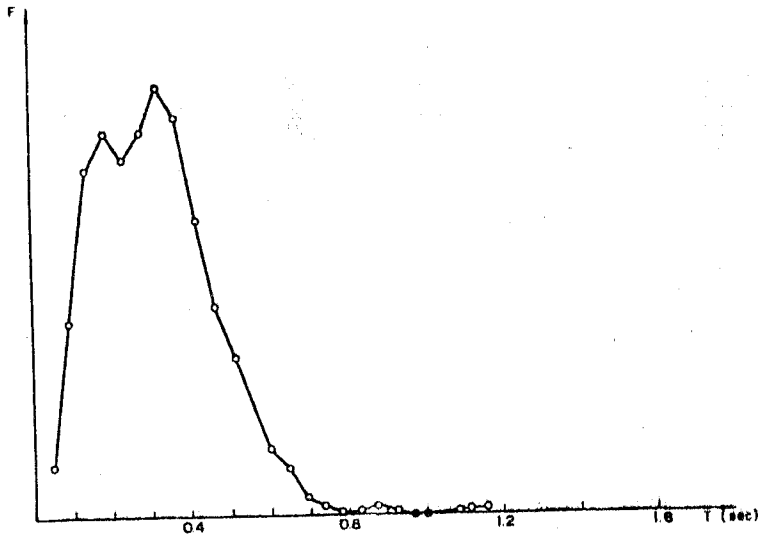


Fig. A-6-9

POINT No. 21

G.U.E. San Pedro (J. San Pedro Cuadra 1)  
Pick No. 2  
(Cerca Drill de Mez)

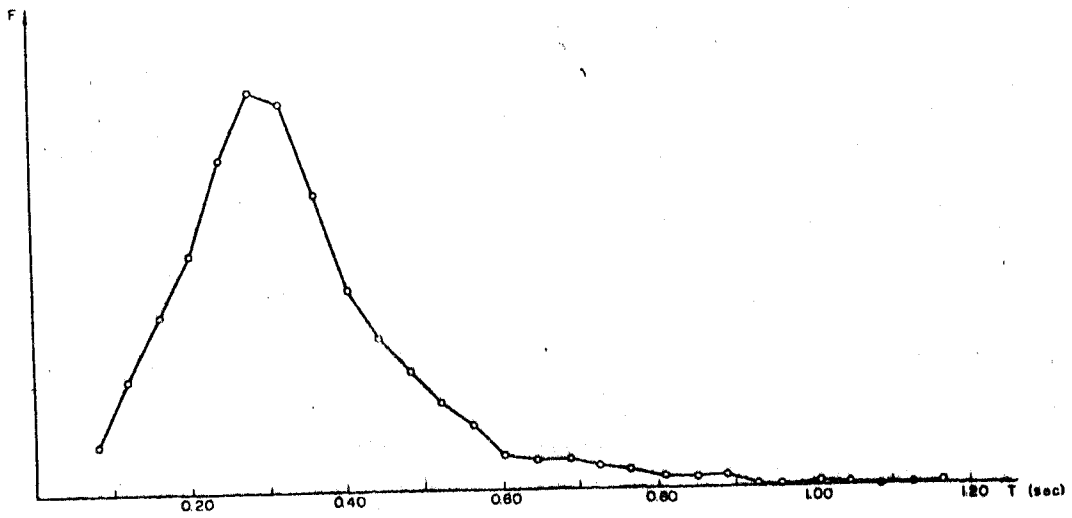


Fig. A-6-10

POINT No. 20

Pozo No. 3 (J. Ica)  
Pick No. 1 (En. El. Buelo)  
Tp = 0.28 F = 50  
F = 5078

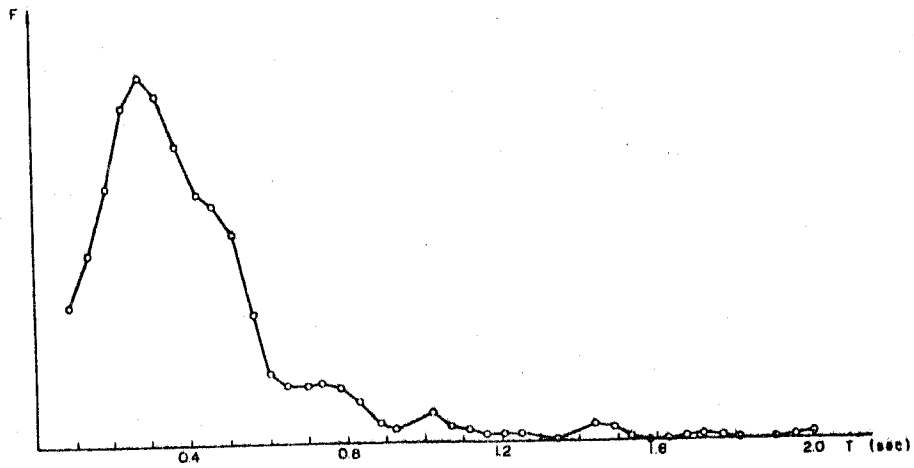
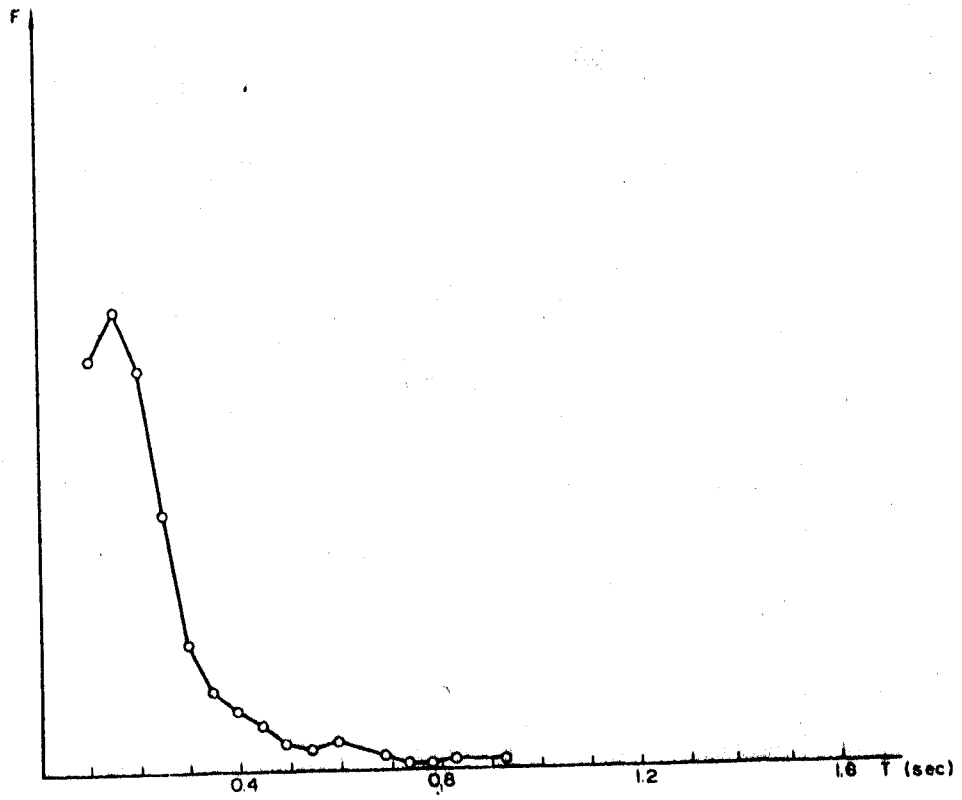


Fig. A-6-11

POINT No. 21

G.U.E. San Pedro  
(J. San Pedro Cuadra 1)  
Pick No. 1 (Campo de Colegio)



POINT No. 6  
Pick No. 1  
Cerro de Sogeso

Fig. A-6-12

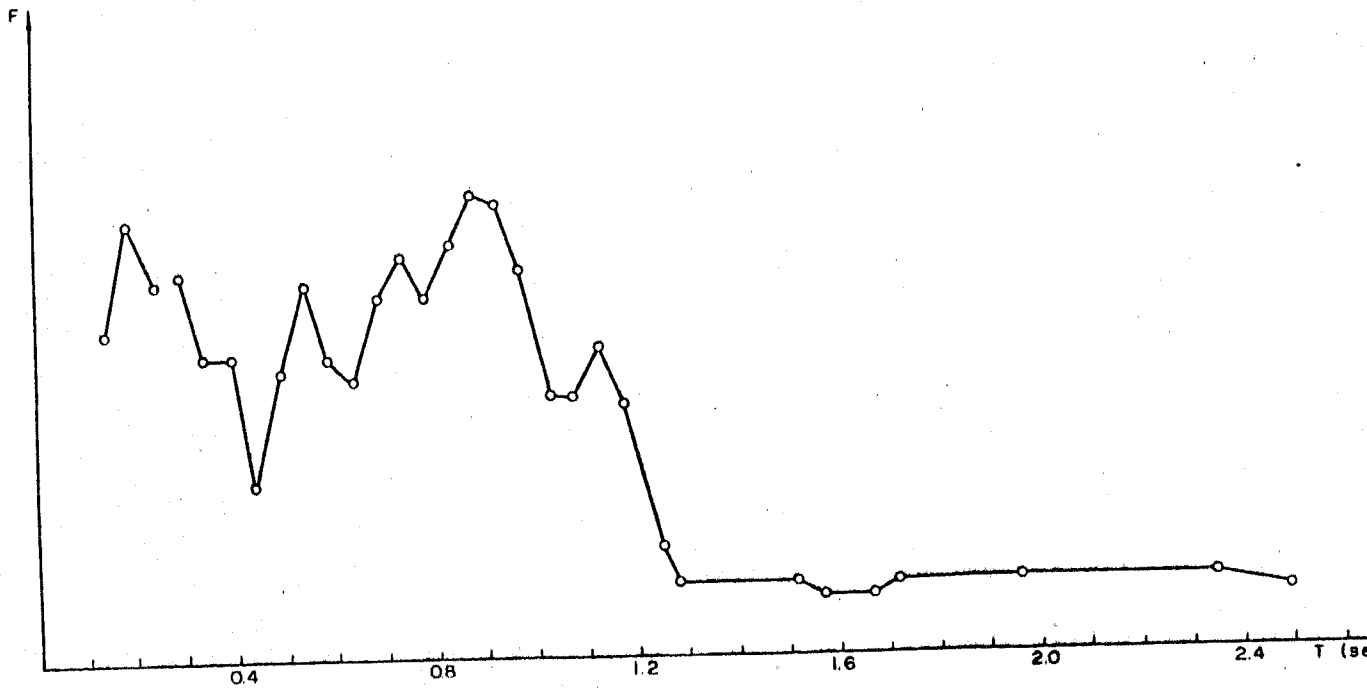


Fig. A-6-13

POINT No. 9  
Pick No. 2

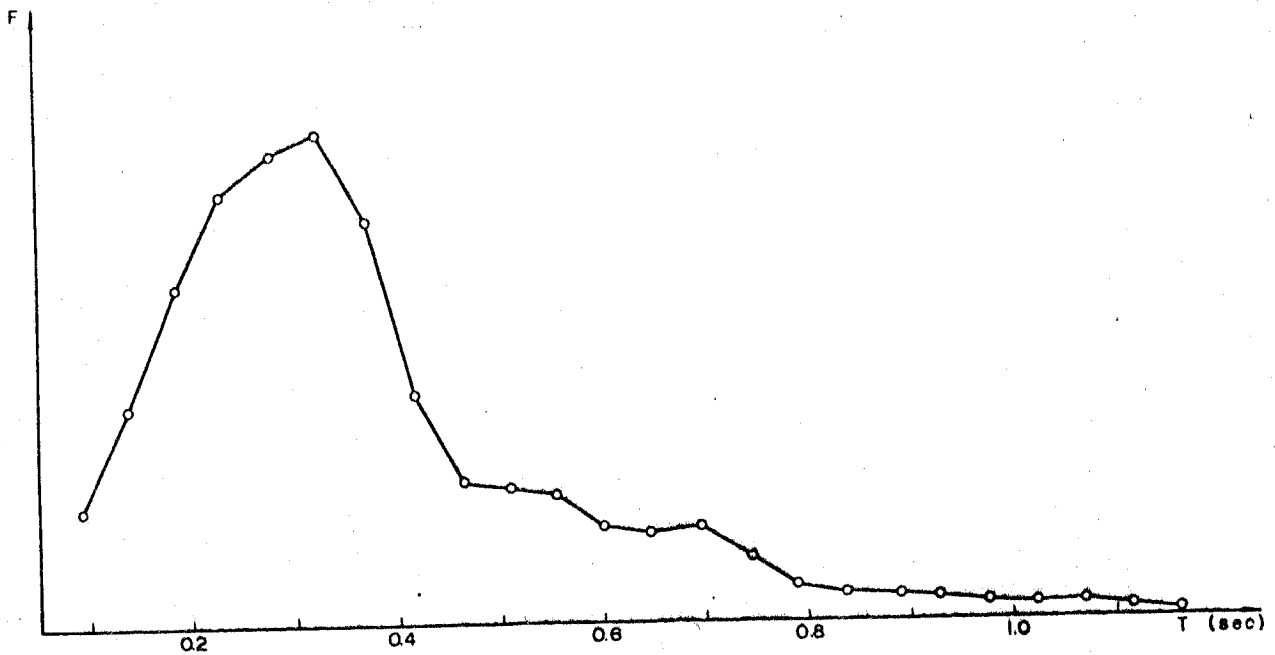


Fig. A-6-14

POINT No. 15  
 Jr. Union Cuadra 6  
 Pick No. 2 (En. El. Suelo)

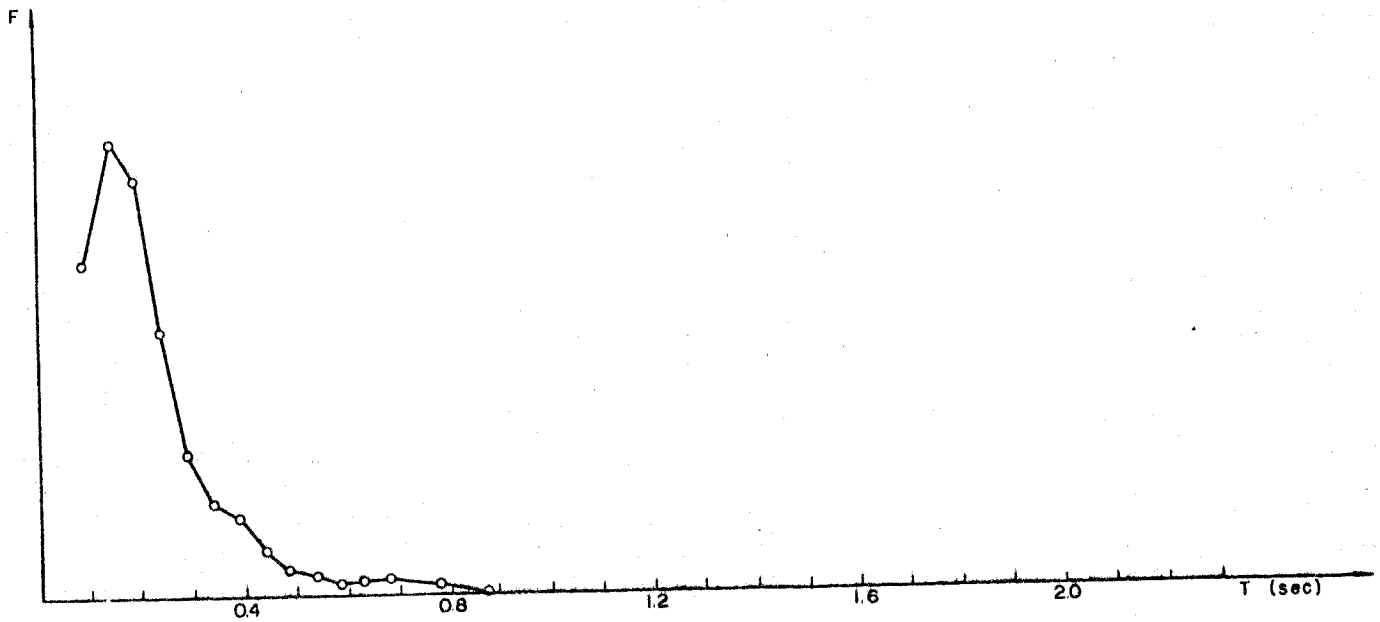


Fig. A-6-15

POINT No. 6  
 Pick No. 1  
 Cerco de Sogeso